The Pennsylvania State University

The Graduate School

Department of Mechanical Engineering

COMBUSTION OF WATER-IN-OIL EMULSIONS OF DIESEL AND FRESH AND WEATHERED CRUDE OILS FLOATING ON WATER

A Thesis in

Mechanical Engineering

by

Ajey Y. Walavalkar

Submitted in Partial Fulfillment
of the Requirements
for the Degree of

Doctor of Philosophy

August 2001

We approve the thesis of Ajey Y. Walavalkar.

Date of Signature

_____	_____
Anil K. Kulkarni Professor of Mechanical Engineering Thesis Advisor Chair of Committee	
_____	_____
Ralph L. Webb Professor of Mechanical Engineering	
_____	_____
Savash Yavuzkurt Professor of Mechanical Engineering	
_____	_____
Sarma V. Pisupati Assistant Professor of Energy and GeoEnvironmental Engineering	
_____	_____
Richard C. Benson Professor of Mechanical Engineering Head of the Department of Mechanical Engineering	

ABSTRACT

Burning of spilled oil on the ocean surface or *in-situ* combustion is one of the techniques used in oil spill clean up operations. With the passage of time, as the crude oil stays on the ocean surface, evaporation of the lighter components of the crude oil and mixing of water with the oil due to wind and ocean turbulence create emulsions that are more dense and more viscous than oil. This makes the ignition of the oil harder to achieve. Prior studies have shown that emulsions containing more than a certain fraction of water do not burn, and thus present a difficulty in applying the *in-situ* combustion technique.

Many normally incombustible materials can be ignited when subjected to a certain minimum heat flux, and sustained fire and flame spread can be achieved on these materials. In the present work, this principle is applied to the emulsion combustion problem so that, if successful, the window of opportunity for *in-situ* combustion of oil spills can be widened. It is proposed that there exists a threshold heat flux level for most of the emulsions such that, when emulsion is exposed to a heat flux equal to or greater than the threshold heat flux, sustained fire and flame spread can be achieved.

A test facility was designed and built to conduct laboratory scale burn tests of water-in-oil emulsions to study the threshold heat flux values for different types of emulsions. The emulsion samples, floating on water surface, could be subjected to radiative heat flux ranging from 1.2 kW/m^2 to 21 kW/m^2 in steps of about 1 kW/m^2.

Experimental measurements of threshold heat flux values were made for emulsions of diesel, Milne Point crude oil and Alaska North Slope crude oil with water. The water fraction in the emulsion was changed from 0% to 80% by volume. The crude oil samples were also tested for effects of evaporation of the lighter fractions from the crude oil. Laboratory scale experiments clearly verified that there exists a threshold heat flux for each type of emulsion studied. For example, emulsions of fresh Milne Point crude oil containing 35% water by volume could not be ignited with external heat flux of 11 kW/m^2. But the same emulsion composition could be ignited with external heat flux of 13 kW/m^2. 15% weathered Milne Point crude oil could not be burned, in unemulsified

state, without external heat flux of 10 kW/m^2. Emulsions of 26 % weathered Alaska North Slope crude oil containing 50% water by volume could be successfully burned with the help of external heat flux of 9 kW/m^2.

The data indicate that higher threshold heat flux is required to cause successful burning of emulsions having higher water content or emulsions of more weathered oil. Upon correlating the threshold heat flux data for the crude oils with the density of the crude oil, it was observed that the threshold heat flux values increase with increasing density of the crude oil.

Previous studies have proposed that it is the oil that separates from the emulsion that burns and not the emulsion itself. Combining this idea with the results presented, it can be argued that in order to create a sustained emulsion pool fire, the emulsion must be separated into water and oil at such a rate that the rate at which the oil is separated from the emulsion must be at least equal to the rate at which the oil is consumed by combustion. The results from the study also suggest that in order to achieve flame spread, the fire must be of such size as to impose the surrounding emulsion pool with heat flux equal to or more than the threshold heat flux.

The combustion process of a water-in-oil emulsion layer floating on top of a water surface, as in case of *in-situ* burning of oil, spilled at sea that has turned into emulsion, was modeled using comprehensive mathematical treatment. Mathematical models are available in the literature for oil pool fires but not for emulsion pool fires. This model is unique as it incorporates the separation of emulsion into water and oil, a phenomenon that governs the emulsion pool fires. The burning process is divided into three regimes, as follows.

1. The initial regime, when the emulsion layer floating on the ocean surface receives heat flux from an external source such as an igniter or a burning oil pool;
2. The intermediate regime, from the instant when there is first appearance of oil layer on the top of the emulsion layer due to breaking of emulsion until the oil starts evaporating; and,

3. The final regime, which is characterized by the combustion of oil vapor and continues till the fire extinguishes.

The model was solved numerically using finite difference method and it was validated using the data from the laboratory scale burn experiments involving emulsions of diesel with water. The model predictions were used to study the effects of emulsion composition and oil weathering on important emulsion pool fire characteristics such as, the average burning rate, total duration of the burn, the volume of the oil residue and the overall oil burning efficiency.

The average oil burning rate, total duration of burn, the volume of the oil residue and the burn efficiency decreased with increasing water content of the emulsion. Average oil burn rate and the overall burn efficiency decreased with increased weathering of the oil whereas the total burn time and the volume of the oil residue increased with increased weathering of the oil. Comparisons of the model predictions with the experimental observations showed that most of the model predictions were found to be within 25% of the observed values. The model has captured the description of significant processes involved in emulsion combustion, and thus is able to describe the experimental observations with sufficient accuracy.

TABLE OF CONTENTS

LIST OF FIGURES

LIST OF TABLES

NOMENCLATURE

Symbols:

C	Stretching factor
C_o	Fraction of heat flux not absorbed at the surface
C_1	Inverse of oil content of emulsion, on mass basis
c_{po}	Specific heat of oil
H	Emulsion thickness
h	Convective heat transfer coefficient
k	Thermal conductivity
L	Oil thickness
L_p	Rate of oil layer production due to emulsion breaking
L_d	Rate of oil layer depletion due to oil evaporation
$\dot{q}''$	Incident heat flux
$\dot{q}''_{\max}$	Maximum heat flux incident on the slick
Q_{comb}	Energy released by combustion of oil per unit mass
Q_{Lo}	Energy consumed in oil vaporization
Q_{Lw}	Energy consumed in water vaporization
t	Time
T_{eb}	Emulsion breaking temperature
T_{ov}	Oil vaporization temperature
T	Temperature
x_e	Emulsion coordinates
x_o	Oil coordinates
x_w	Water coordinates
y_w	Coordinates in transformed water region

Greek Symbols:

α	Thermal diffusivity
β	Inverse absorption depth

ε	Emissivity
ρ	Density
σ	Stefan-Boltzmann constant

Subscripts:

e	Emulsion
o	Oil
w	Water
1	For initial regime
2	For intermediate regime
3	For final regime
i	Initial conditions

ACKNOWLEDGEMENTS

Many people have contributed to successful completion of this work. I would like to thank my advisor, Dr. Anil Kulkarni. His insightful guidance throughout the entire project is very much appreciated. His support and encouragement, in academic as well as non-academic matters, during my graduate studies at Penn State made the whole experience highly enjoyable and educational. I would like to thank Dr. Sarma Pisupati for his help in setting up my emulsion pool fire test rig at the Combustion Lab of the Energy Institute. I also want to thank Dr. Ralph Webb and Dr. Savash Yavuzkurt for their time and effort in directing my thesis work.

The support of the staff at the Combustion Lab of the Energy Institute, especially that of Ron Wincek, Mike Hill, Dave Johnson and Kevin Witt is greatly appreciated. The work would not have completed without cooperation and help from Ron Gathagan and Dave McCloskey. I would also like to thank Michelle Pisarchik, Jennifer Benson, Brad Oakes, Karem Munir, Leena and Aparna Krishnamurthy for working with me on this project.

My sincere thanks are due to LaRue Jackobs for her help with the accounts of the project. This project was funded by the National institute of Standards and Technology. I would like to thank Mr. Doug Walton of the National Institute of Standards and Technology, US DOC, and Joe Mullin and Sharon Buffington of Mineral Management Service, US DOI, for their technical and financial support for the project. I thank Ms. Charlene Hutton of the Alaskan Clean Seas, Prudhoe Bay, Alaska for donating the crude oil samples used in this work. I also thank Ellen Sue Spicer for meticulous proofreading of the thesis and all the suggestions made for improving the thesis.

Friendship of Arun, Gautam, Michelle, Jaya, Saurabh, Nilesh, Aniruddha, Sameer, and Kanchan made my stay at Penn State a pleasant memory. I would not have come this far without the love and encouragement of my parents and my sister Jai. Love, support, understanding, patience and encouragement from my dear wife Leena made the journey towards the dream of a doctoral degree the most enjoyable one.

Chapter 1

INTRODUCTION

1.1 Oil Spill Problems

The growth of technology is driving up the rate of consumption of energy. Presently, about 96% of the energy demand is met by the conventional non-renewable energy sources. Petroleum products form a major part (about 60%) of the energy source available today. (International Energy Association Web Page, 1998 data) The world uses around 2.7 billion gallons of oil every day. The sources of the crude petroleum are concentrated in certain areas of the world. Many times, economic or geographic conditions need the crude oil refineries to be built away from the source, and the crude oil needs to be transported from the oil well to the refinery. This transport takes place mostly via ocean or under-sea pipelines. Ships carry crude oil from the source to the refinery. Sometimes, refined petroleum products are also carried from the refinery to the market via the ocean. In some cases, such as the oil fields in Alaska, the crude oil is transported through a direct pipeline that may run under the ocean. Every day, 31.5 billion gallons of oil are being transported at sea (From Oil Spill Intelligence Report, Arlington, MA, USA).

In spite of all the precautions, the incidents of oil tanker breakage or oil pipeline leakage continue to occur. Although the number of accidents and the total amount of oil spilled have decreased in the past five years, every year about 100 million US gallons of oil spill. The biggest spill occurred during the 1991 Persian Gulf War, when about 240 million gallons of oil spilled from the oil terminals and tankers off the coast of Saudi Arabia. The second biggest spill occurred during a ten-month period, from June 1979 to February 1980, when 140 million gallons of oil spilled at the Ixtoc I well blowout in the Gulf of Mexico near Ciudad del Carmen, Mexico. The Exxon-Valdez spill in Alaska was the 35^{th} largest spill in the world, although it was the largest one in the US, when 11 million gallons of oil were spilled at Bligh Reef in Prince William Sound, Alaska on March 24, 1989. (From Oil Spill Intelligence Report, Arlington, MA, USA)

Accidents with the oil transporting media result in spillage of crude petroleum oils on the ocean surface. Due to winds, waves and surface tension effects, the oil spreads on the ocean surface. As the spilled oil, floating on the ocean surface, is exposed to the surroundings, the oil starts to weather. Weathering consists of various processes such as evaporation, emulsification, dispersion, photo-oxidation, adsorption, and biodegradation.

The wind and the ocean turbulence supply the energy required to break the oil-water interface layer. A complex process known as emulsification takes place. Over a period of time emulsions of oil and water are formed. Numerous small droplets of water are trapped in the continuous oil phase. The resulting mixture is called water-in-oil emulsion. The emulsion may contain as much as 80% water by mass. The emulsification process increases the volume of the spill. Impurities, such as asphaltines, resins and waxes, present in the crude oil increase the extent of emulsification by precipitating out the surfactants. These surfactants help the emulsion stabilize and make the demulsification process difficult. The viscosity and the density of emulsions are higher than those of the oils. The viscosity of the emulsion can be more than 100 times higher than that of the oil.

The process of evaporation of lighter components of the crude oil into the surrounding atmosphere causes reduction in spill volume. As the oil is allowed to stand on the water surface for a longer time, the lighter components in the oil evaporate. Up to 20% of the volume of the spilled oil can evaporate in the first 24 hours. (Galt J. A., 1994). As the lighter components evaporate, the solubility of the oil decreases, resulting in precipitation of the surfactants. The precipitation of the surfactants aids the process of emulsification and makes the resulting emulsions more stable.

Other weathering processes that affect a small fraction of the total spill volume are as follows (From National Oceanic and Atmospheric Administration Web Page at http://response.restoration.noaa.gov/oilaids/crudes.pdf):

1. Dispersion, in which the spilled oil is distributed into the upper layers of the water column by natural wave action,
2. Photo-oxidation, in which small fractions of crude oil chemically react with oxygen in air, due to energy obtained from sun light,

3. Adsorption, where by oil adheres to the surfaces of various bodies such as sand, algae, silt in the ocean, and
4. Biodegradation, in which the oil is used by certain bacteria, fungi and yeasts as source of food and thus consumed

The oil spill not only results in economic losses but also poses a major threat from an environmental point of view. A prolonged stay of spilled oil on the ocean surface disrupts the ecological balance. Marine life is threatened as the supply of oxygen and sunlight is blocked by the presence of the emulsion surface of the ocean. The lighter fractions of the crude oils are the hydrocarbons, escaping directly into the atmosphere due to evaporation. These are damaging to the environment as they cause the depletion of ozone layer. Hence, an oil spill, once occurred, needs to be cleaned up as soon as possible.

The tanker T/V Exxon-Valdez ran aground on Bligh Reef and spilled an estimated eleven million gallons of North Slope crude oil into Prince William Sound, Alaska. About 140 miles of beach were heavily oiled and about 1500 miles of shoreline had some oiling. The clean-up efforts continued for three summers from 1989 to 1992. In 1989, more than 11000 people and 1400 marine vessels were involved in this effort. Techniques used to remove or clean the oil included: chemical dispersants, high pressure/hot water washing, cold water washing, fertilizer-enhanced bioremediation, and manual and mechanical removal of oil and oil-laden sediments. *In-situ* burning technique was also used with success, but only on exploratory scale (Allen, 1990). Scientists estimated that 35% of the spilled oil evaporated, 40% was deposited on beaches within Prince William Sound, and 25% entered the Gulf of Alaska, where it either became beached or was lost at sea. The estimated cost of this multi-year clean up was more than two billion dollars or roughly $200/ gallon of oil spilled. The affected habitat restoration is still going on (Exxon Valdez Oil Spill Restoration Web Page).

1.2 Clean up Techniques

The clean up operation for oil spills consists of various techniques. Some of the most commonly used oil spill clean up techniques are:

1. Containment and mechanical recovery: Shortly after the spill, the oil spreads over a large area, and needs to be collected by using some sort of containment devices. Containment involves surrounding the oil with a floating barrier called a boom. The mechanical recovery method involves picking up oil and/or emulsions from the ocean surface and carrying them to the ground and dumping them in the pits. This method is very costly requiring a substantial amount of equipment and human power. However, if the emulsification has gone too far, sometimes the mechanical recovery proves to be the only viable method. This method is also effective for on-shore spill clean-ups. The oil is soaked in pieces of absorbent material, like cloth or cotton wool, and then disposed off in a landfill. The oil, however, eventually escapes to the atmosphere, creating severe pollution problems. Thus, though effective, the mechanical recovery method has drawbacks of being costly, labor intensive and environmentally damaging.
2. *In-situ* Burning: The burning of spilled oil on the ocean surface is an effective method that has been used sporadically in the past thirty years. The spilled oil and/or emulsion are first restricted from spreading by containment devices such as fire resistant booms. The booms are then towed to collect the spillage together. The spillage is ignited and left to burn until it extinguishes. The residue is then scooped up mechanically to finish the clean up. The decision of whether or not to burn an oil slick at sea is often contentious. Issues such as the distance of the oil from the damaged vessel or from a populated area, the potential toxicity of the smoke generated, the likelihood of the burn being successful depending on the surrounding sea and weather conditions, the fate of the unburned residue, and the safety of the clean up crew all need to be taken into consideration. With conditions optimal to cause the burn, the *in-situ* burning technique can remove up to 98% of the spill volume. The burning efficiency in the case of the Exxon Valdez oil spill was more than 98% (Allen, 1990).
3. Dispersants: Dispersants are a group of chemicals designed to be sprayed onto oil slicks in order to accelerate the process of natural dispersion. Natural dispersion of an oil slick occurs when waves and other turbulence at the sea surface cause all

or part of the slick to break up into droplets and enter into the water underneath. Spraying dispersants may be the only means of removing spilled oil from the sea surface, particularly when mechanical recovery and *in-situ* burning are not possible. Their use is intended to minimize the damage caused by floating oil. Dispersants have very little effect on very viscous floating oil as they tend to slide off the oil into the water before they can penetrate. Even the oils that can be dispersed initially become resistant after a period of time, as the viscosity increases because of evaporation and emulsification.

4. Bioremediation: This technique involves enhancing the natural biodegradation process by natural oil-eating bacteria by providing them with the necessary fertilizers or oxygen. Although the idea of bioremediation is attractive, the rate of oil removal from the surface is very slow. In addition, some of the more complex components of oil, such as resins and asphaltenes, remain partially or completely undegraded. Thus, bioremediation is not a viable technique for oil spill clean up at present.

1.3 The In-Situ Burning

The *in-situ* burning is an effective method of oil spill clean up. Table 1 shows some of the major oil spill burning efforts in the past thirty years. *In-situ* burning requires fewer personnel and less equipment when compared to the mechanical recovery process. As the spilled oil is burned, the hydrocarbons are converted to combustion products. Hence, the emissions from the fire are not as damaging to the environment as are the pure hydrocarbons escaping into the atmosphere. The efficiency of this method has been found to be very high.

However, the *in-situ* burning of spilled oil is not effective if a considerable amount of time has elapsed after the spill. In such cases, the extent of emulsification is very high. The emulsions that contain high amounts of water cannot be burnt easily. Thus, this method is useful only within the ‘window of opportunity’, which has not yet been defined systematically.

Table 1. Selected Historical Oil Spill Burns (adapted from Fingas M. F., 1998)

Year	Country Location	Description	Major Conclusions
1967	Britain	Torrey Canyon	Cargo tanks difficult to ignite with military devices
1970	Sweden	Othello/Katelysia[1]	Success in burning amongst ice
1975	Canada	Balena Bay-experiment	Demonstrated ease of burning oil on ice
1981	Canada	McKinley Bay-experiment	Noted difficulty in burning emulsions
1983	USA	Beaufort Sea-experiment[2]	Ability to burn in broken ice
1986-91	USA	NIST-experiments	Science of burning, rates, soot, heat transfer
1989	USA	Exxon Valdez[3]	A burn demonstrating practicality and ease
1992	USA	Texas Marsh Burn[4]	Resulted in very little impact on the environment
1993	Canada	NOBE[5]	Oil removal efficiency over 99%. Emission sample analysis showing no major environmental damage.
1994	Norway	Series of Spitzbergen burns	Large area ignition results in burn of emulsions
1996	Britain	Burn Test	Demonstrated practicality of technique
1997	USA	North Slope Tank tests	Waves not strongly constraining on burning
1998	USA	Fifth set of Mobile burns	Emissions measured and booms tested

(1: Chemical Week, 1970; 2: O'Rourke, 1976; 3: Allen, 1990; 4: Gonzalez and Lugo, 1994; 5: Fingas *et al*., 1995c)

The *in-situ* combustion of spilled oil is not the final solution for the oil spill clean up problem. It needs to be followed by removal of the residue. The amount of residue left depends on the burn efficiency, which depends on the surrounding conditions and the emulsion characteristics. Although, the residue needs to be scooped up from the ocean surface, the volume of such residue is often quite low compared to the spill volume. Hence, the *in-situ* burning can be an effective tool for oil spill clean up.

1.4 Challenges in Application of the In-Situ Burning Technique

One of the main factors that determine the success of the *in-situ* burning as an oil spill clean-up technique is the time that has elapsed since the occurrence of the spill. If applied early, the technique may yield a high burning efficiency and ease of ignition. This window of opportunity, within which the *in-situ* burning can be a success, has not yet been defined with sufficient accuracy.

The success of *in-situ* burning as an oil spill clean up technique also depends on the type of oil involved in the spill. During the *in-situ* burning, it is the vapors of hydrocarbons above the slick that burn, not the liquid itself. The temperature at which the oil produces vapors to ignite is called the flash point. A temperature above the flash point at which the oil produces vapors at sufficient rate to support continuous burning is called fire point. In order to burn the oil slick successfully, it must be heated to its fire point. The oils with higher flash and fire point temperatures are more difficult to burn.

The climatic conditions present at the ocean surface, such as wind and the turbulence on the ocean at the time of spill, can significantly affect the effectiveness of this technique. These factors will determine the extent of emulsification and evaporation of the oil. Evaporation of lighter components of crude oil increases the flash and fire point temperatures. This makes ignition and flame spread after ignition more difficult to achieve. Evaporation also helps in emulsification. When water and oil emulsify, small droplets of water are trapped in the continuous oil phase. This type of emulsion is termed as water-in-oil emulsion. Stable emulsions can contain up to 75% of water by volume. For oils with fire points higher than 100 °C, the water in the emulsion must either be boiled off or removed before the oil can reach the fire point. For stable emulsions, the burn rate declines significantly with increasing water content of the emulsion. Compared

to unemulsified slicks, emulsions are much more difficult to ignite, and once ignited, show reduced flame spreading and more sensitivity to wind and wave action. (Buist I. A., 1998). Wind hinders flame-spread in the upwind direction, but helps flame-spread in the downwind direction by bending the flame over the slick to increase the heat feedback from the flame to the slick.

For ignition to occur, the oil must reach its flash point temperature. If the oil slick thickness is small, most of the heat from the igniter or the surrounding fire is lost to the water body underneath. Thus, thin slicks are difficult to ignite and sustain the burning process. The minimum thickness required to cause ignition and sustain the fire depends on the oil type, the amount of evaporation and the extent of emulsification. It ranges from 1 mm to 10 mm. (Buist I. A., 1998). As the fire consumes the oil, the slick starts to thin out. When the slick thickness falls below the minimum thickness, the heat loss to the water layer makes it difficult to produce oil vapors at sufficient rate to sustain combustion and the fire extinguishes, leaving unignitable residue behind.

1.5 Outline of the Thesis

The focus of the present is research is to understand the processes involved in the *in-situ* burning of the oil spills. A new technique to achieve successful combustion of water-in-oil emulsions floating on top of the water surface is proposed and validated. Data from laboratory scale experiments for three oils are presented. A mathematical model is developed to predict various important characteristics of emulsion pool fires, such as total burn time, thickness of the residue left, and average burn rate. Using the experimental data, the model is validated.

Chapter 2 describes the state of the art in the field of *in-situ* combustion of oil spills. The entire process of *in-situ* burning is divided into three stages, viz.: before, during and after the combustion. Efforts from various researchers in these fields are summarized and key findings of these efforts are presented. Based on the review of the literature, motivation for the work presented is discussed.

Chapter 3 presents the overall goals of the project. The chapter also lists the specific objectives of the present work. Background and description of the new technique

proposed to expand the applicability of *in-situ* burning as an oil spill clean up technique is presented in this chapter.

A detailed description of the mathematical model developed is provided in chapter 4. To create the mathematical model, description of the physical processes occurring during the emulsion combustion was developed. Based on this description, some simplifying assumptions were made. The numerical scheme used to solve the model is described. Preliminary validation of the model was achieved by comparing the model predictions with an analytical solution of a simplified one-dimensional conduction problem.

A detailed description of the experimental investigation is described in chapter 5. Designs of the apparatus used are discussed along with the schematic representations of the apparatus. A detailed description of the experimental procedure is also provided in this chapter.

Chapter 6 presents data from laboratory scale pool fire experiments of diesel-water emulsions. The tests provided validation for the proposed technique. The data from these tests were also used to validate the mathematical model. Analysis of the results from these tests is also presented.

Experimental data for two crude oils and the predictions from the model for the two crude oils are presented in chapter 7. Analysis of the results presented is also provided.

Chapter 8 summarizes the work presented. Conclusions and recommendations for future work are also presented in this chapter.

Chapter 2

REVIEW OF OIL SPILL COMBUSTION STUDIES

2.1 Background

In-situ combustion of oil or water-in-oil emulsion, supported on top of a water-base, is a complex process. It may be examined in three stages -- before, during, and after the actual combustion. Spreading and emulsification of oil prior to combustion strongly influence the ease of ignition, the rate of burning, and the oil removal efficiency. Surrounding physical conditions, including wind velocity, waves, and the presence or absence of a containment device, such as a fire boom, determine continuation of the combustion process. The resulting smoke, residue, and aquatic toxicity should be within the acceptable limits for the clean up measure to be a success. In the past, researchers have studied various aspects of the process of *in-situ* combustion of spilled oils. An overview of these efforts is presented in this chapter.

2.2 Pre-Combustion Considerations

As soon as the oil spills on water, it starts spreading. For small amounts of oil spilled onto clean water, it was found that the surface tension effects dominated the initial spreading. If large amounts of oil are spilled even onto previously oiled surfaces, the spreading occurs by gravity inertial mechanisms (Brown and Goodman, 1995). The oil layer thickness decreases as it continues to spread, and a continuous film of oil as thin as 0.01 mm to 0.1 mm may be formed by light crudes and 0.05 mm to 0.5 mm by heavy crudes (Fingas and Laroche, 1990). Most of the crude and refined oils, depending on the type of oil, will burn on water if the layer thickness is at least 1 mm to 3 mm. Oil layers thinner than a critical thickness will cause excessive heat loss to water and leave either insufficient energy to pyrolyze the oil or cause boilover of water under the layer (Arai *et al.,* 1988). Thus, spreading dynamics are important when considering the implementation of oil spill combustion as a clean up countermeasure.

Mackay *et al.,* (1980) modeled the spreading of the spilled oil on the ocean surface. The model was based on the works of Fay (1969) and divided the spreading of the oil into thin and thick slicks. It then predicted the evolution of each type of slick as a function of time. The spreading of thin slicks was considered to be mainly a surface tension phenomenon, while the spreading of thick slicks was due to gravity and viscosity. Mackay *et al.,* (1980) assume that the thin slick is of constant thickness (1 μm), and as it spreads, it draws oil from the thick slick. Garcia-Martinez *et al.,* (1996) suggested corrections which include physical properties of oil and water in the model, in place of constants suggested by Mackay *et al.,* (1980).

Crude oils contain various hydrocarbons. As the oil is spilled and exposed to the surroundings, the lighter hydrocarbon fractions of the oil start evaporating. Evaporation is a very important process for most of the oil spills. The loss of the lighter fractions from the crude oils makes ignition and flame spread harder to achieve. In a few days, light crude oils can be reduced by as much as 75% of their initial volume, and medium crude oils by as much as 40% of their volume due to evaporation. Temperature and time are the two most important parameters in this regard (Fingas, 1994). As the lighter components of oil escape, the emulsifiers --asphaltenes, resins and waxes --which are present in oil and are soluble in lighter components of oil, precipitate out and aid emulsification (Bobra, 1992).

Stiver and Mackay (1984) proposed an analytical approach to model the rate of evaporation of oil. In this model, the oil is treated as a single substance with a vapor pressure that varies with the fraction evaporated. This model requires the slope of the distillation curve, which may not be available for many oils. Another approach to the evaporation modeling is the so-called pseudo component modeling. In this approach the oil is modeled as a mixture of a number of components. Each component is characterized by a mole fraction and a vapor pressure. The total evaporation rate is set equal to the sum of the evaporation rates of the components (Jones 1997). Fingas (1996) tested approximately sixty oils and petroleum products to study the rate of evaporation as a function of temperature and time. The analysis showed that the percentage of oil evaporated by mass varied with time as either a logarithmic or a square root function of

time. Best-fit equations were suggested for both types of oils. For the oils that followed logarithmic relationship,

Percentage evaporated = [0.165(%D) + 0.045(T-15)]ln(t).

Where as for the oils that followed the square root relationship,

Percentage evaporated = [0.0254(%D) + 0.01(T-15)] $\sqrt{t}$.

Here *% D* is the percentage weight of the oil distilled at 180 °C, T is the temperature in °C, and *t* is time in minutes. With the high correlation of the distillation data and the evaporation data it was suggested that evaporation, like distillation, is largely governed by intrinsic oil properties, rather than environmental properties such as the boundary layer factors.

Oil starts forming emulsion with water in a matter of a few hours. Formation of water-in-oil emulsions (water droplets trapped in continuous oil phase) is one of the major difficulties in the clean up techniques of oil spills, including *in-situ* burning. Under some conditions, water-in-oil emulsions can form rapidly and contain up to 80% volume of water. The rate of formation and the stability of these emulsions are dependent on prevailing sea conditions and on the physical and chemical properties of oil. As discussed earlier, evaporation of the lighter fractions from the crude oil increases the rate of formation and the stability of the emulsions. One of the most important characteristics of emulsion is its greatly enhanced viscosity compared to oil or water.

To form a water-in oil emulsion, the interface between oil and water must be broken. This allows small droplets of water to enter the continuous oil phase. If the droplets are small enough that the surface tension forces between the oil and water can hold them in the oil phase, a stable water-in-oil emulsion is formed. Fingas *et al.*, (1998 and 2000a) presented summarized results from studies to determine the stability of the water-in-oil emulsions. They classified the water-in-oil emulsions of about 100 oils into three main categories: stable, unstable and meso-stable. Unstable emulsions are formed when the oils have very high viscosity (over about 50000 mPa s) or very low viscosity (under about 6 mPa s) and when resins and asphaltenes are less than about 3%. The authors have summarized the salient points from the recent literature in this field to be:

1. Stable and less stable emulsions exist.

2. Emulsion stability results from the viscoelastic films formed by asphaltenes at the oil water interface.
3. Asphaltenes produce more rigid films than do resins.
4. Water content does not appear to correlate directly with stability; however, very low or very high water contents (<50% or >90%) are not found to form stable emulsions.
5. Most researchers use visible phase separation to classify emulsion as stable or unstable, and most concede that this is not an optimal technique.

Fingas *et al.,* (2000b) studied the energy and work threshold required to form stable emulsions. Their studies showed that although a minimum energy threshold is necessary to start the process of emulsification, the work (energy expended over time) threshold is what determines the stability of the emulsion.

To ignite a layer of oil or emulsion floating on top of water successfully, the layer must have some minimum thickness. The minimum slick thickness required for igniting various oils are: 1 mm for fresh crude, 3 mm to 5 mm for evaporated crude oils and light diesels; and, up to 10 mm for residual fuel oils (Buist and McCourt 1998). The reason that these thicknesses are required is heat loss to water. Sufficient heat is required to vaporize the oil for continued combustion. For very thin slicks, most of the heat from the igniter is lost to the water and combustion is not sustained. As the oil is spilled on an ocean surface, the oil starts to spread, thus forming a very thin layer. In order to burn the oil or emulsion layer efficiently, the oil or emulsion needs to be corralled to form an ignitable thickness of the slick. The use of a fire-resistant containment boom is the method most often proposed for maintaining the necessary, minimum slick thickness. For a successful burn to take place, the boom must be capable of withstanding the fire exposure while containing the oil. Failure of the boom due to extreme heat often results in leakage of oil, thus reducing the effectiveness of the burn. Bitting and Coyne (1997) have reported detailed oil collection performance data on five commercially available booms that were tested. The data were collected without fire and were meant to provide guidance in determining the tow speeds. McCourt *et al.,* (1997) have presented the description of the state of the art in the boom technology. Efforts currently underway to

standardize the testing of the fire resistant containment boom by the American Society for Testing and Material (ASTM) F 20 committee are summarized by Walton (1998).

In order to burn the emulsified oil, the two phases, oil and water need to be separated. The breaking of emulsions can be achieved by chemical agents, sometimes referred to as demulsifiers or emulsion breakers, and heat (Strom-Kristiansen *et al.*, 1995). The stability of a water-in-oil emulsion and its response to an emulsion breaker and heat depend on the chemical composition and the physical properties of the oil from which it is formed. Extensive studies on the properties of emulsion, emulsification process, initial dynamics and combustibility of emulsions have been carried out (Lewis and Walker, 1995; Bobra, 1992; Fuji, 1995; and Buist *et al.*, 1995).

If the oil layer thickness, degree of emulsification, weathering and surrounding physical conditions (such as wind velocity and waves) are suitable, the spilled oil may be ignited. Use of appropriate igniters and ignition methods is necessary to initiate sustained *in-situ* combustion of spilled oils. To ignite heavy oils, longer heating times and a hotter flame are required compared to lighter oils. Typical methods used for ignition in field experiments have been pyroid igniters, Dome igniters, laser igniters, and Helitorch igniters with gelled gasoline. The “Dome igniter”, developed by Dome Petroleum, is a relatively simple device consisting of cans and propellants having a burn time of approximately ten minutes (Allen and Simpson, 1986). The pyroid igniter was developed by Environment Canada and the Canadian military. After pulling on a firing pin which strikes a primer cap, a 25-second delay allows for manual tossing and setting on the oil slick surface of the igniter. The flame from the edge of the igniter lasts for two minutes (Allen and Simpson, 1986). Attempts to develop a laser ignition device have also been made. A device called “Helitorch” is also used for the purpose of ignition. It is a helicopter-slung device that distributes packets of burning, gelled fuel. Typical burning globules have a burning time of four to six minutes (Evans and Walton, 1989). Gelled crude oil was found to be a better igniter than gelled gasoline (Guenette *et al.,* 1995a). The combination of gelled gasoline and crude oil has also been found to be effective for the ignition of weathered crude emulsions (Buist *et al.,* 1995). Guenette *et al.,* (1995b and 1997) developed and tested a new type of igniter design. The igniter is designed to burn

the stable water-in-oil emulsions by using a mixture of gelled fuels (gasoline, diesel and Bunker C oil) and an emulsion breaker (Alcopol 060). The igniter, called the emulsion breaking igniter, differs from the so-called break and burn approach (i.e. breaking of the emulsion by use of the emulsion breaker prior to the burn, and then applying the igniter to initiate the burn) in that it offers a single step approach to ignition by both breaking and igniting a stable slick of water-in-oil emulsion in one step.

Lab studies show that ignition delay increases with the evaporation of lighter components and water content of the emulsion (Buist *et al.,* 1995). In 3 m diameter pool spill experiments, the ignition delay was found to be directly proportional to the square root of spill volume. Ignition time for evaporated oils was found to be less than 90 seconds and was not affected by slick thickness while emulsions of fresh crude ignited in 25 seconds. Demulsifiers were found to enhance ignition and flame spread. The minimum ignitable thickness for emulsions tended to be greater than that of water-free oil slicks (in the range of 5 mm to 10 mm). Sensitivity of emulsion burning to wind is also more than that of water-free oil burning. A guide for ignition of weathered and emulsified fuels was presented by Putorti *et al.,* (1994), using measured ignition characteristics of diesel pools of various sizes.

2.3 Combustion of Spilled Oil

Once the oil or emulsion layer is ignited, sustained burning can be achieved if energy feedback at the surface is at least equal to the heat losses to the surroundings and to the interior, and to latent heat of vaporization. Typically, the oil layer thickness reduces at a rate of approximately 2 mm/min (for heavy crudes) to 3 mm/min (for lighter oils) (Three mm/min is approximately 0.07 gal/min.ft^2, 4100 L/day.m^2, or 100 gal/day.ft^2.). With increasing emulsion water content, the rate of oil removal by burning decreases. An increase in water content from 0 to 25% by volume reduces the oil burn rates by 1/3 to 1/2 for oils that form stable emulsions. By increasing the water content to 50% by volume, the oil removal rate is reduced further by a total of 1/2 to 1 (i.e. no burning). It should be noted that the *in-situ* burning of some oils that form emulsions does not appear to be greatly affected by water content as noted above (Buist and McCourt, 1998). The burn rate decreases during the final stage due to the increased rate of heat sink to water

substrate. However, the burn rate does not vary significantly with different oil types, degrees of weathering and water content (Fingas, 1990).

The mechanism of water-in-oil emulsion combustion is far more complex than oil combustion. It has been postulated that it is not the emulsion that burns; rather a layer of oil separated out of emulsion and floating on top of emulsion that burns (Guenette *et al.*, 1995a). Thus, the controlling factor in emulsion burning is the rate of removal of water. This can be done either by breaking the emulsion (especially for unstable emulsions) or boiling it out (emulsion must reach about 100 °C). In an extensive experimental study on liquid fuel layer combustion on water, Inamura *et al.,* (1992) estimated that a considerable amount of heat could be "lost" to the water via in-depth radiation absorption and conduction, making the water boil, breaking through the oil layer, and affecting the oil combustion. In the case of emulsions, water present in the emulsion layer also may boil away, making the process very complex.

Some observations of emulsion burning reveal that:

1. Incident heat helps separate water and oil in emulsion (Strom-Kristiansen *et al.*, 1995).
2. When water content exceeds 25%, the emulsion is difficult to ignite (Buist *et al.*, 1995).
3. For a stable emulsion, water must be removed by boiling before igniting.
4. Emulsions above 50% can be successfully ignited and burned only if demulsifiers are introduced in the emulsion (Guenette *et al.,* 1995).
5. Burn efficiencies with emulsions, even with water content as high as 50%, are in excess of 90%.
6. Emulsions under certain conditions show a peculiar behavior of combustion characterized by flashing and then extinguishing over a large surface in a repetitive manner (Buist *et al.,* 1995).

The efficiency of burning is the percentage of the original oil that is removed by burning. As there are finite heat losses to the water surface, the burn efficiency is always less than 100%. Experiments on small, as well as large, scales have revealed that well over 90% and often more than 99% of the oil can be burnt. For example, the burning

efficiency in the recent large scale NOBE (Newfoundland Offshore Burn Experiment) was found to be over 99% (Fingas *et al.*, 1995) and in the case of the Exxon Valdez oil spill, the burning efficiency was over 98% (Allen, 1990). Burn efficiency decreases with increasing water content and evaporation (Buist *et al.,* 1995). Important to note is that the efficiency is strongly dependent on the initial thickness of the emulsion, since the final thickness is governed by the heat loss mechanisms that cause the extinction of the fire. The dependence of the efficiency on the initial emulsion layer thickness is discussed in detail in chapter 6.

The oil spill combustion is unsteady when the burning oil spreads and also when the flames advance over a relatively stagnant oil layer. If the spill area is ignited at its periphery, the flames spread outward with the burning oil, and inward over the oil aided by the fire-induced air convection (Buist *et al.,* 1995). Flame spread alone accounted for a rate of approximately 1 m/min on a four-hour aged Alberta Sweet mixed blend with 0.25 m/s wind. Flame spread rate over fresh crude was approximately four times faster than the weathered oil. It was also found that the spread rate on 38%-evaporated oil was very slow, and almost zero on 40% water-in-oil emulsion. The burning oil was found not to spread significantly faster on water than the cold oil. Flame spread almost always keeps up with the spread of oil. The other unsteady combustion phenomenon observed on burning emulsion exhibited a very peculiar behavior of intermittent flashover and extinction of the fire. It is believed to occur because the rate of water-free oil layer production may be less than the rate of oil removal by burning, or this can be due to foaming of the emulsions (Buist *et al.,* 1995).

The key mechanism for a sustained combustion of the oil or water-in-oil emulsion layer (the fuel) on water is the energy balance at the surface. If sufficient energy from combustion is fed back to the fuel layer, the evaporation and pyrolysis of fuel continues; if excess energy is available from combustion, flame spread and more intense burning occurs; and if sufficient energy is not available, the fire extinguishes. Thompson *et al.* (1979) proposed a simple energy balance for the oil layer burning on top of water,

$$Net\ Energy = 0.02\ Q_{com} - Q_{Lo} - c_{po}\ (T_{ov} - T_o). \qquad (1)$$

This equation assumes that 2% of heat of the combustion is returned to fuel in order to compensate for the heat of evaporation and sensible heat. Since crude oils have several components (light and heavy) which have a range of vaporization temperatures *(T_{ov})*, the Net Energy can be positive, negative, or zero for the individual components. From a sustained combustibility point of view, crude oils were categorized as:

1. Most combustible in the form of an oil slick: Over 67% of crude oil components by volume have a positive Net Energy.
2. Moderately combustible: Between 40% and 67% of crude oil components by volume have a positive Net Energy.
3. Not combustible: Less than 40% of crude oil components by volume have a positive Net Energy.

The above energy balance provides a practical approach to classifying fuels and has some scientific basis. However, a more detailed energy analysis is needed to predict ignition and burning rate accurately under specific conditions, such as the one proposed by Putorti, (1994). He made a transient analysis of surface heating of viscous oils under external radiation flux under three conditions at the surface; no heat loss, radiation heat loss, and convective heat loss. It was found, after comparing the results to experiments, that the heat transfer at the surface is dominated by the convective loss, and a proper accounting of such loss allows for an accurate prediction of ignition.

Once the oil layer is ignited, the sustained burning rate can be determined by examining the energy transfer processes at the surface at a steady state. A detailed analysis of combustion of oil-emulsion layer was presented by Guenette *et al.*, (1994) which was based on the work of Brzustowski and Twardus (1982). The burn rate for oil emulsions was given by:

$$r = \frac{q''_{\mathrm{r}} - U_o \Delta \mathrm{T}}{\rho_{\mathrm{o}} \Delta \mathrm{H}_{\mathrm{v,o}} + \rho_{\mathrm{O}} C_{p,o} \left(\mathrm{T_e} - \mathrm{T_o}\right) - \rho_{\mathrm{w}} \Delta \mathrm{H}_{\mathrm{v,w}} \mathrm{f_w} / \left(1 - \mathrm{f_w}\right)} \qquad (2)$$

where $f_W(t)$ is the fraction of water in emulsion at time t, U_O is the overall heat transfer coefficient, and ΔT is the average temperature drop across the slick. This is a steady state, zone model that allows computation of burning rate based on averaged quantities.

Putorti and Evans (1994) performed transient analysis of surface heating of viscous oils under external radiation flux, under three heat loss conditions at the surface. The model comprised of the following governing equation:

$$k_o \frac{\partial^2 T}{\partial y^2} + (1 - C_o) q \beta e^{-\beta y} = \rho C_p \frac{\partial T}{\partial t} \quad . \tag{3}$$

The model was limited to a pure oil layer floating on water receiving incident radiant heat flux. Ignition delay was computed under various heat flux conditions. It was concluded, after comparing the results to experiments, that the heat transfer at the surface is dominated by convective loss at the surface, and its proper accounting allowed a better prediction of ignition time.

Wu *et al.,* (1997) used a transient solution for the flame spread velocity *(V_f)* for a one dimensional conduction problem with time varying externally imposed heat flux, $\dot{q}_e''$. The integro-differential equation (Quintiere, 1981) for the flame front position was given by:

$$T_{ig} - T_i = \frac{\dot{q}_f''}{h} \frac{2}{\sqrt{\pi}} \sqrt{\frac{a \delta_f}{V_f}} \left(1 - \frac{\sqrt{\pi}}{2} \sqrt{\frac{a \delta_f}{V_f}} \right) + \frac{\sqrt{a}}{h\sqrt{\pi}} \int_0^t \frac{\dot{q}_e''}{\sqrt{t-s}} ds$$

$$- \frac{a}{h} \int_0^t \dot{q}_e'' e^{a(t-s)} erfc\left(\sqrt{a(t-s)} \right) ds \, . \tag{4}$$

Here $\dot{q}_f''$ is the flame heat flux, δ_f is the region with uniform heat flux from the flame, s is the temporary variable used for integration, $a = \alpha (h/k)^2$, T_{ig} is the ignition temperature and the flame spread velocity is defined in terms of flame front position x_f as $V_f = \frac{dx_f}{dt}$. Using this expression, combustion of fuel on water base was analyzed by dividing the process into three parts, viz. ignition, flame spread and extinction. Equation 4 was simplified by assumptions that characterize each of these three parts. They also extended the work of Arai *et al.,* (1990) and Garo *et al.,* (1994) to obtain an expression for average regression rate using a one-dimensional, two-layer conduction model. These models, however, do not predict the burning of emulsion, as they do not account for any emulsion breaking mechanism.

To achieve efficient removal of emulsion from ocean surface, once the ignition takes place on one region of the emulsion pool, the flame must spread to the adjacent regions till the entire emulsion pool is ignited. Winds and waves on the ocean surface affect the rate at which the flame spreads. Short waves, in general, do not affect the ignition of emulsion drifting in the burning region. However, swells of the order of 30 cm high and 3 m long can reduce the burn efficiency and make ignition impossible. Heat radiated from fire could ignite emulsions with 50% water in a current of 0.3 m/s and waves 15 cm in height (Guenette *et al.,* 1995). The mid-scale burn tests have shown that oil and emulsion slicks of Alaska North Slope crude oil and Milne Point crude oil could be successfully burned in waves. Increasing wave steepness (or wave energy) appeared to have reduced both burn rates and burn efficiencies of the unemulsified oil slicks. For emulsified slicks, increasing wave steepness did not appear to appreciable affect the oil burning rates, but did reduce the oil removal efficiencies (Buist *et al.,* 1998). Air temperature (-11 ^{o}C to 2 ^{o}C), water temperature (-1 ^{o}C to 17 ^{o}C) and ice coverage were shown to have negligible effect on the burning of oil. It was found that for wind over 30 knots, the fire would not spread; however, at higher wind speeds the fire continued in windward direction.

Under certain conditions, the water sublayer starts boiling, penetrates the fuel layer and ejects water drops into the surroundings. This is the boilover phenomenon (Arai *et al.,* 1990). An oil layer that is thinner than a critical thickness will cause excessive heat loss to water and leave either insufficient energy to pyrolyze it, or cause boilover of water, under the layer. If the oil layer is sufficiently thin, the heat from the combustion is absorbed by the water body underneath the oil layer, causing boilover of water. The boiling water beaks out through the oil layer, carrying with it droplets of oil which burn above the surface. To maintain a sufficient thickness of oil layer, a practical consideration is to contain the oil in an area restricted by the boom, vessel, shoreline, ice or other means, so that it does not spread itself too thin (Allen and Simpson, 1986). Since booms are portable, there is considerable interest in developing fire-resistant booms for the containment of oil slick.

2.4 Post-Combustion Considerations

A large amount of research has been carried out in the field of emissions from the *in-situ* fires. Polyaromatic Hydrocarbons (PAHs) are found to be lower in the soot than in the starting oil and are consumed by the fire to a large extent. The burn products are typically CO_2- 75%, water vapor- 12%, soot- 10%, CO- 3% and other products including PAHs- 0.2% (Tennyson, 1994).

A series of tests was conducted in 1994 and 1998 to study emissions from diesel oil burning *in-situ*. Extensive sampling and monitoring were conducted to determine the emissions at various downwind, upwind and side ground stations, as well as in the smoke plume using a remote controlled helicopter. The results indicated that the burns produced an abundance of particulate matter. PAHs in the soot and residue were found to be lower than those in the starting oil, although higher concentrations of the larger molecules PAHs were found in the soot and residue. Particulates in the air were found to be greater than the recommended exposure levels, only up to 100 m downwind at the ground level. Combustion gases such as carbon dioxide, sulphuric acid aerosols, sulphur dioxide and carbon monoxide were very low and did not reach exposure level maximums. Volatile organic compound emissions were measured, and more than 100 compounds were identified and quantified. Most concentrations were too low to be considered a health risk (Fingas *et al.*, 2000c and Fingas *et al.*, 1996). A summary of literature on soot production during *in-situ* burning of oil is presented by Fraser *et al.*, (1997).

Perhaps the most extensive aquatic and air pollution studies conducted on large-scale oil spill combustion were in NOBE (Newfoundland Offshore Burn Experiment) in 1993 (Daykin *et al.*, 1995; Fingas, *et al.*, 1994). Smoke measurements and air sampling were done using miniblimp and helicopter deployed instrumentation (Walton *et al.*, 1994 a, b). It was found that up to 150 m downwind at ground level, emissions were of concern; however, beyond 500 m, they were negligible. Large eddy simulations of the smoke trajectory from this and other experiments have been done with success (McGrattan *et al.*, 1994; Baum *et al.*, 1994).

The work conducted until now has not shown any serious air pollution problems from the oil spill combustion emission. The most damaging pollution in an oil spill

occurs when lighter compounds are evaporated from the spill. The laboratory test burns have indicated that residues from thick, batch type *in-situ* burns of heavier crude oils will sink. The research on the aquatic toxicity has revealed very little, if any, toxicity from the oil burn.

2.5 Summary of the Literature Survey

An extensive survey of the literature in the field of *in-situ* burning of spilled oil shows that this is a promising technique for oil spill clean up operation. When feasible, *in-situ* burning offers a very high rate of oil removal from the ocean surface. The technique is shown to be cost effective as compared to the mechanical recovery of spilled oil.

The success of *in-situ* combustion as an oil spill clean up technique depends on various factors. The initial spreading, evaporation and emulsification of the spilled oil are very important. Thin, highly emulsified and evaporated oil slicks are known to present difficulties in achieving ignition. The type of the oil spilled and climatic and ocean conditions are the key factors that determine the spreading and weathering of the oil. The amount of time elapsed since occurrence of the spill is also important in determining the success of ignition. Use of demulsifying agents and the choice of appropriate igniters are also crucial to the success of ignition. Creating thick slick by use of fire resistant booms is an effective way to ignite thinly spread oil slicks.

After the ignition of the oil slick is achieved, the effectiveness of the burn is decided by the fraction of the oil that is consumed during the burn. *It is postulated that it is the oil that burns and not the emulsion itself, after the emulsion separates into oil and water*. Hence the removal of water from emulsion is a key to effective emulsion burn. Spreading of the flames is also essential to achieving high efficiency of burn. The type of the oil spilled, the extent of emulsification of the oil, evaporation of the oil, ocean conditions such as steepness of the waves, and climatic conditions such as wind speed, are some of the most important factors that determine the efficiency of the burn. Emulsion continues to burn until the heat feedback from the fire to the emulsion pool surface continues to break emulsion and produce oil at sufficient rate to sustain combustion. As the emulsion layer thins out, the heat loss to the water under the emulsion

layer becomes excessive. Experiments have shown that burn efficiencies in excess of 95 % are possible to achieve. This makes the *in-situ* burning a very attractive technique for oil spill clean up operations.

Smoke emanating from the oil spill combustion has caused concerns about the harmful environmental effects of this technique. A large amount of research has been conducted in the field of emissions from the emulsion pool fires. The results show that the emissions at ground level about 500 m downwind of large scale experimental fire were not of any concern. Studies of residue and aquatic toxicity have also not revealed any cause of concern.

Chapter 3

MOTIVATION AND OBJECTIVES OF THE PRESENT WORK

3.1 Motivation for the Thesis

An examination of the past research efforts in the field of *in-situ* oil spill combustion shows that the focus in the past has been primarily on solving immediate practical problems.

Extensive studies by Buist and McCourt, 1998, Bech *et al*., 1992, and Guenette *et al.*, 1994 have shown that emulsions containing more than a certain amount of water do not burn. Unburnable slicks of emulsion are reported to have water content ranging from as low as 20% to 30% for extremely weathered oils that form stable emulsions, to as high as 70% for less weathered oils that form less stable emulsions. This maximum possible water fraction in an emulsion that can be burned depends on various factors, including the oil type and the degree of weathering the oil undergoes. Also it is reported that the use of emulsion breakers to aid the ignition of emulsions often does not extend the maximum ignitable water content for emulsions of a given type of oil (Buist *et al.*, 1998). Thus, emulsification and weathering are some of the key factors that limit the scope of application of *in-situ* burning as an oil spill clean up technique. Therefore, in order to achieve effective clean up, the spilled oil must be burned within a narrow window of opportunity defined by degree of emulsification and degree of weathering. *Expanding this window of opportunity was one of the main motivations behind this thesis work.*

In order to expand the window of opportunity for application of *in-situ* burning as an oil spill clean up technique, a fundamental understanding of the processes involved in burning of water-in-oil emulsions floating on top of water surface must be developed. Based on this understanding, a technique can then be developed to create conditions suitable to cause a successful burn for a given oil spill.

To decide whether *in-situ* combustion will be an effective clean up technique, and to plan clean up using *in-situ* combustion for a given situation, it is essential to be able to predict various parameters of the *in-situ* combustion technique before its application. With the information about the type of oil spilled, the time that has elapsed since the spill

and the conditions at the location of the spill, a tool should be designed that will predict the types and number of igniters to be used in order to initiate the burning, the time the burn will continue, for and the amount of residue that will be left on the ocean surface after extinction. Such a tool can be developed by mathematically modeling the processes occurring during the oil spill combustion. The mathematical model developed in the present study can serve as a first step towards this goal.

3.2 Objectives of the Thesis

The basic goal of this project is to develop an understanding of the nature of the processes that occur during the emulsion combustion on top of the water surface, and use this understanding to suggest a new technique that will expand the applicability of *in-situ* combustion to emulsion slicks that are considered to be unburnable.

It has been known in the field of fire research that several materials, such as most woods and certain plastics, do not sustain fire on a small scale unless assisted by external heat flux. A large fire returns a significant amount of heat back to the burning area and also to the yet-to-be–ignited area, allowing fire to sustain and spread. Prior work shows that when a material (normally incombustible in the absence of external heat flux) is subjected to a minimum (also known as threshold or critical) heat flux, it can be ignited, and a sustained fire and flame spread can be achieved (Brehob and Kulkarni, 1998). In the present work, this principle is applied to the oil spill and emulsion combustion problem, so that, if successful, the window of opportunity for *in-situ* combustion of emulsions can be widened.

The important question one may ask is, how can an emulsion pool be subjected to external heat flux when it is floating on an open water body? Among other possibilities, it is proposed here that the external heat flux may come from an adjacent pool fire. As shown in Figure 1, a small pool fire will not produce sufficient heat flux, but if the pool size is sufficiently large, it will provide the needed heat flux for the surrounding emulsion to ignite and burn. This will make the pool size and fire size grow, providing an even larger heat flux to the yet-unburned emulsion around the pool, and causing the mixture to ignite and continue to burn, and the process will continue. Thus, the emulsion layer, that was considered incombustible, can now be burnt with this technique.

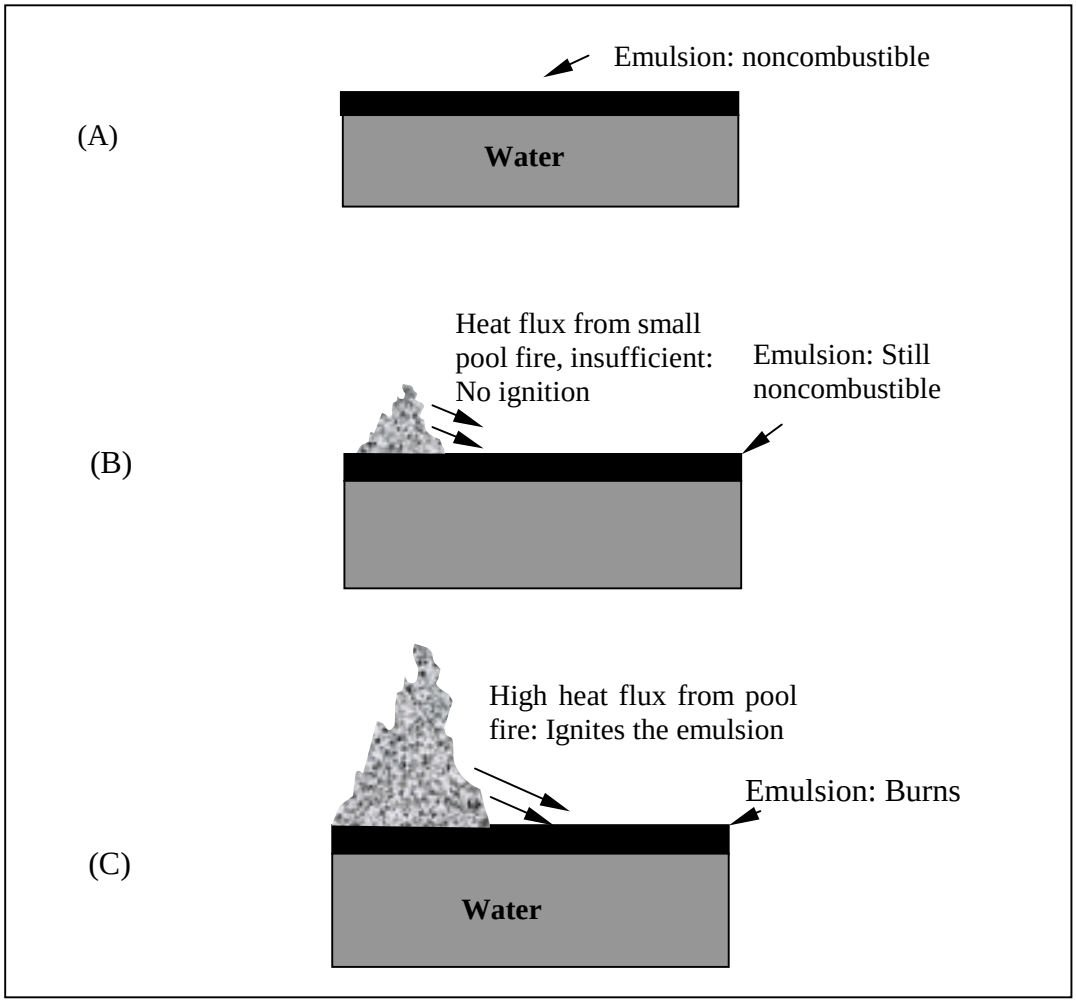

Figure 1 A noncombustible oil-water emulsion (A) can not be ignited with heat flux less than the threshold heat flux value (B), but it may be ignited with high heat flux from an adjacent pool fire of sufficiently large size (C).

The initial pool fire of desired size might be achieved by one of several different means, such as, intentionally starting a fresh oil fire, using a special large size igniter, using artificial external heat flux, etc. Correlation of the radiant heat flux to the surrounding area as a function of the fire size depends on the type of fuel and other factors, such as how much soot the flames have and the height of flames. Heat feedback from a known size of pool fire to its base has been modeled (see, for example, Tien, 1985, Khater *et al.,* 1990, Hamins *et al.,* 1994), and measured for large fires (see, for example, Yamaguchi and Wakasa, 1986).

In order to use the new technique described above to widen the window of opportunity for *in-situ* combustion of emulsions, we must first validate the technique and then quantify the threshold or critical heat flux necessary to cause sustained burning of emulsion slick as a function of oil type, water content of emulsion and degree of weathering. Also, a tool that can predict various characteristics of the emulsion pool fires such as ignition delay, burn rate, and burn efficiency needs to be developed. A mathematical model of the processes involved in combustion of water-in-oil emulsion floating on top of the water surface is needed to develop such a tool. Thus, the specific objectives of this thesis are as follows:

1. To verify that there exists a threshold or critical heat flux value that is necessary to cause sustained combustion of the emulsion slick for each type of emulsion.
2. To quantify the threshold or critical heat flux necessary to cause sustained burning of emulsion slick as a function of oil type, water content of emulsion, and degree of weathering.
3. To develop and numerically solve a mathematical model describing some of the most important physical processes involved during combustion of water-in-oil emulsion floating on top of the water surface.
4. To validate the mathematical model by laboratory scale experiments.
5. To study the effects of various factors such as type of oil, degree of weathering, water content of emulsion and initial thickness of the emulsion slick on important characteristics of the emulsion pool combustion such as ignition delay, average burning rate, total duration of the burn, thickness of the residue left, and overall burn efficiency.

To validate the technique proposed and to quantify the threshold heat flux data, laboratory scale experiments were conducted. These experiments were designed, set up, and conducted in order to:

1. Evaporate lighter fractions of crude oils and reduce the oil volume by predetermined amount,
2. Prepare oil emulsions of different types and composition,
3. Measure certain properties of the emulsion which are needed as input to the mathematical model and currently not available in literature (such as minimum external heat flux necessary for ignition and sustained fire), and
4. Study the combustion of those emulsions and record various emulsion pool fire characteristics under controlled conditions for comparison with the model predictions.

These experiments provided information about emulsion pool fire characteristics, such as the minimum heat flux required to generate a sustained fire for an emulsion pool fire, the effectiveness of burning in terms of the residue left after extinction of the fire, and average burning rate and interdependence of these characteristics. Effects of the extent of emulsification, weathering, and type of oil on the above-mentioned characteristics were also studied. The experiments were conducted on emulsions with water of three different oils. They were the commercially available Diesel oil, Alaska North Slope crude oil, and Milne Point crude oil. The data from the experiments were then used to validate the mathematical model.

To predict the applicability of the *in-situ* combustion technique, a mathematical model that considers various factors affecting the combustion of water-in-oil emulsions was developed. The model uses the oil properties and the emulsion characteristics, such as the water percentage present in the emulsion and the surrounding conditions as input data. Some assumptions are made to simplify the effort. The mathematical model is solved numerically using finite difference method. The solution is programmed, in Fortran, to study the effects of important controlling parameters on characteristics of the oil spill combustion. This model is able to predict the total duration of burn, the rate of burning, the thickness of the residue left, and the burn efficiency for a particular case of

oil spill. The model predictions were verified by the laboratory scale experimentation described above.

Some of the factors such as wind, ocean turbulence, water temperature, etc. were not considered in this study. These factors are known to affect the emulsion pool fire characteristics significantly. Hence there is a need to continue this work further to investigate the effects of these factors on emulsion pool fires.

The mathematical model accounting for some of the most important physical processes occurring during combustion of emulsion layer floating on the top of ocean surface is presented in the next chapter.

Chapter 4

MATHEMATICAL MODEL

4.1 Physical Model

Combustion of an oil emulsion layer floating on top of a body of water is a complex phenomenon. The *in-situ* burning of water-in-oil emulsions floating on top of a water body involves several different processes as compared to the burning of unemulsified oils. Mathematical models are available in the literature for oil pool fires but not for emulsion pool fires. The basic premise of this model is that it is not the emulsion, per se, that burns, but rather the oil that evaporates and burns. Therefore, to cause ignition, the emulsion must first separate into water and oil. It is the layer of oil floating on top of the emulsion that burns. This model incorporates the separation of emulsion into water and oil, a phenomenon that governs the emulsion pool fires.

We will first describe the physical processes that occur during the *in-situ* burning of water-in-oil emulsions floating on top of water surface. Heat is transferred from a source, such as an igniter or adjacent fire, to the emulsion. As the emulsion heats up, it separates into water and oil. The breaking of emulsion into water and oil can occur in two ways: by boiling off the water contained within the emulsion and by reduction of the surface tension force between the oil and the water as the emulsion heats up. Both of these processes may be present simultaneously (Buist *et al.*, 1998). When the emulsion is heated, the surface tension between the entrapped water droplets and the continuous oil phase decreases because of increasing temperature. As the surface tension forces fall below a certain level, the water droplets cannot be held in the oil phase any longer. Thus these droplets coalesce and form bigger droplets that drop out of the emulsion, thus creating an oil layer that floats on top of the emulsion. For some emulsions, however, the emulsion temperature may reach around 100 °C before the thermal separation of emulsion into oil and water can occur. For such stable emulsions, the water will start boiling off the emulsion layer. In case of thermal separation, the separation starts at the top of the emulsion layer, as the emulsion is heated from the top. However due to high

viscosity of the emulsion layer, the separated water may not be able to escape through the bottom of the slick until the viscosity of the entire slick becomes low enough (Guenette *et al.,* 1994). As the emulsion starts to break into oil and water, the oil floats on top of the emulsion layer.

The condensed phase now consists of an oil layer, an emulsion layer and the water base. At the free oil surface, there is partial absorption of incident heat flux, in-depth radiation absorption, heat loss to the surroundings by radiation and convection, and conduction in the condensed phase. As the top layer of oil receives heat, it heats up, vaporizes, and pyrolyzes. The pyrolysis gases mix with the oxidizer from the air, which is supplied by diffusion, aided by wind and turbulence. The mixture is ignited by the available ignition source or fire above the oil layer. The oil burning process is sustained by partial energy feedback to the emulsion slick from the combustion. In addition to pyrolysis, the energy is distributed in the form of the sensible heat of raising the temperature of the condensed phase, reradiation to the surroundings, convection to the surroundings, latent heat of water evaporation, latent heat of oil vaporization, and heat loss into the water (Guenette *et al.,* 1995). Figure 2 shows, schematically, all these processes occurring during emulsion combustion. Depending on the thickness of the emulsion layer, the water substrate may boilover. The process ends after the emulsion layer is completely consumed or there is excessive heat loss. The excessive heat loss reduces the rate at which the oil vaporizes. As the oil vaporization rate drops down, the energy feedback to the slick starts to decrease, which further reduces the oil vaporization rate and eventually extinction occurs (Arai *et al.,* 1990).

For the modeling purpose, the overall burning process is divided into three regimes as follows:

1. *Initial Regime* ($t = 0$ to t_1): The model starts with an application of external heat flux to an emulsion layer floating on ocean surface. The entire slick is at a uniform temperature equal to the surrounding temperature. A constant heat flux is incident on the emulsion surface. The heat flux may be because of an igniter placed on the emulsion surface or by the surrounding fire. The emulsion layer is heated and eventually the top surface reaches the emulsion-breaking temperature. This marks the end of initial regime.

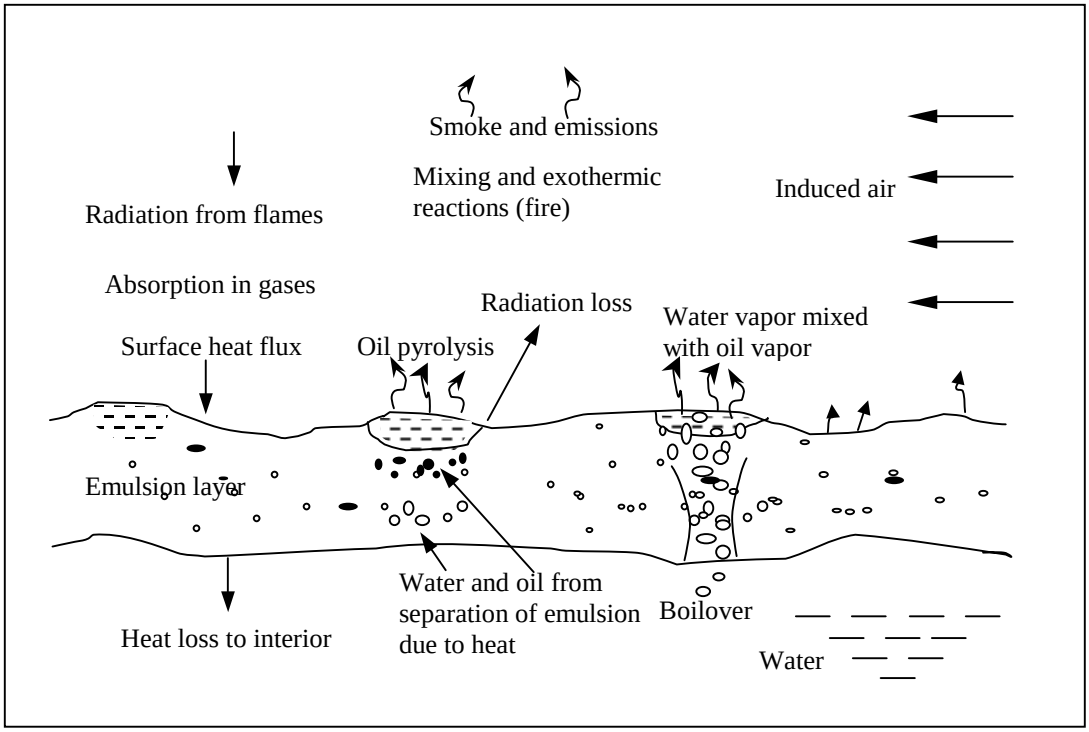

Figure 2. Schematic of the processes of emulsion combustion

2. *Intermediate Regime* ($t = t_1$ to t_2): As the emulsion surface reaches the emulsion breaking temperature, the emulsion separates into water and oil. Water being heavier than the emulsion, it sinks to the bottom. This results in the appearance of oil on top of the emulsion. Though it is believed that the emulsion separation occurs over a range of temperatures, we model this as a process occurring at a constant temperature. Thus, there are three layers in this regime: oil, emulsion, and water. The oil layer grows and the emulsion layer thins out. Now the oil layer receives incident heat flux directly. The oil, not being optically thick, absorbs only a part of the incident heat flux at the surface, and some of the radiation energy is absorbed in-depth. A part of the heat flux that reaches oil-emulsion interface, without getting absorbed in oil, is completely absorbed at the oil-emulsion interface. The temperature of the oil layer increases while the oil-emulsion interface temperature remains constant at the emulsion breaking temperature. When the oil surface temperature reaches vaporization temperature, the intermediate regime ends.

3. *Final Regime* ($t = t_2$ to t_3): The vaporized oil burns, the energy is released by oil combustion, and a part of it is fed back to the oil. The incident heat flux increases rapidly to the prescribed maximum value, $\dot{q}''_{\max}$,which depends on the type of crude oil, fire size, wind velocity, and other combustion conditions. The surface temperature of the oil now remains at the oil vaporization temperature. The vaporization causes the oil layer to deplete, while the breaking up of the emulsion layer causes the oil layer to grow. The process continues until the emulsion layer completely depletes, the oil layer continues to burn, and finally extinction occurs because the loss of heat to the water becomes greater than the heat feedback to the oil surface.

4.2 Assumptions

A number of assumptions are made to make the model mathematically tractable. The model with these assumptions, it is believed, still captures most of the main dominating processes involved in the emulsion combustion floating on top of the water surface, while the assumptions make the model easier to solve numerically.

The assumptions involved are as follows:

1. Initially, the emulsion layer floating on the water surface, and the entire water body are at a uniform temperature of T_i.
2. The energy transfer into the interior of the condensed phase is by one-dimensional conduction. This assumption is made because the emulsion layer is heated from the top and the density gradient does not set up natural convection currents. The high viscosity of oil and very high viscosity of emulsion (typically one or more order of magnitude greater than that of the oil) allows an assumption of quiescent layers. The model is an energy balance of a representative portion of the large oil/emulsion slick. Hence, the heat transfer only in a direction normal to the ocean surface is considered.
3. Representative properties for emulsion are approximated by the weighted averages of the oil and water properties, and constant throughout the time of operation. While forming the emulsion, the oil and the water do not react chemically. If the water is dispersed into the oil phase uniformly, the overall properties such as thermal conductivity, specific heat and density for the emulsion will be very close to the averages of the respective properties of water and oil, weighted according to the mass fractions of water and oil.
4. The thermo-physical properties of oil, water and emulsion are assumed to be constant with time and temperature. From the laboratory observations, the surface temperature of the emulsion pool may reach up to 200 °C, while the initial temperature is the room temperature of about 25 °C. It can be seen that the water properties vary by less than 5% in this temperature range. The crude oil properties also have a very weak dependence on the temperature (Cragoe, 1929).
5. When the oil begins to vaporize, a prescribed maximum heat flux, $\dot{q}''_{\max}$, is reached; and after that, the heat flux remains constant. Studies by Tien, 1985, Khater *et al.*, 1990, Hamins *et al.*, 1994 have reported a steady state heat flux value for heat feedback from the pool fires to the pool surface.

Hence the assumption, that the heat flux absorbed by the pool surface reaches a maximum and remains constant at that maximum value, is a valid one.

6. Emulsion is assumed to separate into water and oil at the emulsion breaking temperature. Pisarchik *et al.,* 1997 have reported, and the observations during the laboratory test have revealed, that at a particular temperature a visible layer of oil is seen floating on top of the emulsion surface. It is postulated that as the temperature of the emulsion layer increases, the surface tension forces holding the water droplets inside the continuous oil phase decrease. For example, surface tension of water against air decreases from 73 dynes/cm at 20 °C to 63 dynes/cm at 80 °C nonlinearly (with the reduction in surface tension increasing with increasing temperature), and then continues to fall off significantly as the temperature approaches the boiling temperature. Accurate data for temperature dependence of surface tension of water against the oils used in the current experiments is, however, not available. As the surface tension falls below a certain value, it cannot hold the water droplets inside the oil phase any longer and the emulsion starts to separate into water and oil. The process may occur, however, over a range of temperatures.
7. The water that is freed after separation of emulsion is assumed to sink out of the emulsion layer. Guenette *et al.,* 1994 argue that the water separating out from the emulsion cannot settle out of the emulsion layer due to the viscous nature of the slick and that the main process by which the water is removed from the emulsion slick is vaporization or boiling. Buist and McCourt (1998) report that the separated water may accumulate inside the slick until the slick is fluid enough for the water to pass through. It is possible that the water may not leave the emulsion slick entirely as soon as it is separated from the emulsion. However it is felt that, if the viscosity of the emulsion layer below the layer of emulsion that is separating is low

enough for the water to pass through, the water that is present interstitially will not affect the dynamics of the emulsion combustion in a major way.

8. The oil evaporates at the fixed oil vaporization temperature. Crude oils contain various different hydrocarbon fractions. These different crude oil fractions evaporate at different temperatures. Thus overall, the crude oils evaporate over a range of temperatures. However, in the absence of the exact data for the crude oils and with the view of keeping the model computationally simple, it is assumed that the oil evaporates at a constant oil vaporization temperature.
9. Wind and ocean turbulence effects are neglected. Wind and ocean turbulence affect the emulsion combustion. Winds change the convective heat transfer coefficient at the surface. This effect can be captured by appropriate input of the convective heat transfer coefficient at the surface. The winds also bend the flames towards or away from the emulsion surface thus increasing or decreasing the total heat feedback to the slick. Selecting proper values for the maximum heat flux $\dot{q}''_{\max}$ can simulate this effect. In laboratory setting, these effects were absent. The wave effects are more complex in nature as they cause mixing of the emulsion and water. These effects need to be studied separately.
10. Emulsion is assumed optically thick. This was assumed because the emulsions are heterogeneous. The boundary surfaces between the water and oil phases absorb the radiation, and hence the optically thick assumption is valid.
11. The seawater base is modeled as a semi-infinite medium. The duration of the burn is short so that the temperature of the seawater at sufficient depths is practically unaltered.

4.3 Mathematical Model

The mathematical representation of the physical model described in section 4.1 is presented in this section. The governing differential equation is the transient one-

dimensional conduction equation. It is applied to oil, emulsion and water layers. For the governing equation in the oil layer, a source term accounting for in-depth radiation absorption is introduced.

Depending on the regime, different boundary conditions are applied at the top surface. Since the domain is semi-infinite, at the semi-infinite boundary, the temperature is always equal to the initial or surrounding temperature *(T_i).* As the emulsion starts separating into oil and water, the oil-emulsion interface temperature is fixed at the emulsion breaking temperature *(T_{eb}).* As the temperature of the top surface of the oil layer reaches the oil vaporization temperature, *(T_{ov})* it is kept constant. Energy balance conditions are used at the oil-emulsion and emulsion-water interfaces. For the initial regime, the initial temperature is equal to T_i throughout the domain. The temperature field at the end of the initial regime is used as an initial condition for the intermediate regime and the temperature field at the end of the intermediate regime is used as the initial condition for the final regime. Governing equations and boundary conditions for each regime are presented below.

4.3.1 Initial Regime

A schematic representation of the initial regime is shown in Figure 3.

Governing equations:

$$\frac{\partial T_{e1}}{\partial t} = \alpha_e \frac{\partial^2 T_{e1}}{\partial x_e^2} \tag{5}$$

$$\frac{\partial T_{w1}}{\partial t} = \alpha_w \frac{\partial^2 T_{w1}}{\partial x_w^2} \tag{6}$$

Initial conditions:

$$@\ t = 0,\ T_{e1} = T_i \tag{7}$$

$$T_{w1} = T_i \tag{8}$$

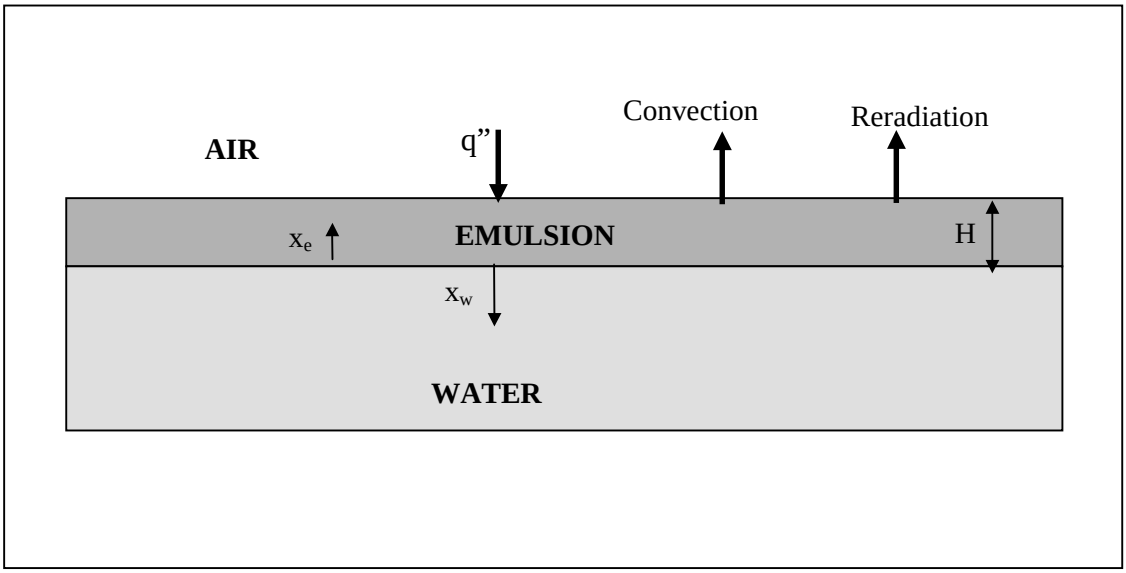

Figure 3. Schematic representation of initial regime of emulsion combustion.

Boundary conditions:

$$@\ x_e = H,\ k_e \frac{\partial T_{e1}}{\partial x_e} = \dot{q}'' - h_e(T_{e1} - T_i) - \sigma\varepsilon_e(T_{e1}^4 - T_i^4) \tag{9}$$

$$@\ x_e = 0,\ x_w = 0,$$

$$k_e \frac{\partial T_{e1}}{\partial x_e} = -k_w \frac{\partial T_{w1}}{\partial x_w} \tag{10}$$

$$@\ x_w = \infty,\ T_{w1} = T_i \tag{11}$$

The initial regime ends when $T_{e1} = T_{eb}$ @ $x_e = H$.

At the end of the initial regime, $t = t_1$, $H = H_i$.

4.3.2 Intermediate Regime

A schematic representation of the intermediate regime is shown in Figure 4.

Governing equations:

$$\frac{\partial T_{o2}}{\partial t} = \alpha_o \frac{\partial^2 T_{o2}}{\partial x_o^2} + \frac{C_0 \dot{q}'' \beta e^{-\beta(L - x_o)}}{\rho_o c_{po}} \tag{12}$$

$$\frac{\partial T_{e2}}{\partial t} = \alpha_e \frac{\partial^2 T_{e2}}{\partial x_e^2} \tag{13}$$

$$\frac{\partial T_{w2}}{\partial t} = \alpha_w \frac{\partial^2 T_{w2}}{\partial x_w^2} \tag{14}$$

Initial conditions:

$$@\ t = t_1,\ T_{o2} = T_{eb} \tag{15}$$

$$T_{e2} = T_{e1} \tag{16}$$

$$T_{w2} = T_{w1} \tag{17}$$

$$L = 0 \tag{18}$$

$$H = H_i \tag{19}$$

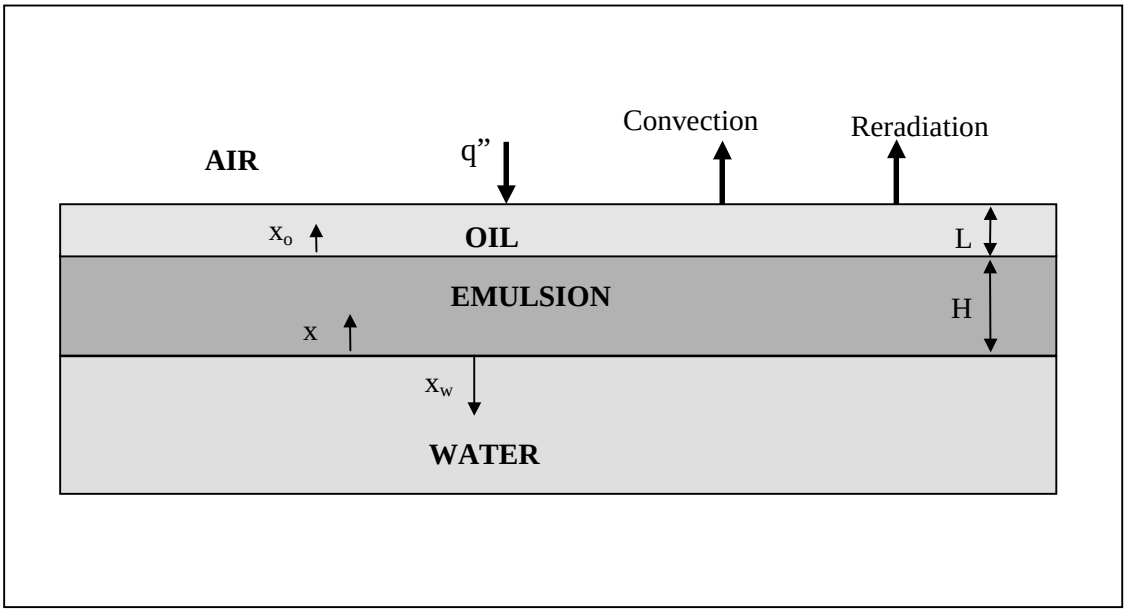

Figure 4. Schematic representation of intermediate regime of emulsion combustion.

Boundary conditions and auxiliary conditions at the boundaries:

$@\ x_o = 0,\ T_{o2} = T_{eb}$ (20)

$@\ x_o = L,$

$$k_o \frac{\partial T_{o2}}{\partial x_o} = (1 - C_o)\dot{q}'' - h_o(T_{o2} - T_i) - \sigma\varepsilon_o(T_{o2}^4 - T_i^4) \quad (21)$$

$@\ x_e = 0,\ x_w = 0,$

$$k_e \frac{\partial T_{e2}}{\partial x_e} = -k_w \frac{\partial T_{w2}}{\partial x_w} \quad (22)$$

$@\ x_e = H,\ T_{e2} = T_{eb}$ (23)

$@\ x_w = \infty,\ T_{w2} = T_i$ (24)

$@\ x_o = 0,\ x_e = H,$

$$k_o \frac{\partial T_{o2}}{\partial x_o} - k_e \frac{\partial T_{e2}}{\partial x_e} = aC_0\dot{q}''e^{-\beta L} \quad (25)$$

The intermediate regime ends when $T_{o2} = T_{ov}$ @ $x_o = L$.

At end of the intermediate regime, $t = t_2$, $H = H_2$, $L = L_2$.

4.3.3 Final Regime

A schematic representation of the final regime is shown in Figure 5.

Governing equations:

$$\frac{\partial T_{o3}}{\partial t} = \alpha_o \frac{\partial^2 T_{o3}}{\partial x_o^2} + \frac{C_0\dot{q}''\beta e^{-\beta(L - x_o)}}{\rho_o c_{po}} \quad (26)$$

$$\frac{\partial T_{e3}}{\partial t} = \alpha_e \frac{\partial^2 T_{e3}}{\partial x_e^2} \quad (27)$$

$$\frac{\partial T_{w3}}{\partial t} = \alpha_w \frac{\partial^2 T_{w3}}{\partial x_w^2} \quad (28)$$

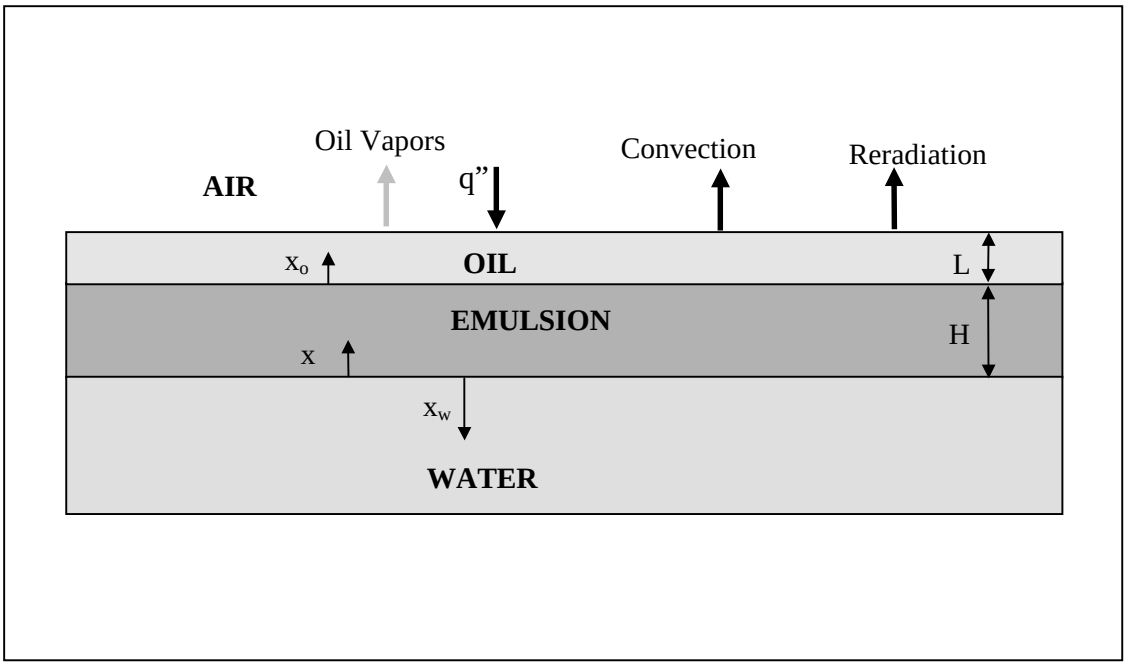

Figure 5. Schematic representation of final regime of emulsion combustion.

Initial conditions:

$$@\ t = t_2,\ T_{o3} = T_{ov} \tag{29}$$

$$T_{e3} = T_{e2} \tag{30}$$

$$T_{w3} = T_{w2} \tag{31}$$

$$L = L_2 \tag{32}$$

$$H = H_2 \tag{33}$$

Boundary conditions and auxiliary conditions at the boundaries:

$$@\ x_o = 0,\ T_{o3} = T_{eb} \tag{34}$$

$$@\ x_o = L,\ T_{o3} = T_{ov} \tag{35}$$

$$@\ x_e = H,\ T_{e3} = T_{eb} \tag{36}$$

$@\ x_e = 0,\ x_w = 0,$

$$k_e \frac{\partial T_{e3}}{\partial x_e} = -k_w \frac{\partial T_{w3}}{\partial x_w} \tag{37}$$

$$@\ x_w = \infty,\ T_{w3} = T_i \tag{38}$$

$@\ x_o = 0,\ x_e = H,$

$$k_o \frac{\partial T_{o3}}{\partial x_o} - k_e \frac{\partial T_{e3}}{\partial x_e} = aC_0 \dot{q}'' e^{-\beta L} \tag{39}$$

$@\ x_o = L,$

$$k_o \frac{\partial T_{o3}}{\partial x_o} = (1 - C_o)\dot{q}'' - h_o (T_{o3} - T_i) - \sigma \varepsilon_o (T_{o3}^4 - T_i^4) - \rho_o Q_{Lo} \frac{dL}{dt} \tag{40}$$

The final regime ends when either the rate at which the oil vaporizes decreases to a very low number (10^{-6} mm/s) or the oil layer completely evaporates out. Either of these situations occurs when the emulsion layer becomes thin so that there is excessive heat loss.

4.4 Numerical Solution

The emulsion layer was divided into a 0.5 mm grid for numerical computation. The oil grid spacing was calculated such that one emulsion formed one grid length in oil after break up. Thus the oil grid spacing was a function of the fraction of oil present in the emulsion. The grid for the water base was stretched to accommodate the semi-infinite

medium using coordinate transformation. The original semi-infinite region was transformed to a finite region in the transformed coordinate system. The transformation rule used was,

$$y_w = 1 - \frac{1}{1 + Cx_w}, \tag{42}$$

where y_w is the transformed coordinate in water domain. Using this rule, equations (5), (13), (27) which are of the type

$$\frac{\partial T_w}{\partial t} = \alpha_w \frac{\partial^2 T_w}{\partial x_w^2}$$

were transformed to the type of

$$\frac{\partial T_w}{\partial t} = \alpha_w C^2 (1 - y_w)^4 \frac{\partial^2 T_w}{\partial y_w^2} - 4\alpha_w C^2 (1 - y_w)^3 \frac{\partial T_w}{\partial y_w}. \tag{43}$$

The boundary conditions (9), (21), (36) which are of the type

$$k_e \frac{\partial T_e}{\partial x_e} = -k_w \frac{\partial T_w}{\partial y_w}$$

transformed to the type

$$k_e \frac{\partial T_e}{\partial x_e} = -Ck_w (1 - y_w)^2 \frac{\partial T_w}{\partial y_w}. \tag{44}$$

Explicit time accurate finite difference scheme with pseudo time stepping was used to solve the resulting set of simultaneous partial differential equations and the boundary and auxiliary conditions. A general partial differential equation selected for finite differencing can be represented as

$$\frac{\partial T}{\partial \tau} + \frac{\partial T}{\partial t} = \alpha C_{t1} \frac{\partial^2 T}{\partial x^2} + C_{t2} \frac{\partial T}{\partial x} + \frac{aC_0 \dot{q}'' \beta e^{-\beta(L-x)}}{\rho_o c_{po}} \tag{45}$$

where, $C_{t1} = C^2(1 - x)^4$ and $C_{t2} = -4\alpha_w C^2(1 - x)^3$ for water base and $C_{t1} = 1$ and $C_{t2} = 0$ for oil and emulsion layers. Also, $a = 1$ for oil layer to account for the in-depth radiation absorption and $a = 0$ for emulsion and water layers. The pseudo time (τ) derivative added to the governing equation is driven to zero by attaining steady state in pseudo time, for each time step in real time (t), thus assuring a converged solution. A two-point difference in time and central difference in space is used. Details of the finite differencing are

presented in Appendix A. The equations were coded in Fortran. The code was compiled and run on SGI Irix 6.2 system. Typical run time for the code was around 20 minutes. The Fortran code is provided in Appendix B

4.5 Preliminary Model Validation

The model was validated by comparing the numerical results for a simple case of conduction through one-dimensional, semi-infinite body with the analytical solution. The semi-infinite body with constant uniform initial temperature was subjected to a constant heat flux at the boundary. Temperature as a function of time and space was obtained from the analytical solution as

$$T = T_i + \frac{\dot{q}''}{k}\left(\frac{2}{\sqrt{\pi}} \cdot \sqrt{\alpha t} \cdot e^{\frac{-x^2}{4\alpha t}} - x \cdot erfc\left(\frac{x}{2\sqrt{\alpha t}}\right)\right). \quad (46)$$

For a test case, a material with conductivity of 0.58 W/mK and a thermal diffusivity of 0.137×10^{-6} m^2/s was considered. The semi-infinite body was heated from initial uniform temperature of 0 °C until the surface temperature reached 107 °C by a constant heat flux source of 20 kW/m^2. The time predicted by the model is 59.1 seconds, whereas the analytical solution predicts the time to be 55.2 seconds. A comparison of the temperature profiles obtained by solving the analytical solution and predicted by the model is shown in figure 6. The comparison showed the model predictions of the in-depth temperature profile to within 1% of the analytical temperature profiles.

The choice of time step and the gird spacing was made by trial and error. At large values of time step or the grid spacing, the model proved to be unstable. Hence a time step of 0.1 second and a grid spacing of 0.5 mm in emulsion were chosen.

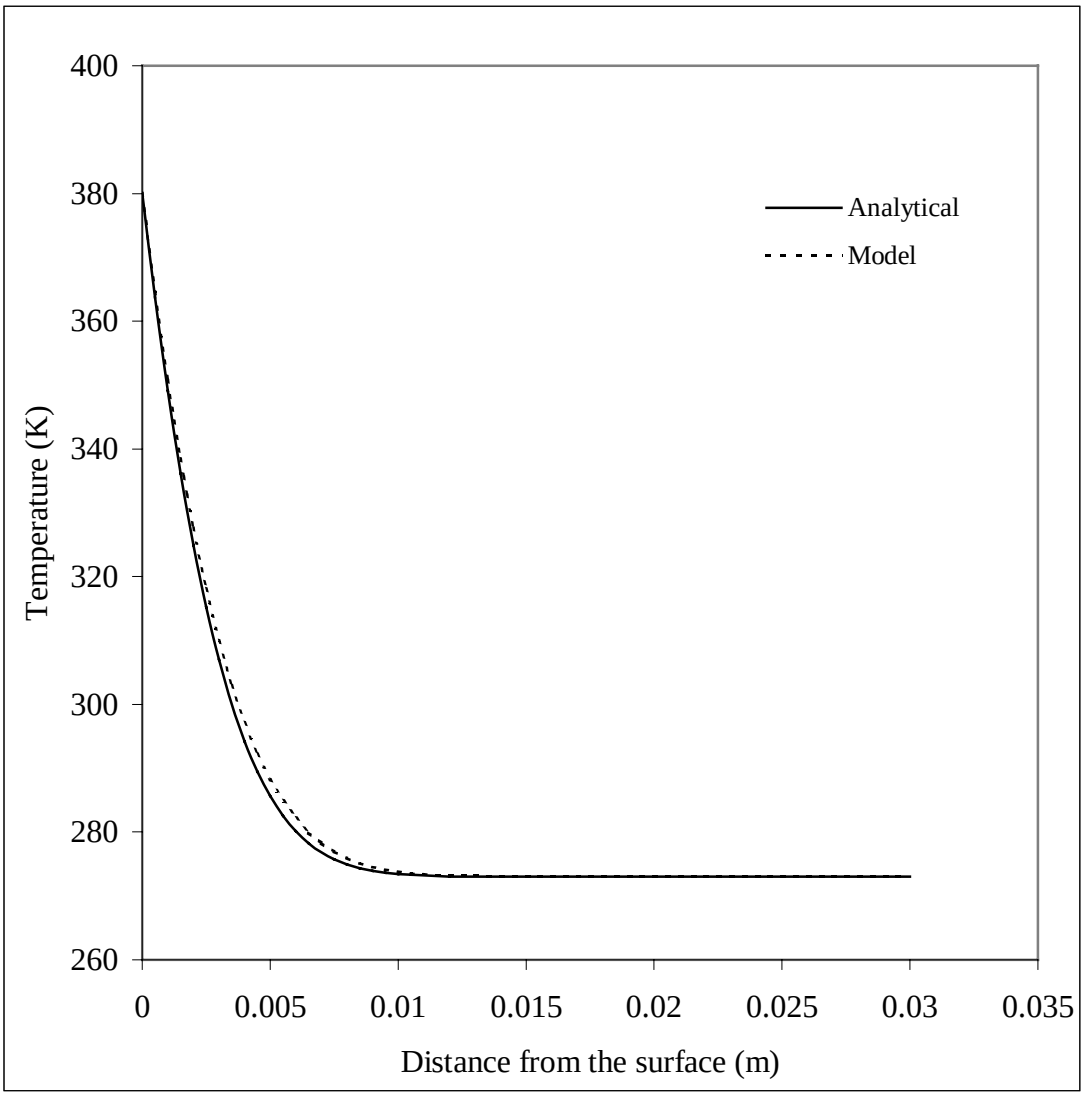

Figure 6. Comparison of temperature profiles from analytical solution and model for a semi-infinite body subject to a constant heat flux at the surface

Chapter 5

EXPERIMENTAL INVESTIGATION

5.1 Introduction

The overall objective of the experimental investigation was to determine the range of conditions under which oil or a water in oil emulsion burns efficiently, and if so, how to increase this range of combustibility of the oil or the water in oil emulsion floating on top of water. The primary concern was to simulate the important combustion characteristics of the actual, *in-situ* burning of oil spill on ocean, in laboratory scale experiments as accurately as possible. This requires the following considerations in the laboratory experiments:

1. The fire must be turbulent. A laminar flow experiment would significantly differ from the large scale. While the actual scale of turbulence in large fires could not be precisely simulated in a small scale experiment, a turbulent fire and a surrounding turbulent flow field in a laboratory experiment would have many characteristics close to those of the large fire, such as the convective heat feedback and local or small scale mixing (but not, for example, the radiation level). Although the laboratory scale experiment is not completely similar to a full-scale fire, a carefully designed laboratory scale experiment outweighs the costs of conducting large-scale experiments while retaining the scientific benefits.
2. The strong radiative heat feedback to the burning and yet-to-burn areas is another characteristic of a large-scale fire. In a laboratory scale, external heat radiation was imposed in order to compensate for the lack of radiation from small size flames with less soot.

An experimental set up facility was developed based on the above needs. Details of the set up are presented in the next section.

5.2 The Experimental Set up

The design of the emulsion burning experiments was divided into four basic parts, viz.: weathering of fresh oil to desired degree, preparation of the emulsion needed for the test, pool burning of the prepared emulsion under controlled conditions with necessary instrumentation to collect the important data, and accurate volume or mass measurement of the residue left from the burn.

5.2.1 Weathering of Fresh Oil

Evaporation of lighter components from the oil alters the oil properties. In case of an oil spill on ocean surface, the oil that is spilled undergoes evaporation of lighter fractions in the oil as it is exposed to the surroundings until the clean up operations start. In the field of oil spill studies, evaporation of lighter components of the crude oil is termed as weathering of crude oil. Hence the term weathering is used henceforth to describe the evaporation of the lighter fractions of the crude oil. In order to study the effect of this weathering phenomenon, the crude oils used in the study were weathered under controlled conditions.

To evaporate the lighter components from the fresh crude oil, continuous bubbling of air through the oil column was carried out. This increased the rate of evaporation. Samples of each of the crude oils were evaporated to different degrees of weathering. The vapors were vented out of the laboratory using a fume hood. The bubbling of air was continued until the desired volume fraction of the oil was removed. The degree of weathering was measured by the percentage of the initial volume that was evaporated and was calculated using the following equation:

$$\%\ weathered = \frac{(Initial\ Volume - \ Voulme\ after\ Evaporation)}{Initial\ Volume} \times 100 \qquad (47)$$

A schematic of the set up used for weathering oils is shown in figure 7. Due to violent bubbling, sometimes the oil spilled out of the glass cylinder used for weathering. This has introduced some error in the weathering percentages reported. However, it is estimated based on the inspection of the oil that spilled that the error in the reported weathering percentage did not exceed 1%.

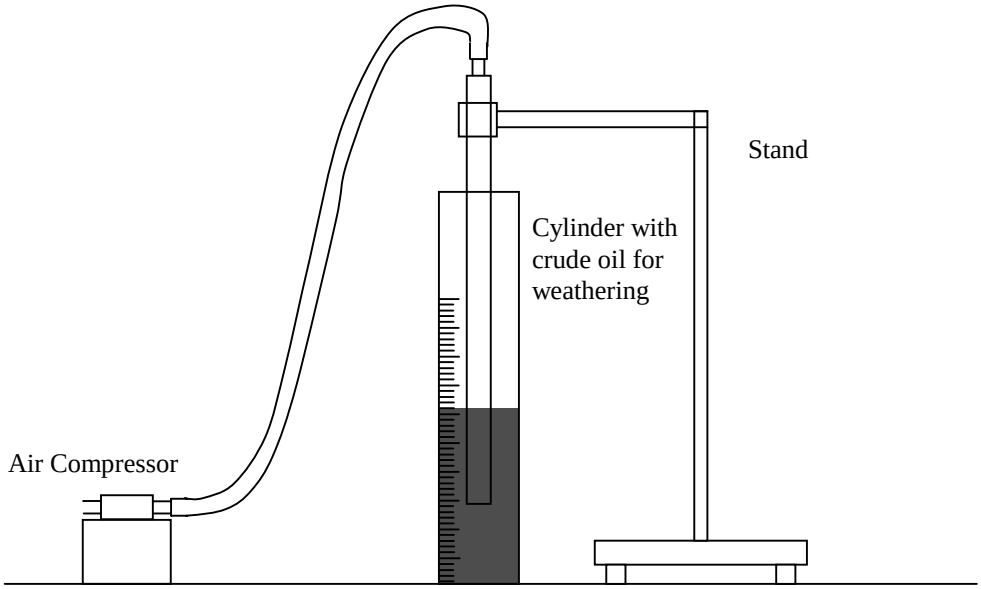

Figure 7. Schematic representation of the experimental set up for weathering of crude oil

5.2.2 Emulsion Preparation

To study the effect of extent of emulsification and isolate the effects of other factors on the important emulsion pool fire characteristics, it was essential to use emulsions with accurately known compositions. This was achieved by mixing measured amounts of emulsion constituents to form the emulsion. The schematic of the emulsion making apparatus is shown in figure 8. The apparatus holds four 1-quart (approx. 800 ml) Ball home canning jars. The jars were filled with measured amounts of emulsion constituents. They were then rotated about a horizontal axis at a speed of 30 rpm (Hokstad *et al.,* 1995) using a variable speed motor. An emulsion was considered to be stable if the emulsion that was left over after using the necessary amount for the burn test showed no visible separation until the end of the burn test. This level of stability was typically achieved after 24 to 48 hours of rotation. Pisarchik *et al.,* (1997) have reported that from stability and emulsion separation point of view, the emulsion of fresh water and emulsions of seawater behave similarly. Hence, fresh water was used in this study for emulsification.

5.2.3 Emulsion Pool Fire

The stable emulsions made using the emulsion making apparatus were then burned in the pool fire set up. This set up was designed and instrumented for collecting data from pool fires of water-in-oil emulsions floating on water. The schematic of the pool fire set up is shown in figure 9. A 23 cm x 23 cm size pool was made in the center of a 150 cm x 120 cm x 25 cm deep, water pool. The central pool was supported inside the outer pool by a metallic, supporting mechanism. This central box, made of sheet metal, could be removed and replaced so that the size of the pool could be changed. The fuel, oil or water-in-oil emulsion was poured in the center pool to a desired height. The outer water pool was needed for protection from the accidental spillover and flame spread from the fuel. For visual accessibility to the fire, the outer tank was made of clear plexiglass. Additionally, to aid visual access from underneath the emulsion pool, a mirror was installed at a 45 ° angle under the plexiglass tank.

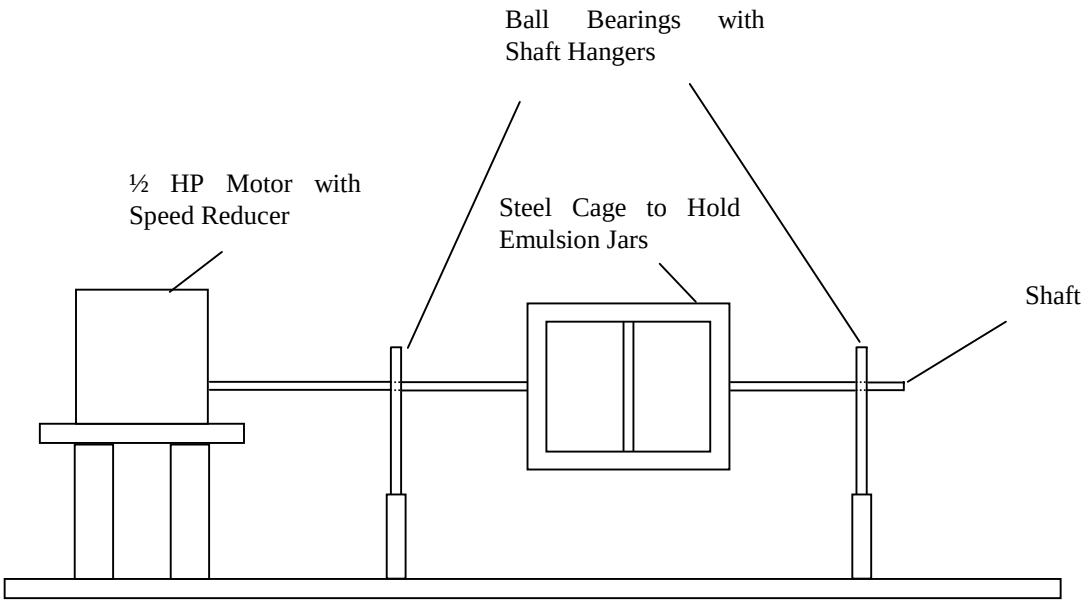

Figure 8. Schematic of the emulsion making apparatus

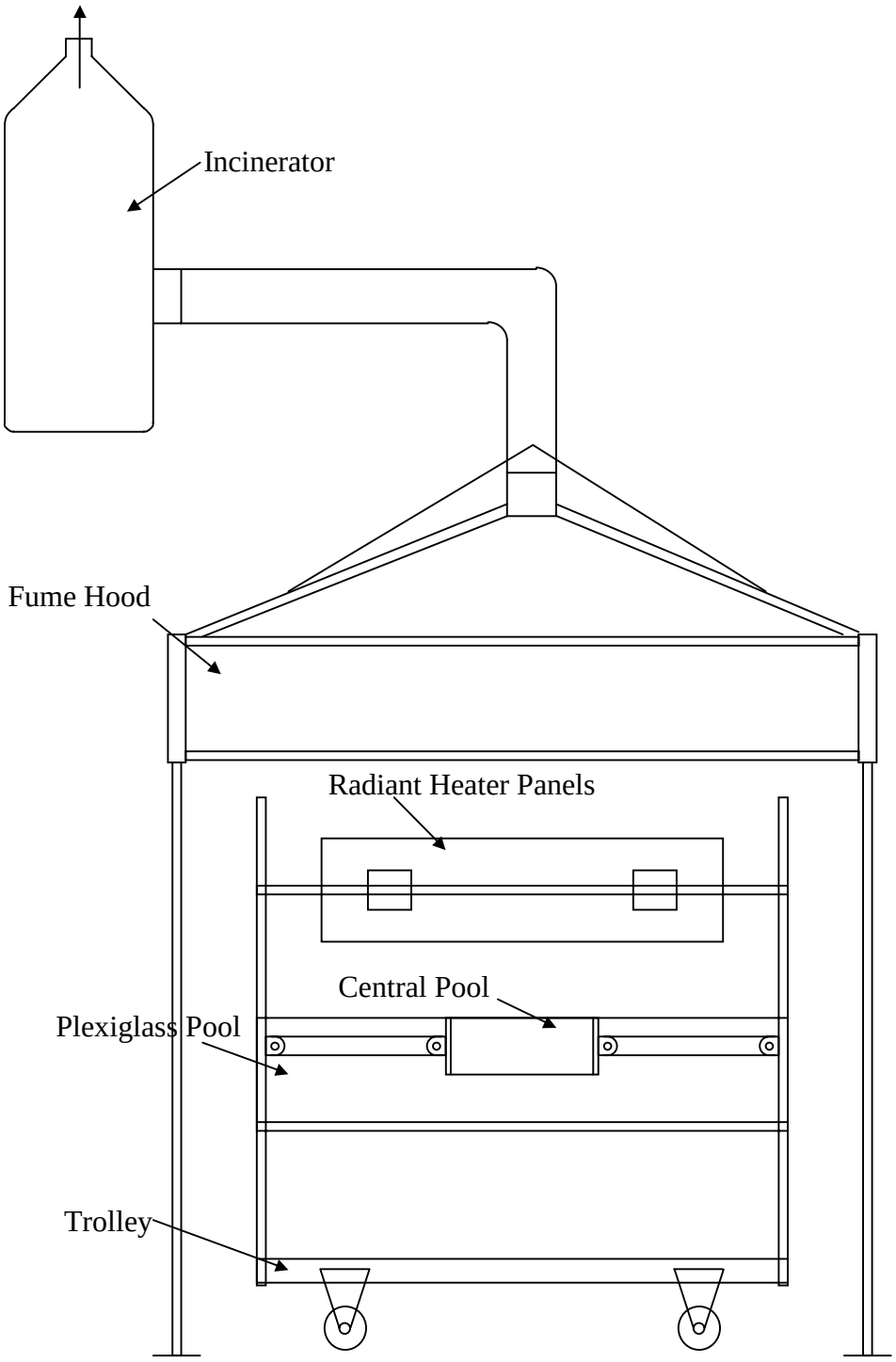

Figure 9. Schematic of the pool fire set up

Two electrically operated heating panels (constructed by Therma-Tech Corporation) were used to supply external radiation. The panels have rows of heating elements embedded in a ceramic material and have a Corning Vycor face plate. They were electrically heated by a 440 V, three phase, 60 amp power and controlled by a silicon control rectifier (SCR), which allowed the panels to reach a maximum temperature of 815 °C that produced a maximum radiative heat flux of about 60 kW/m^2 at the panel surface. The panels were mounted facing toward the pool at an angle to irradiate the oil/emulsion pool with a uniform heat flux. Based on the geometry and view factor estimated, the fuel pool could be subjected to radiative heat flux from 1 kW/m^2 to 21 kW/m^2. Depending on the requirements, this maximum radiative heat flux level could be changed by raising or lowering the panels.

The entire pool assembly was mounted on a movable base and was covered with a flame hood. The hood outlet was connected to a down-fired combustor (DFC) through an electric blower. The exhaust of the pool fire underwent 'after burning' in the DFC. This converted the unburned fuel particles and the intermediate products of combustion in the exhaust plumes to final products of combustion.

Ignition of the pool was achieved by use of either 11 inch long matchsticks supported at the front end of a wooden rod or a small natural gas pilot flame close to the emulsion surface. The flow rate of the natural gas to the pilot flame was kept at a constant minimum level. This ensured that the pilot flame did not provide any substantial heat flux on to the fuel surface.

Type K thermocouples were used to monitor the in-depth temperature distribution and the oil-water interface temperature. A thermocouple rake of five thermocouples with a spacing of 5 mm between the consecutive thermocouples was mounted inside the inner pool. Though radiation shielding for the thermocouples was not used, the thermocouples did not receive the external radiation from the heater panels, as they were submerged in the emulsion pool. A 16-channel data acquisition board was used to collect the temperature data during the burn and the data were stored on a PC.

A video camera was used to record the test runs. These measurements were needed to determine the flame height, the conditions at which ignition takes place (or

does not take place) to provide input to numerical models, and in general, to understand the interdependence of the variables (for example, the relation between heat flux and burn rate). Observations such as total burning time and presence of boilover were noted for each burn.

5.2.4 Residue Measurement

After extinction of the fire, some unburned residue was left floating in the central pool. The knowledge of initial volume of emulsion, volume of residue left, and the total burning time provided an estimate of the average burning rate for the test run. In order to measure the residue accurately, it was necessary that the measurement included the entire residue volume. For the diesel-water emulsions tested, the residue after each burn was collected using a wet vacuum cleaner (Shop-Vac) and its volume was measured in a measuring apparatus shown in figure 10.

This method of measurement proved to be unsuitable for measuring the residue of the crude oil emulsions, as the crude oil residues were more viscous and would stick to the vacuum cleaner assembly. Thus, to obtain more accurate measurements of the crude oil emulsion residues, the center pool used was closed from the bottom. The mass of water and mass of emulsion poured in the center pool were measured using an electronic balance with accuracy of 1 g. The entire assembly was then measured after the burn test. The difference between the initial and final mass measurements was considered to be the mass of the oil burned in the experiment. This measurement, coupled with the measurement of the total burn time, provided an estimate of the average burning rate of oil. This method may overestimate the burning rates, as the mass of the water that might have evaporated out and the mass of the oil that might have evaporated prior to the start of the burn are not taken into consideration. Thus, the actual mass of the oil burned would be less than the mass of the oil considered to have burned. Based on the observations made during the tests, it was estimated that the error in the measurement could be up to 15%.

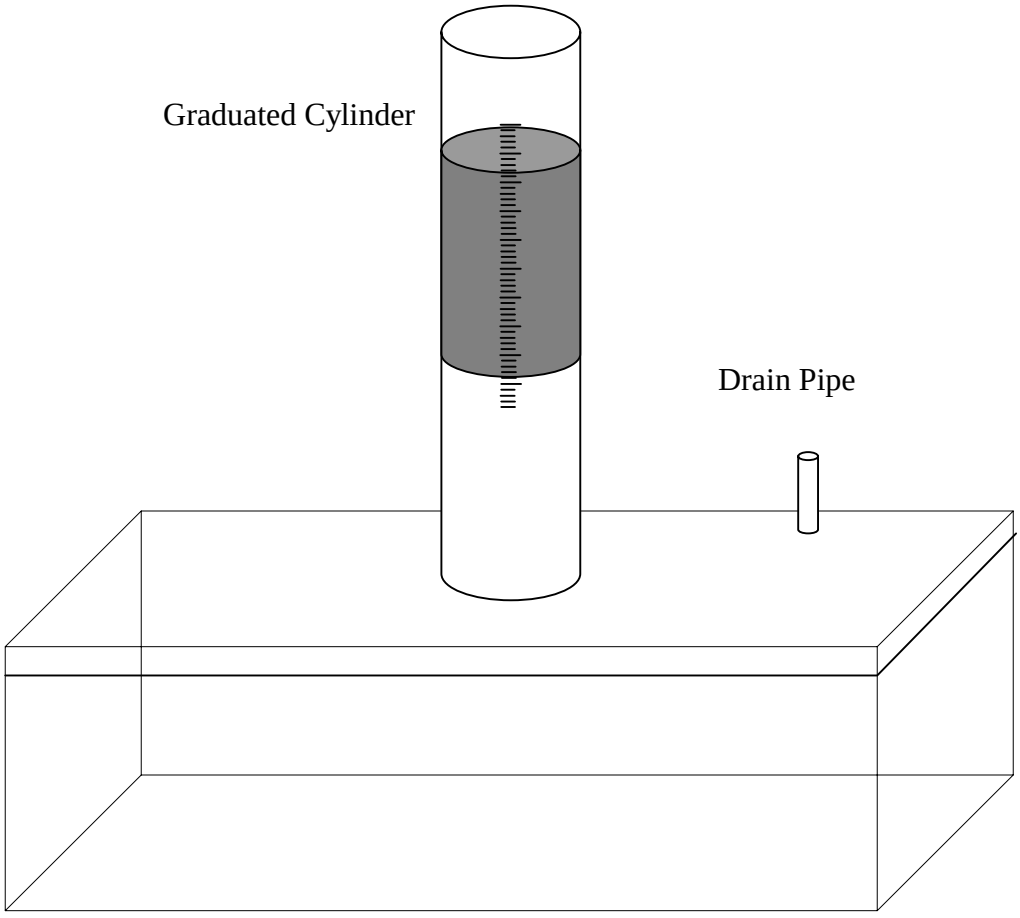

Note: Not to Scale

Figure 10. Schematic of the apparatus for residue measurement

5.3 Heater Panel Calibration

The SCR controls the heat flux incident on the emulsion pool surface by the electrically operated, radiant heater panels. In order to know the value of the heat flux incident on the pool surface for a particular controller setting, calibration of the heater panels was conducted.

A circular foil, radiant heat flux gage was used to make the heat flux measurements. The heat flux transducer is 12.7 mm diameter, a water cooled, circular foil, heat flux gage manufactured by Medtherm Corporation (model number is 32-5-1.0-18)

For the heater panel calibration, nine locations were chosen to cover the entire emulsion pool surface and measurements were taken at steady state. The heat flux distribution on the pool surface was found to be quite even. The average of the nine readings for a particular setting of the controller was taken as the heat flux on the emulsion pool surface at that controller setting. The maximum and minimum heat flux measurements for any particular setting were within ± 5 % of the average heat flux value at that setting. A plot of average heat flux values on the pool surface for the two heater panel mountings at various SCR dial settings is shown in figure 11. Tables 2 and 3 show the heater panel calibration chart from lowest to the highest settings of the SCR controller at the upper level mounting and lower level mounting of the heater panel. The calibration was checked periodically to ensure that the heat flux value readings were accurate. Also, the calibration for the heat flux gage itself was checked against a master gage at National Institute of Standards and Technology (NIST), Gaithersburg, MD. The comparison of the heat flux, measured by the NIST master gage with the calibration chart provided for the gage by the manufacturer, is presented in figure 12. The maximum variation between the NIST gage calibration and the calibration provided by the manufacturer was about 8%. This was considered to be within acceptable limits. Hence the gage calibration charts provided by the manufacturer were used for the heater panel calibration.

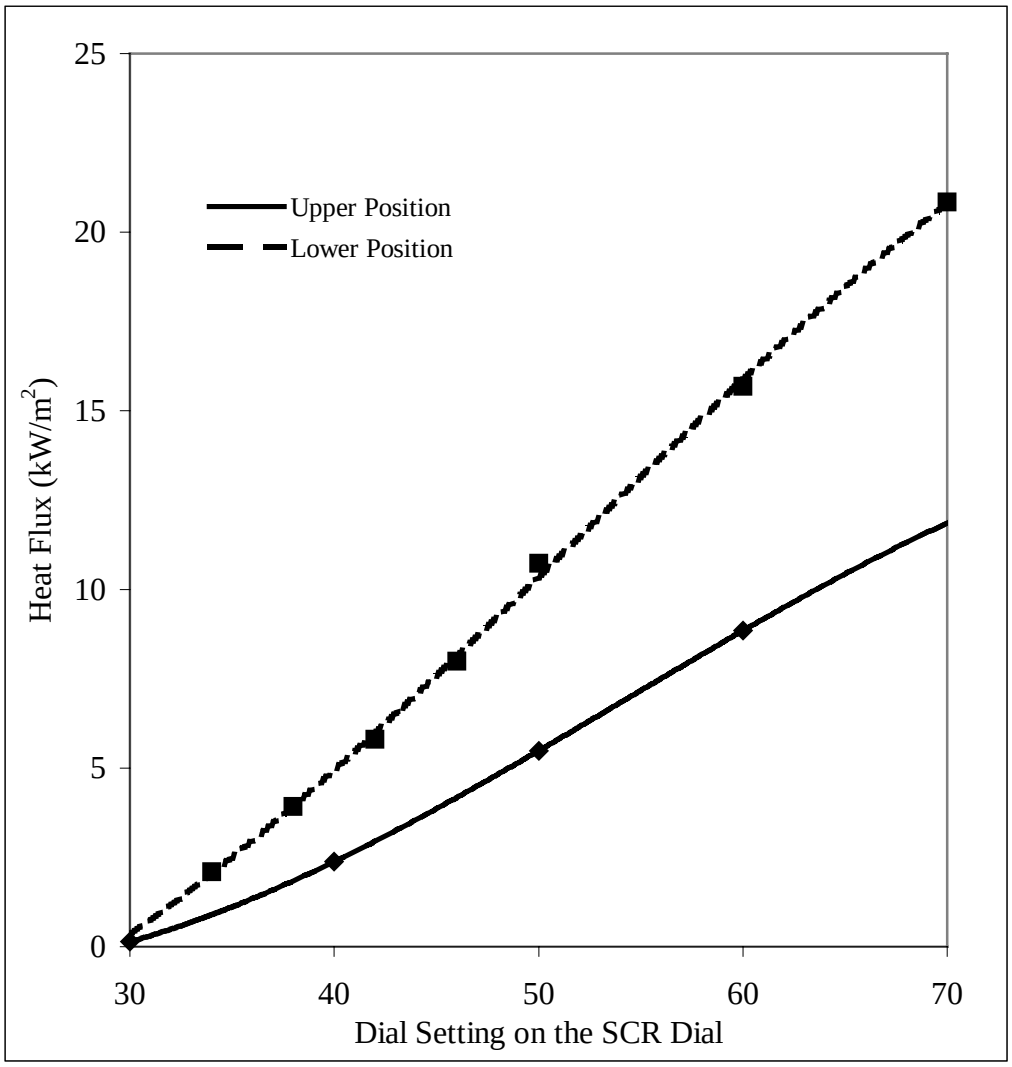

Figure 11. Heat flux variation for different SCR dial settings at lower and upper level mountings of the heater panel

Table 2. Heat Flux Variation on the Pool Surface from Minimum to Maximum Settings of the SCR at the Upper Mounting Level

Position No	**Heat Flux in kW/m^2 for SCR Setting of**			
	40	**50**	**60**	**70**
1	3.18	4.43	6.02	7.33
2	3.01	4.46	5.98	7.23
3	3.18	4.56	6.29	7.61
4	3.18	4.49	6.09	7.33
5	3.01	4.29	5.98	7.23
6	2.97	4.29	5.74	6.92
7	3.04	4.43	5.95	7.12
8	2.97	4.49	5.95	7.23
9	3.11	4.43	6.22	7.47

Table 3. Heat Flux Variation on the Pool Surface from Minimum to Maximum Settings of the SCR at the Lower Mounting Level

Position	**Heat Flux in kW/m^2 for SCR Dial Setting of**						
No	**34**	**38**	**42**	**46**	**50**	**60**	**70**
1	2.06	4.16	5.70	8.04	11.12	15.78	20.49
2	2.04	4.06	5.49	7.86	10.76	15.72	20.01
3	2.16	4.20	5.98	8.28	11.18	14.27	21.10
4	2.03	4.08	5.74	7.92	10.88	15.41	20.13
5	1.99	3.83	5.56	7.80	10.46	14.99	19.78
6	2.07	4.05	6.01	8.16	11.12	16.20	21.52
7	2.18	3.90	5.87	7.98	10.58	16.14	21.09
8	2.04	3.79	5.65	7.80	10.34	15.54	20.67
9	2.21	3.87	6.07	7.92	10.94	15.90	21.76
10	2.19	3.81	5.95	8.16	10.70	16.26	21.88
11	2.06	3.58	5.70	7.86	9.97	15.66	20.37
12	2.16	3.83	5.98	8.10	10.76	16.38	21.28

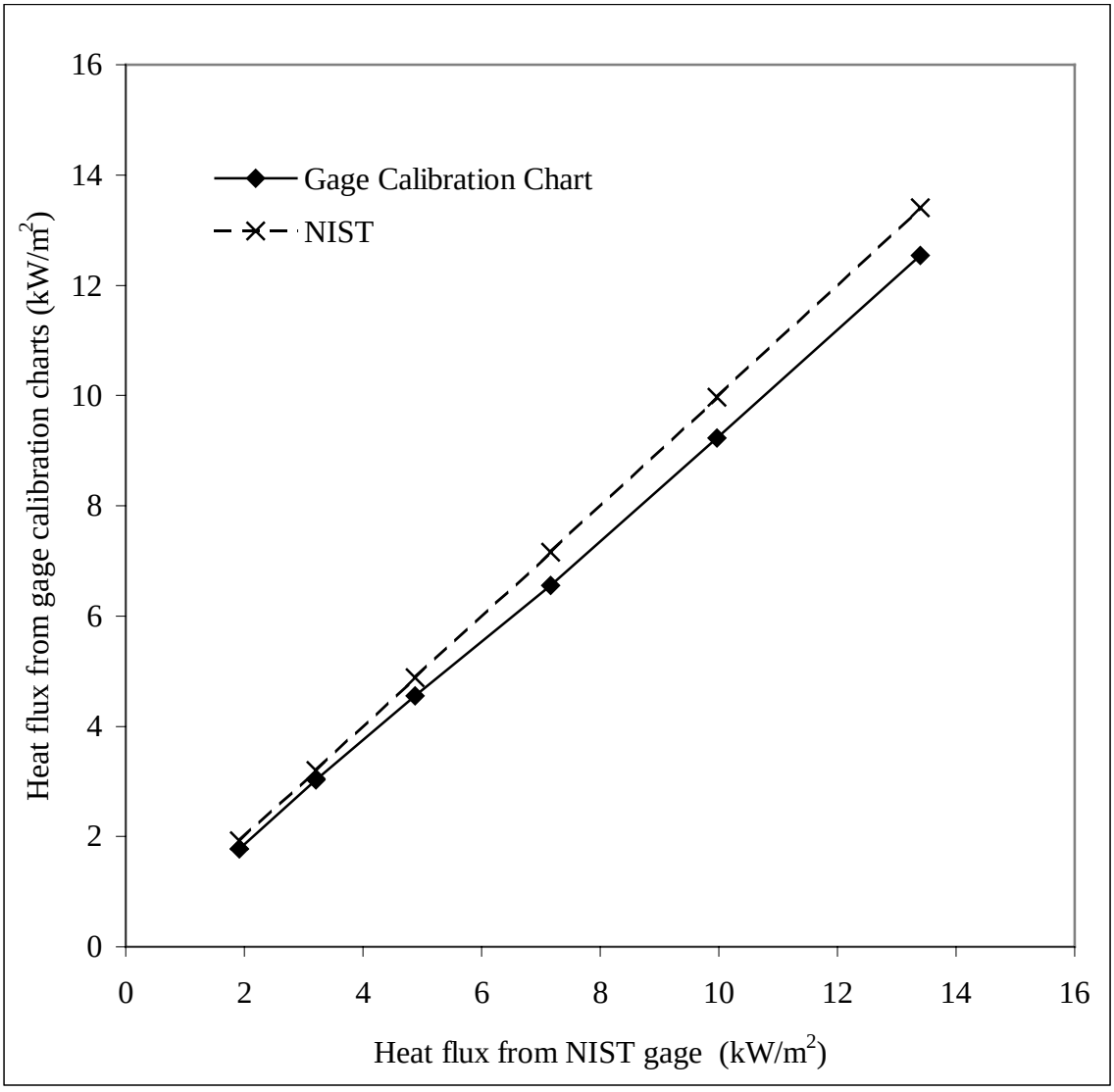

Figure 12. Comparison of the calibration chart provided by the manufacturer of the gage with the NIST master gage.

5.4 Experimental Procedure

A measured amount of oil was first weathered, using the set up shown schematically in figure 7. By measuring the initial and final volumes of the oil, the degree of weathering for the oil sample was determined.

Depending on the proportions of oil and water required in an emulsion, measured volumes of oil and water were poured into four quart sized Ball jars. The jars were then placed into the emulsion making apparatus shown schematically in figure 8 and rotated about the horizontal axis. Continuous rotation for about 48 hours resulted in water-in-oil emulsions with desired proportions of oil and water.

A predetermined amount of the emulsion was poured evenly over the center section of the water in the tank. Initially, the emulsion pool was covered and the heater panels were set to a predetermined heat flux setting. The emulsion pool was uncovered and exposed to the heat flux from the heater panels after the heater panels reached steady state. It was observed during the heater panel calibration that it took approximately 5 minutes for the heater panels to reach steady state at any given heat flux setting. As the emulsion pool was uncovered and exposed to the radiation heat flux, the emulsion would start to heat up. After the surface temperature reached the preset value of 90 °C, an attempt was made to ignite the sample. Upon failure to cause ignition after repeated ignition attempts, the sample was removed from the pool and the panels were turned off and allowed to cool down. After the panels cooled down sufficiently, a new sample of the same type of emulsion was poured evenly over the center section of the water in the tank, the pool was covered from the heater panels and the heat flux level of the panels was increased by a constant, small, predetermined amount. The sample was exposed to the radiation from the panels, after the panels reached the steady state at that particular heat flux setting. Ignition was again attempted as the surface temperature reached the same preset value. The process was continued until sustained combustion was obtained. The resulting fire was monitored with a video camera and other instrumentation as described in the previous section. The minimum value of the heat flux at which successful ignition was achieved was recorded as the threshold heat flux value for the type of the emulsion tested.

For the diesel-water emulsion tests, after the burn was over, the residue was collected by using a wet vacuum cleaner. The contents of the vacuum cleaner were then poured into the residue measuring apparatus shown in figure 10. The apparatus consisted of a measuring cylinder fitted on top of a sealed glass tank. The entire assembly was initially filled with water. Water from the apparatus was removed through the drain and the residue was poured from the top of the cylinder. As the residue is lighter than the water, it floats on top of the water. After all of the residue from the vacuum cleaner was poured, it was left undisturbed for approximately 24 hours so that any excess water that might have gone in the emulsion during vacuuming or pouring could settle down. The volume of the residue was then measured. By using the residue volume measurement, the initial volume of emulsion poured, and the total time of burn, the average burning rate value was calculated.

For the tests involving emulsions of crude oil with water, the center pool used was sealed from the bottom. The mass of the pool with the water and the emulsion in it was measured before the test. The mass was measured again after the burn test. The difference in the mass was considered to be the mass of the oil that burned during the test. The density values for different oils used were measured in the laboratory. Using the density of the oil, the mass of the oil that burned during the test and the time for the burn, the average burning rate value was calculated. Data collected from the lab tests were used as inputs to the mathematical model. Data for the diesel-water tests were also used to validate the mathematical model. The laboratory test data and the results from the mathematical model for the diesel-water emulsions, Alaska North Slope (ANS) crude oil-water emulsions and Milne Point (MPU) crude oil-water emulsions are presented in next chapters.

Chapter 6

DIESEL-WATER EMULSION TEST DATA AND THE MODEL VALIDATION

6.1 Objectives of the Diesel-Water Emulsion Tests

The first series of tests conducted involved diesel-water emulsions. The objectives for this series of tests were as follows:

1. The primary aim of the diesel-water emulsion tests was to verify the concept of a minimum heat flux to cause sustained ignition. Emulsions do not burn when subject to heat flux values lower than this threshold value, and burn when subjected to heat flux equal to or more than the threshold value.
2. It was believed that the threshold heat flux value depends on the amount of water present in the emulsion. This series was designed to evaluate this dependence of threshold heat flux on the water content of the emulsion.
3. Another reason behind conducting the series of tests involving the diesel-water emulsions was to generate experimental data that would be useful in validation of the mathematical model and that would provide insight into the processes involved in the water-in-oil emulsion combustion on top of water surface. In order to validate the model, it was necessary to use the oil for which the thermo-physical property data are available. Commercial # 2 Diesel oil has most of its property data published in the literature.

With these objectives in mind, diesel-water emulsions were tested in the laboratory. Emulsions of diesel and water needed to be made with varying water fractions in the emulsion. Attempts at emulsification of diesel and water did not result in stable emulsions. Commercial # 2 diesel oil, being a refined petroleum product, does not contain the asphaltenes, resins, and waxes that are necessary for formation of stable emulsions with water. Hence, it was decided to add SAE 30 grade motor oil to aid emulsification. The fraction of motor oil was kept constant to 10% by volume. The water

content of the diesel-water-SAE 30 emulsions was varied from 20% to 80% by volume. Tests were conducted according to the procedure described in section 5.4. Observations made during these tests are presented in the following sections.

6.2 Threshold Heat Flux Data for Diesel-Water-SAE 30 Emulsions

As described earlier, the primary objective of the diesel-water-SAE 30 emulsion tests was to verify that there exists a minimum heat flux value such that emulsions that do not burn when subject to heat flux values lower than this threshold value, burn when subjected to heat flux equal to or more than the threshold value.

Table 4 presents a summary of the diesel-water-SAE 30 emulsion tests. The observations made during these tests clearly show that diesel-water emulsions are incombustible when exposed to external radiation heat flux below a certain threshold value. The emulsions, however, can be ignited when exposed to a radiation heat flux equal to or more than the threshold heat flux value. The tests for which the flames spread to cover the entire pool surface, lasting for at least two minutes after the pilot was turned off were classified as successful ignition.

Repeatability of the threshold heat flux values, as observed during the diesel-water emulsion tests, is within 10% of the heat flux values. One or more of the following factors may be responsible for the observed variation in the threshold heat flux values.

1. The heat flux values reported are the average heat flux incident on the surface at a given controller setting. There is variation of ± 5% from the average heat flux over the surface of the pool. The exact heat flux value at the location on the pool where the ignition first takes place may be different from the average heat flux value.
2. Variations involved in manually setting the SCR to the exact dial setting may result in variation in the threshold heat flux reading.
3. The surrounding conditions in the lab, such as the direction and strength of the air currents, the lab temperature, the water temperature, etc. may not be exactly the same for different tests.

Table 4. Summary of the Diesel-Water-SAE 30 Emulsion Tests to Establish the Threshold Heat Flux Values for Varying Water Content of the Emulsion

Emulsion Composition, % by Volume			Radiant Heat Flux (kW/m^2)	Ignition Result
Water	Diesel	SAE 30		
10	80	10	1.40	No Ignition
			1.90	No Ignition
			2.40	**Ignition**
10	80	10	0	No Ignition
			? (Improper heater panel control)	Ignition.
20	70	10	1.4	No Ignition
			1.9	No Ignition
			2.4	**Ignition**
30	60	10	3.1	No Ignition
			3.3	**Ignition**
40	50	10	0.0	No Ignition
			3.1	No Ignition
			3.9	**Ignition**
40	50	10	2.4	No Ignition
			3.0	No Ignition
			3.6	**Ignition**
40	50	10	**8.0**	**Ignition**
50	40	10	2.4	No Ignition
			3.0	No Ignition
			3.6	**Ignition**
50	40	10	? (Improper heater panel control)	Ignition
50	40	10	**3.6**	**Ignition**
50	40	10	**4.5**	**Ignition**

Table 4 (continued). Summary of the Diesel-Water-SAE 30 Emulsion Tests to Establish the Threshold Heat Flux Values for Varying Water Content of the Emulsion

Emulsion Composition, % by Volume			Radiant Heat Flux (kW/m^2)	Ignition Result
Water	Diesel	SAE 30		
60	30	10	3.6	No Ignition
			3.9	**Ignition**
70	20	10	3.3	No Ignition
			3.6	**Ignition**
70	20	10	**3.3**	**Ignition**
80	10	10	3.3	No Ignition
			3.6	No Ignition
			3.9	No Ignition
			4.2	No Ignition
			4.5	No Ignition
			6.0	**Ignition**
80	10	10	4.5	No Ignition
			4.8	No Ignition
			5.1	No Ignition
			5.4	No Ignition
			5.7	**Weak Ignition, Quick Extinction**
			6.0	**Ignition**

4. Though every effort was made to maintain the same level of the emulsion pool, a slight variation in the level of the emulsion pool will mean that even if the SCR setting is the same, the emulsion surface is exposed to a different heat flux value.
5. Emulsions of similar composition may have different water droplet size distribution, depending on the exact time for which the diesel-water-SAE 30 mixture was rotated in the emulsion making apparatus. Fingas *et al.*, (2000b) have reported that the emulsification process proceeds through four distinct states of water-in-oil, each of which has a different emulsion stability class. Shorter duration of mixing may result in larger water droplet sizes inside the emulsion, which will tend to separate at lower heat flux settings.

Figure 13 shows variation of the threshold heat flux values as a function of water content of the diesel-water emulsion. It can be seen that the threshold heat flux value increases as the water fraction of the diesel-water emulsion increases. Heat flux value plotted is the average heat flux incident on the surface of the emulsion pool. Error bars indicate a variation of ± 5% from the average heat flux value at the surface.

Data points for 70% and 80% water emulsions were not considered while fitting the curve through the data points. When the water content of these emulsions becomes high, the SAE 30 motor oil added to cause emulsification is no longer insignificant as compared to the amount of diesel in the emulsion. This is suspected to alter the behavior of these emulsions. The 80% water emulsion was also found to be unstable.

In order to create a sustained fire, the rate at which the oil is separated from the emulsion must be at least equal to the rate at which the oil is consumed by the fire. If the rate of release of oil is less than the rate of burning of oil, the fire will extinguish. When the external heat flux is at the threshold value, the two rates must be very close to each other. As the water content of the emulsion increases, in order to produce oil at a sufficient enough rate, the rate at which the emulsion breaks must increase. Thus, in order to break the emulsion at a faster rate, the required external heat flux increases.

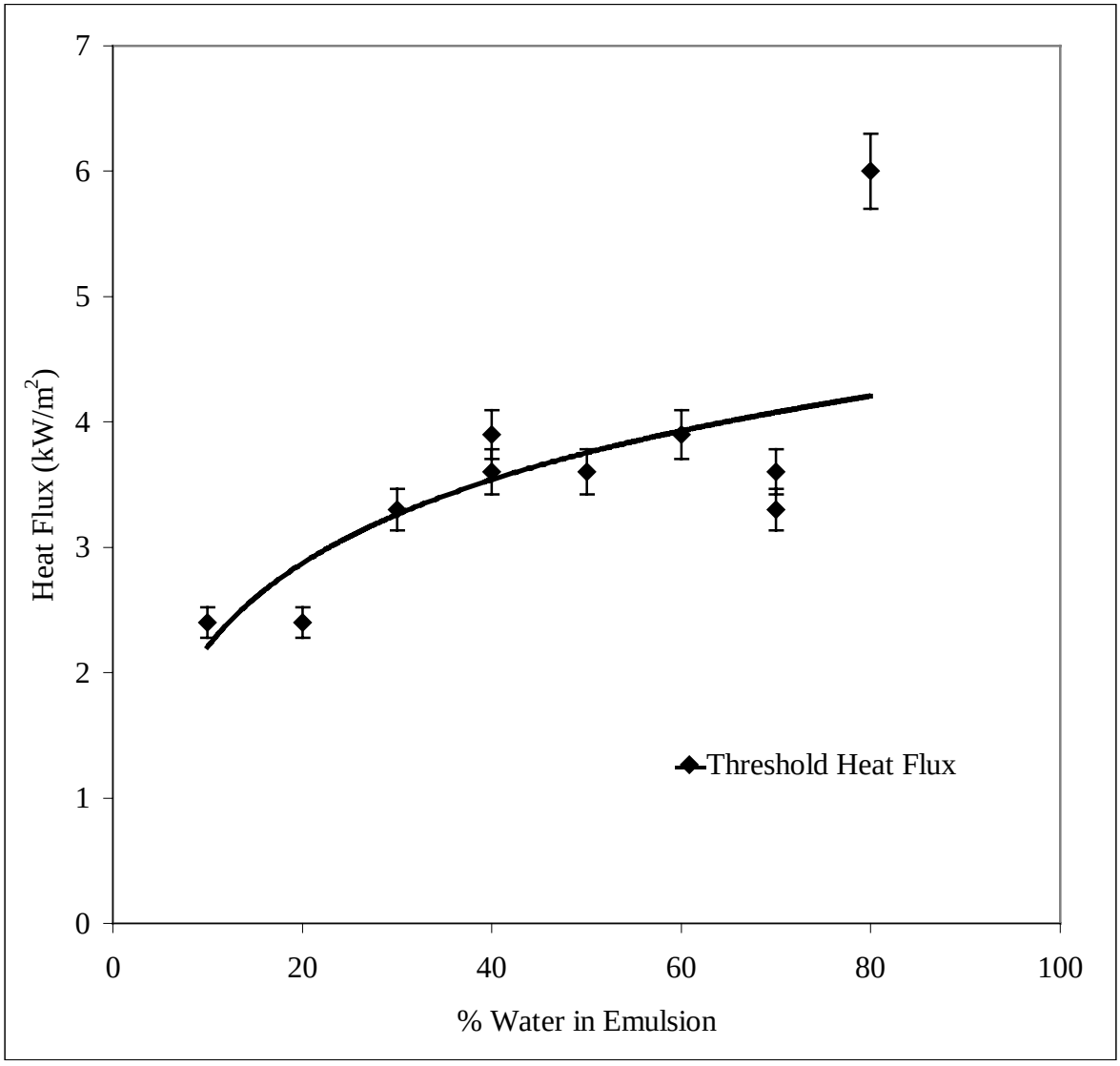

Figure 13. Threshold heat flux required to create a sustained fire as a function of water content of diesel-water emulsion. (Data points for 70% and 80% water in emulsion are not considered in fitting the curve. Please refer to discussion on page 67 for details.)

6.3 Input Data for Validation of the Mathematical Model

The data generated during the diesel-water emulsion tests were used to validate the mathematical model described in chapter 4. The governing equations, the boundary conditions, and the auxiliary conditions were finite differenced, and the numerical solution was programmed in Fortran. To solve the model, various input data were required. The property data required as input to the model are given in table 5. The property data values for commercial # 2 diesel oil were obtained from Vargaftik, 1975 and Arai *et al.,* 1988. The value of optical depth for diesel could not be found in the literature. Hence the optical depth for SAE 30 reported by Putorti (1994) as 1.78 mm was used. Property values used for water were obtained from Incropera and Dewitt (1985). Property values for emulsions were calculated based on weighted values of properties of oil and water in proportion to their mass percentages present in the emulsion. Initial emulsion thickness during the experiments, and hence for the model calculations, was kept constant at 15 mm. For the diesel-water-SAE 30 emulsions, it was observed in our lab and by Pisarchik *et al.,* (1997), that the emulsions begin to separate as the temperature reaches 90°C. This value was used as the constant emulsion breaking temperature.

The values of the initial heat flux incident on the emulsion slick were obtained from the experimental data. When the oil begins to vaporize and burn, the absorbed (not incident) heat flux increases rapidly to the prescribed maximum value, $\dot{q}''_{max}$ (which normally depends on the type of the oil, fire size, wind velocity, and other combustion conditions), and after that, the heat flux is modeled to remain constant. For the diesel-water emulsions, the $\dot{q}''_{max}$ value of 8 kW/m^2 was used. This value yielded a reasonable burn time for one of the test conditions. Hence the value of 8 kW/m^2 was used consistently for all cases. It has been known that a significant amount of flame radiation can be reflected off the oil surface depending on the incident angle, for example, up to 60% for heptane pools at low angles (Hamins *et al.,* 1994). The incident radiative heat flux itself varies considerably from the center to the periphery of a pool fire. For example, for a methanol pool fire, it is about 15 kW/m^2 at the center to about 2 kW/m^2 at the periphery, and for a heptane fire, it is about 20 kW/m^2 at the center to about 15 kW/m^2 at the periphery (Hamins *et al.,* 1994).

Table 5. Property Value Input for the Mathematical Model

	Property	**Value**
Commercial No. 2 Diesel Oil	h_o	10.0 $W/m^2 K$
	ε_o	0.50
	k_o	0.117 W/m K
	α_o	76.77 x 10^{-9} m^2/s
	ρ_o	846 kg/m^3
	c_{po}	1800.0 kJ/kg K
	Q_{Lo}	3.3 x 10^5 J/kg
	Q_{comb}	4.19 x 10^7 J/kg
	T_{ov}	112.0 °C
	β	560.0 m^{-1}
Water	k_w	0.67 W/m K
	α_w	15.7 x 10^{-6} m^2/s
	ρ_w	958.0 kg/m^3
	c_{pw}	4217.0 J/kg K
Emulsion	h_e	10.0 $W/m^2 K$
	ε_e	0.95

The convective heat transfer coefficients for emulsion and oil (10 W/m^{2}K) were based on the value used by Putorti (1994). With T_{ov} = 112 °C and the ambient temperature T_∞ = 25 °C, the convective heat transfer (870 W/m^2) was about 11% of the radiative $\dot{q}''_{\max}$ value (8000 W/m^2). Thus changing the convective heat transfer coefficient from 5 W/m^{2}K to 10 W/m^{2}K to 15 W/m^{2}K, did not affect the model predictions significantly.

6.4 Validation of the Mathematical Model

One of the objectives of the diesel-water emulsion tests was to generate experimental data that could be used to validate the mathematical model. With the input values as described in the previous section, the model was solved numerically for different emulsion compositions. Results obtained from the model were then compared with experimental observations.

Results of the lab scale burn experiments and the corresponding results from the model are presented in tables 6-8. Plots of these and other results are shown in figures 14 to 20. Discussion of the results is presented next.

As described earlier, 90 °C was used as the emulsion separation temperature, and the time from exposure of the emulsion surface to the incident heat flux, to the time required for the top surface of the emulsion to reach 90 °C, was noted. This period was related to the ignition delay, because the ignition occurs soon after the oil starts to appear on the surface of the emulsion. The model could predict the ignition delay based on the time taken for the oil to start vaporizing. Since the oil vaporizes over a range of temperatures, predicting exact ignition delay was difficult from the model results. Also, the ignition delay itself was not measured experimentally, because the ignition delay was very hard to define in present setup. It would be somewhat dependent upon the position of the igniter (because the process is not strictly one-dimensional) and the flashing phenomenon occurring before sustained ignition. Before sustained ignition is achieved, very small sized flames are produced on the pool surface. In the presence of threshold heat flux, these small sized flames keep on flashing until sustained fire is developed. It is very difficult to define the demarcation between the end of flashing and appearance of sustained flame.

Table 6. Comparison of Model Predictions of Emulsion Separation Time with Experimental Data

Plotted in	Figure 14		Figure 15	
%Water	Time for Emulsion Separation at Threshold Heat Flux (s)		Time for Emulsion Separation at a Constant Heat Flux of 8 kW/m^2 (s)	
	Experimental	Model	Experimental	Model
20		540	65	37
30	600	350	65	53
40	430	375	87	68
50	440	470	87	90

Two different values of time for separation are reported in table 6; one was calculated at the threshold heat flux value (which depends on the water content of the emulsion), and the other at a fixed external heat flux value equal to 8 kW/m^2.

Figure 14 shows the time for emulsion separation as a function of the water content of the diesel-water emulsion at the threshold heat flux. For the emulsion with only 20% water, the threshold heat flux value was very low and due to the external cooling effects, in the laboratory setting, the surface temperature did not reach 90 °C before the ignition occurred. Hence no data point was available for this emulsion type.

Figure 15 shows the time for emulsion separation as a function of the water content of the diesel-water emulsion at a constant heat flux of 8 kW/m^2. At a constant external heat flux, time for emulsion separation increases with increasing water content of the emulsion. This may occur because, as the water fraction of emulsion increases, the thermal diffusivity of the emulsion layer increases. This means that the emulsion layer is now conducting more of the heat received than it is absorbing causing a decrease in the rate of increase of temperature. Thus it takes more time for the surface temperature to reach the emulsion breaking temperature.

In both the figures, figure 14 and figure 15, it can be seen that the model predictions show a trend similar to those of the experimental observations. However the trend of the model predictions match the trend of the experimental observations better in Figure 15, but not so well in Figure 14. The reason is that at the threshold heat flux the “flashing” phenomenon is much more prominent. Thus with the presence of the pilot flame from the igniter, small flames are produced locally near the igniter. These flames oscillate a little and spread a little before getting extinguished. As the temperature continues to rise, the flashing flames are sustained and spread to the entire surface. This results in successful ignition. However, the surface temperature fluctuates during the flashing phenomenon and it affects the estimation of the separation time significantly (even with the definition of reaching 90 °C at the surface), particularly at the lower threshold heat flux values (i.e. at the low water content), where the flashing phenomenon lasts longer than at higher heat flux values. Thus, it can be seen in figure 14 that the model predictions agree better with the experimental observations at higher water content.

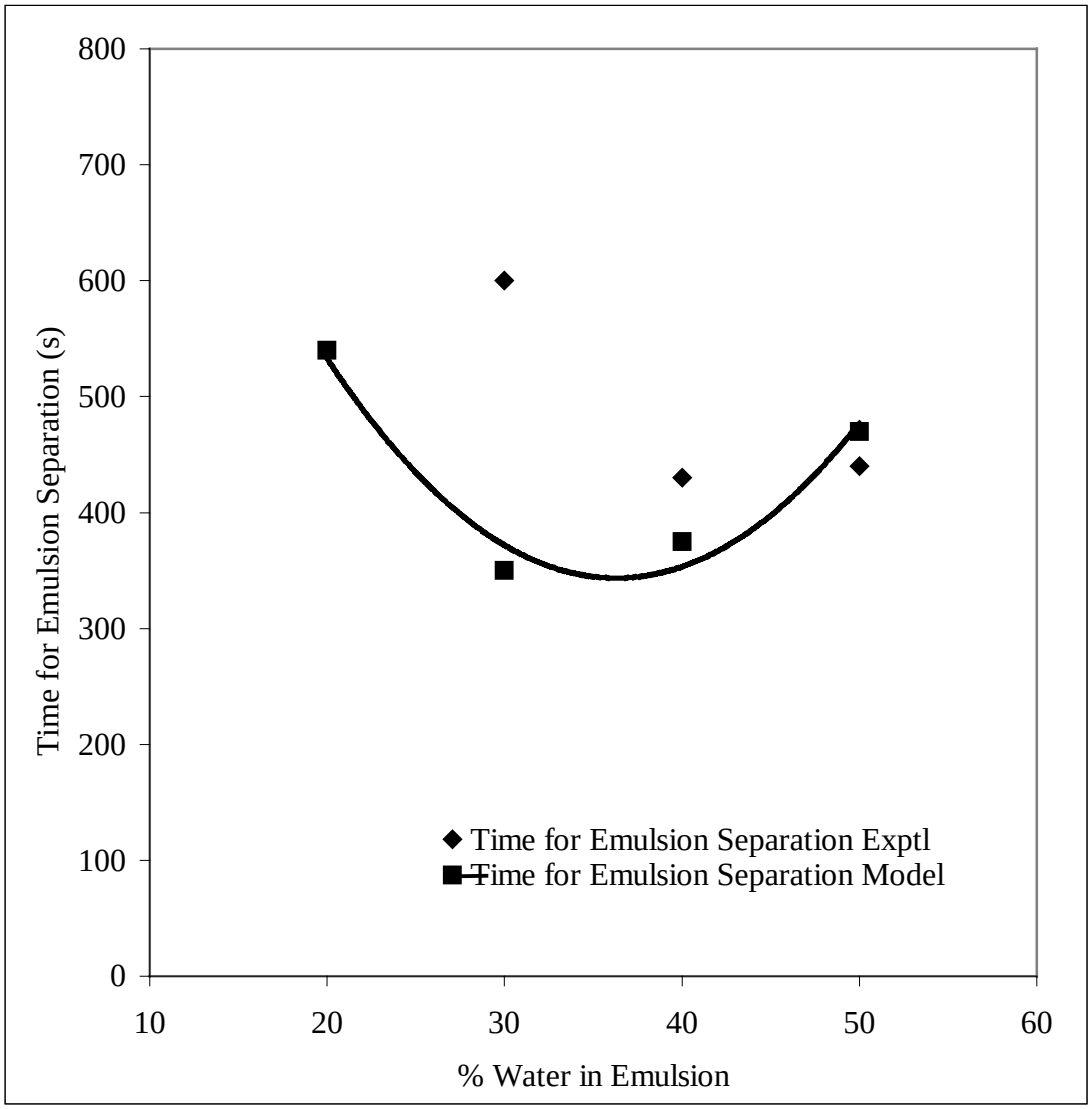

Figure 14. Comparison of model prediction of time for emulsion separation with the experimentally observed values as a function of water content of the diesel-water emulsion at threshold heat flux.

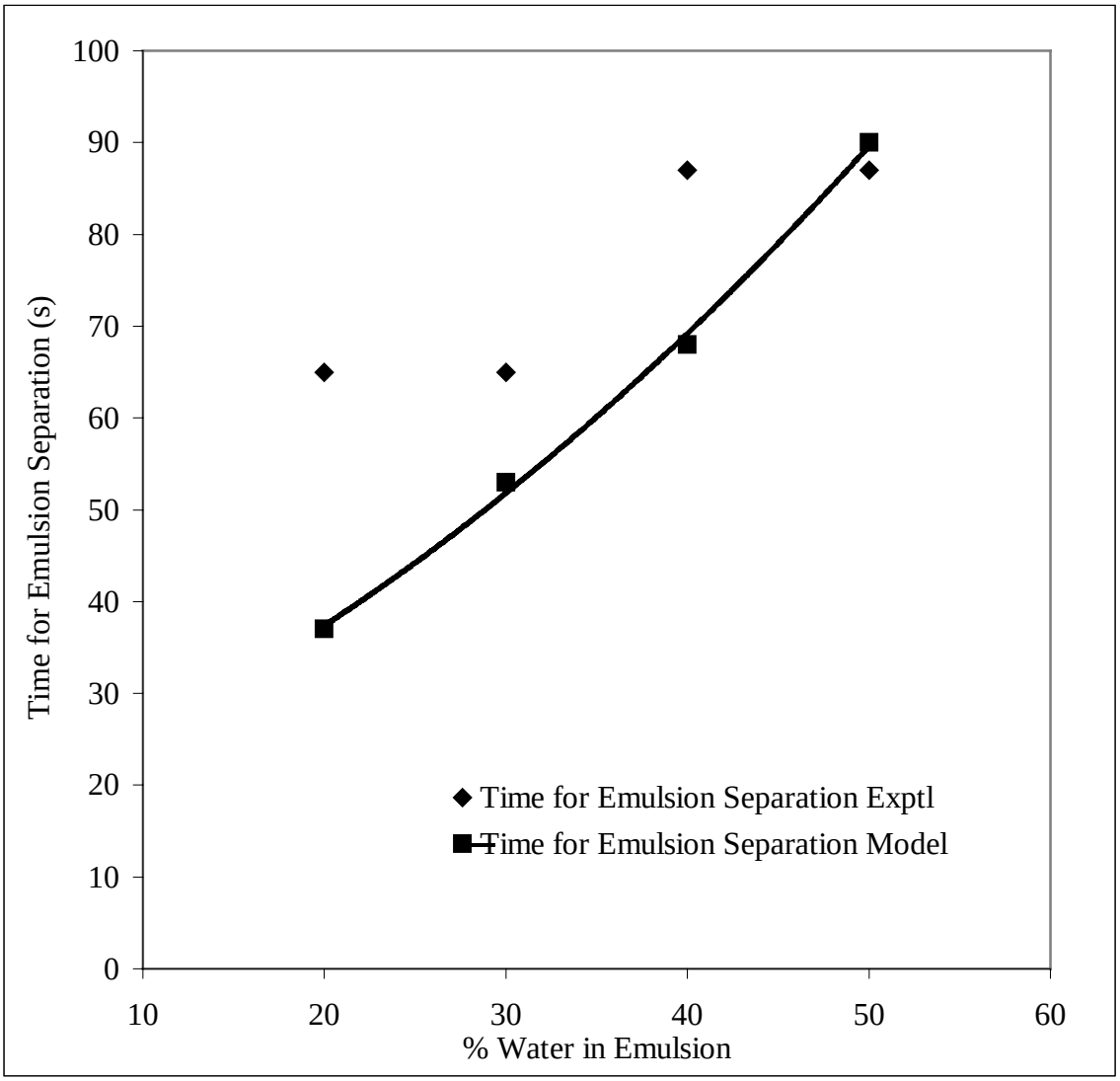

Figure 15. Comparison of model prediction of time for emulsion separation with the experimentally observed values as a function of water content of the emulsion at a constant heat flux of 8 kW/m^2.

Although the model predictions of the time for emulsion separation showed similar trends, they did not match exactly with the experimental observations, as seen in figures 14 and 15. This can be due to a combination of various assumptions involved in the model development such as one dimensional conduction heat transfer inside the condensed phase, no dependence of the water and oil properties on temperature, etc. Errors may also be involved in experimental observations. These can be due to the limitations of the instrumentation as well as due to human factors.

Table 7 and figure 16 present the comparison of the predictions of the temperature profiles from the model with the experimentally observed temperature values at different depths below the surface at various time intervals, after exposing the emulsion pool to the external heat flux. The data presented are for 50 % water in diesel emulsion, heated using heat flux of 3.6 kW/m^2.

Figure 16 shows the temperature variation inside the pool as a function of distance from the pool surface at various time intervals from the start of heating. Continuous lines represent the profiles obtained from the model, whereas the temperature values measured during the experiments are indicated by symbols. It can be seen that the model is able to predict the temperature profile inside the pool at various time intervals with reasonable accuracy. It can be seen that the model predictions for the temperature profile within the emulsion layer match the experimentally observed temperature profiles with less than 10% error. The errors involved in the temperature profiles inside the water body increase with increasing time. Errors involved in exact placement of the thermocouples may be a contributing factor. Errors could be present in arranging the thermocouples in the rake. Additionally, the relative placement of the thermocouples was dependent on placing the top thermocouple exactly at the surface of the pool. Since this was done by visual observation, errors could be present in the placement of the top most thermocouple relative to the pool surface.

Table 7. Comparison of Model Predictions with the Experimental Data of Temperature Profiles Inside the Pool at Different Time Intervals

Distance from the Surface (cm)	Time from the Start of the Heating (s)							
	50		150		250		350	
	Model	Expt	Model	Expt	Model	Expt	Model	Expt
0.0	44.57	42.30	62.14	60.58	73.50	73.34	82.38	82.14
0.5	22.13	21.03	33.60	33.46	43.45	43.00	51.95	50.31
1.0	19.25	19.14	22.50	21.35	28.18	26.65	34.66	31.67
1.5	19.14	19.14	20.03	19.04	23.41	18.65	28.50	22.18
2.0	19.14	19.14	19.99	19.04	23.29	18.65	28.30	19.04

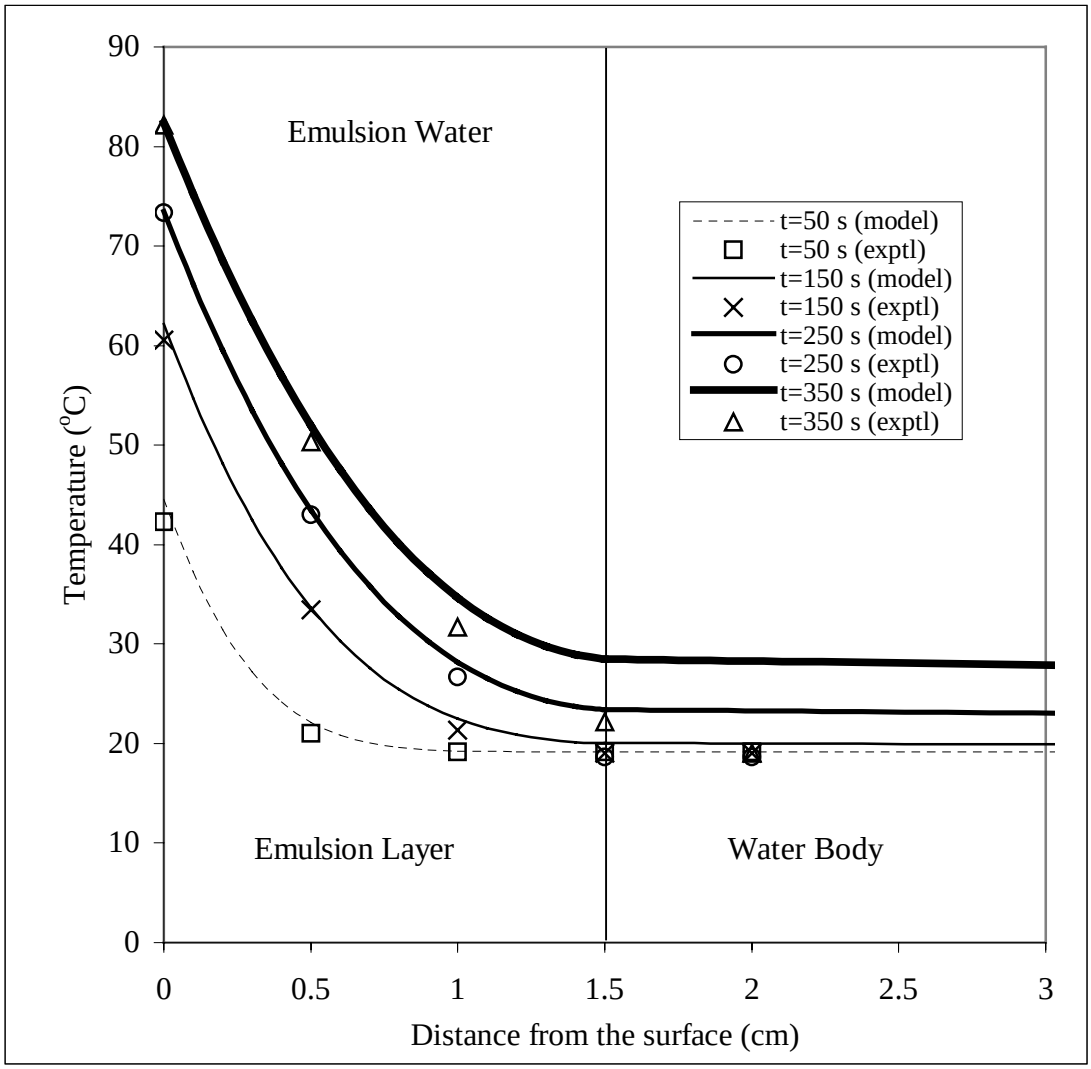

Figure 16. Comparison of model predictions of temperature profiles with the experimentally recorded values of temperatures as a function of distance from the pool surface at various time intervals from start of heating for diesel-water emulsion pool with 50% water in emulsion heated by 3.6 kW/m^2 of external heat flux.

Table 8 shows the comparison of model predictions with the experimental observations for some important pool boiling characteristics such as average diesel burning rate, total burn time, thickness of the diesel residue, and the overall burn efficiency. The results presented in table 8 are plotted in figures 17-20. The discussion of these results is presented next.

Figure 17 shows the comparison of the average diesel burning rate predicted by the model, with the experimental average diesel burning rate values as a function of water content of the diesel-water emulsion. The average burning rate of diesel decreases with increasing water content of the emulsion. This is due to the fact that with more water in the emulsion, there is less diesel separated from the same amount of emulsion. Thus, the diesel available for burning is provided at a slower rate from the emulsion layer. Hence the diesel burning rate is lower. This effect counter balances the fact that with increasing water fraction of the emulsion, the threshold heat flux value will also increase, thus causing the diesel burning rate to increase. The increase in threshold heat flux value with increasing water content ensures the production of diesel layer on top of the emulsion layer at a rate sufficient enough to sustain the fire. Thus though the average burning rate is seen to be decreasing, the rate of decrease is not very high. Even with the increase in water fraction of the emulsion from 20% to 80% the average burning rate decreases only by 25%, as observed by the model predictions.

The experimentally calculated burn rates are consistently lower than the model predictions except for the case of 80% water in the emulsion, which was found to be highly unstable. One of the main approximations involved in the calculation of the average burn rate from the experimental observations was that the residue was assumed to have the same fraction of water by volume as the starting emulsion. However, during the removal of the residue from the pool to the measuring apparatus by use of a vacuum cleaner, it was suspected that the residue emulsified with the water that was also taken up by the vacuum cleaner. Thus, the measured residue may actually have more water than the starting emulsion. Another factor that may have contributed to this observation is the uncertainty in measurement of time at the start of the combustion and the end of the combustion. Due to flashing of fire, it was difficult to measure the exact time at which ignition was achieved.

Table 8. Comparisons of Model Predictions with the Experimental Observations of Important Pool Fire Characteristics

	Figure 17		Figure 18		Figure 19		Figure 20	
% Water	Average Diesel Burn Rate (mm/s) $\times 10^2$		Burn Time (s)		Diesel Residue Thickness (mm)		Overall Burn Efficiency	
	Exptl	Model	Exptl	Model	Exptl	Model	Exptl	Model
20	1.07	1.23	746	695	3.50	3.48	0.67	0.71
30	0.94	1.18	765	651	2.81	2.80	0.69	0.73
40	0.96	0.98	612	578	2.59	3.32	0.65	0.63
50	0.80	1.15	475	439	2.97	2.44	0.50	0.68
60	0.72	0.98	405	361	2.31	2.48	0.49	0.59
70	0.74	0.99	244	240	1.79	2.13	0.40	0.53
80	2.06	0.99	106	129	0.41	1.72	0.73	0.43

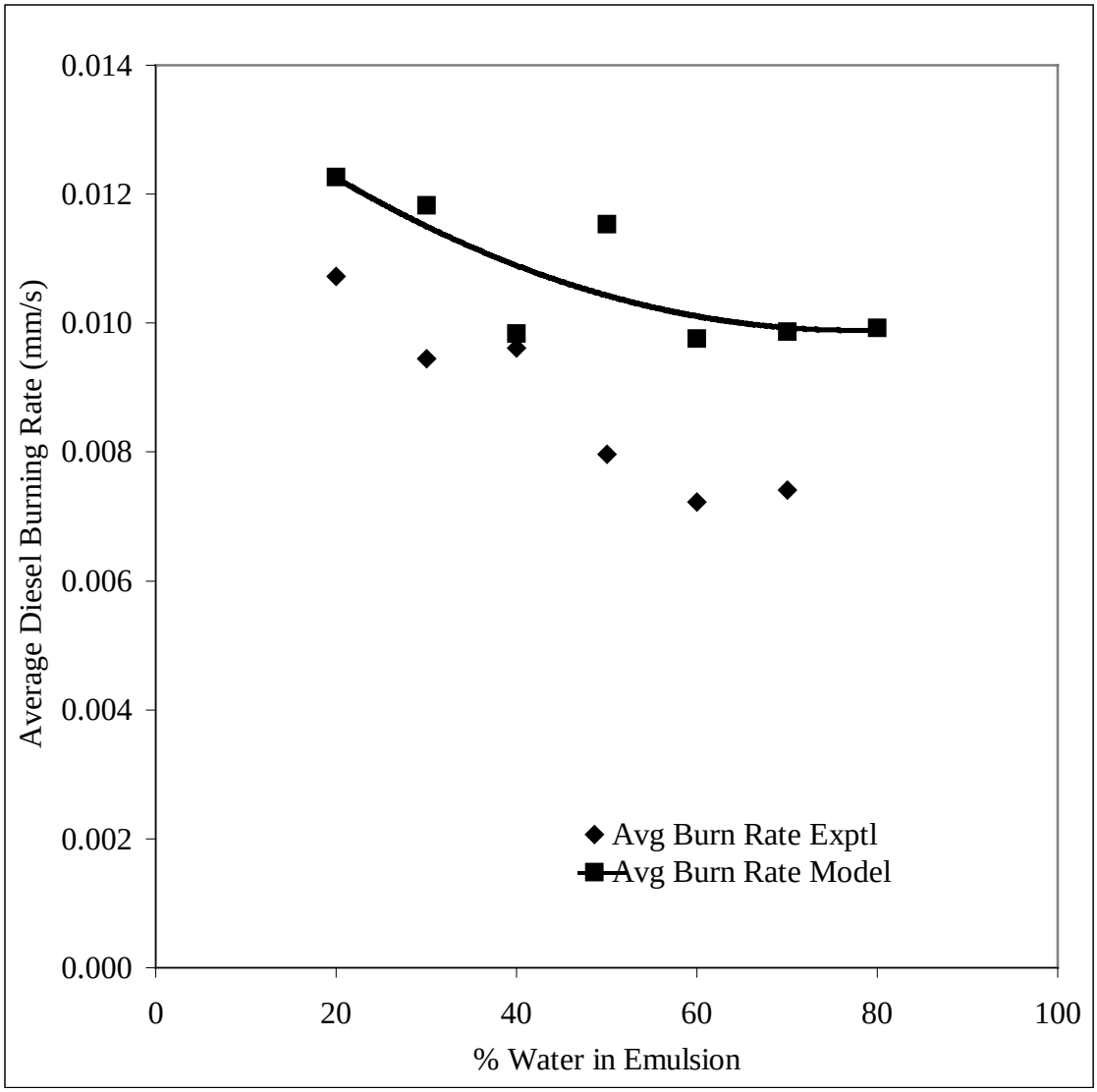

Figure 17. Comparison of average diesel burning rate predicted by the model with the experimental average diesel burning rate values as a function of water content of the emulsion at threshold heat flux.

Figure 18 shows the comparison of the burn time predicted by the model with the experimentally observed values of burn time for different water contents of the emulsion. The burn time is defined as the time from the start of the fire till the fire is extinguished. The comparison between the model predictions and the experimental observations shows a very good agreement. The model predictions are within 20% of the experimental observations.

The total burn time decreases with increasing water content of the emulsion. With increasing water content, the average diesel burning rate decreases, as shown in Figure 17. This effect would result in an increase of the total burn time with increasing water content of the emulsion. However, as the water content of the emulsion increases, for the same starting emulsion thickness, there is less diesel to be burned. This effect results in reducing the total burn time. The latter effect compensates for the increase in burn time due to the reduction in the average burning rate, and reduces the burn time with increasing water fraction in the emulsion.

Figure 19 shows the comparison of diesel residue thickness predicted by the model, with the experimentally measured diesel residue thickness values as a function of water fraction of the emulsion. The diesel residue thickness represents the thickness of the diesel present in the total residue. The diesel residue value was calculated from the measured residue volume, based on the assumption that the residue contained the same fraction of the diesel as the starting emulsion did. The model predictions are found to be within 28% of the experimental observations. Considering the sources of errors present in the experimental measurement technique and the approximations involved in the model, it is believed that the model has predicted the diesel residue thickness with sufficient accuracy to establish the validity of the model.

The diesel residue thickness decreases with increasing water fraction in the emulsion. With more water in the emulsion, there is less diesel to start with. In addition to this, with increasing water fraction of the emulsion, the threshold heat flux value increases. As the extinction occurs because of excessive heat loss to the water body, the emulsion thickness at which the extinction occurs reduces with increasing heat flux. Hence, the combination of these two effects decreases the diesel residue with increasing water fraction of the emulsion.

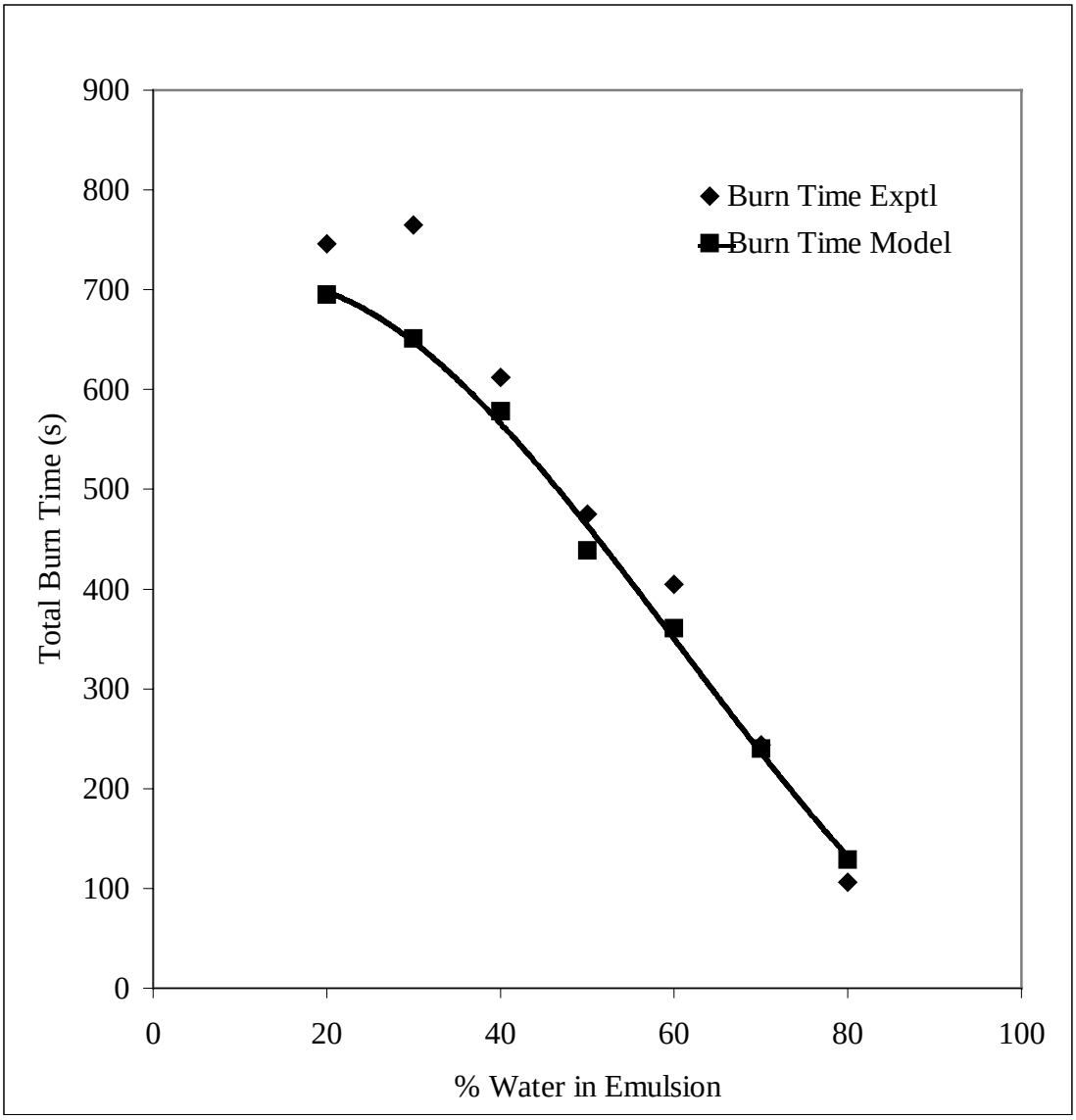

Figure 18. Comparison of the total burn time predicted by the model with the experimentally observed values of the total burn time as a function of water content of the emulsion at threshold heat flux.

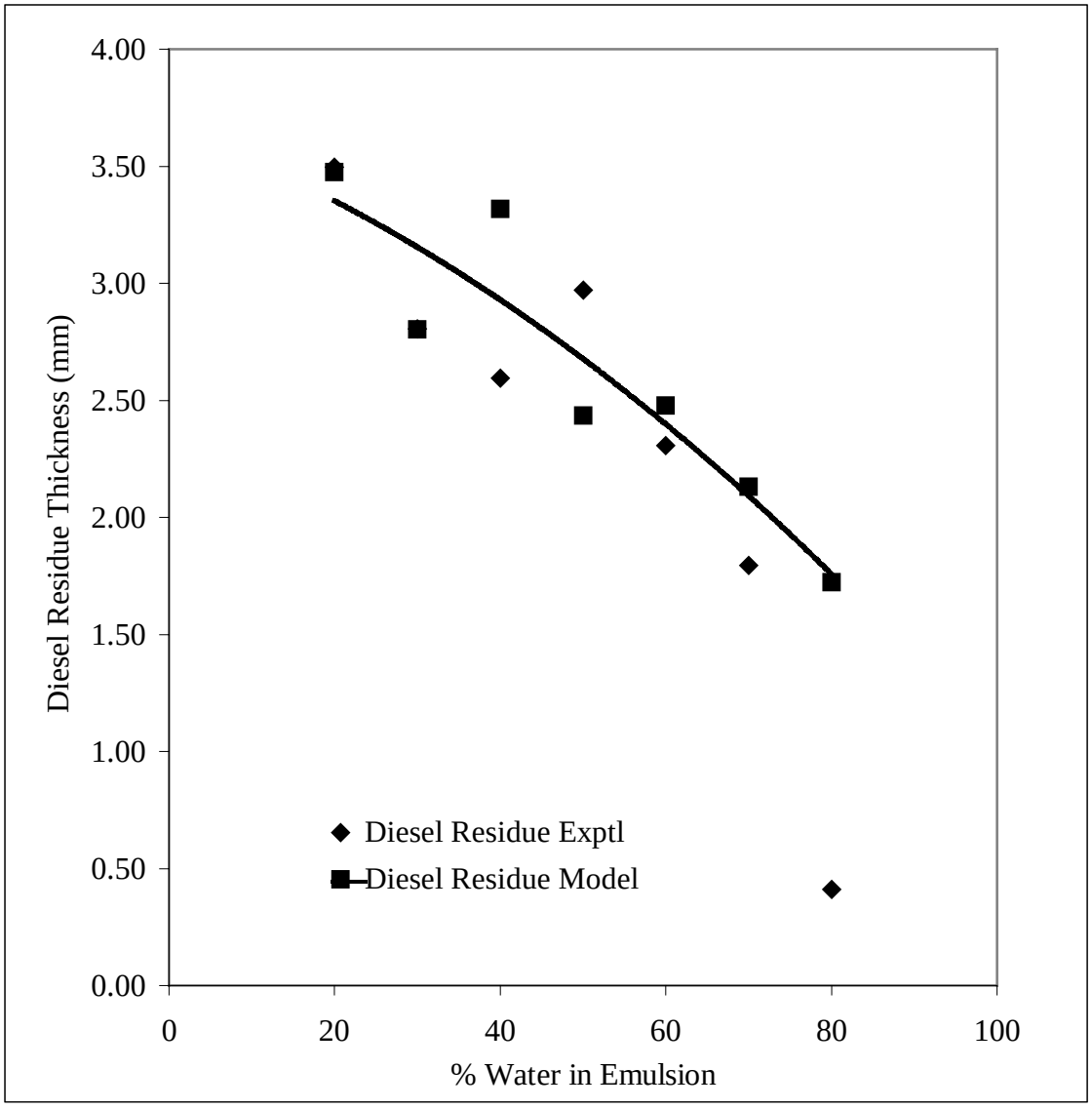

Figure 19. Comparison of the diesel residue thickness predicted by the model with the experimentally measured diesel residue thickness as a function of water content of the emulsion at threshold heat flux.

Figure 20 shows the comparison of the burn efficiency predicted by the model, with the experimentally observed values of the burn efficiency as a function of the water fraction of the diesel-water emulsion. The trend of variation of the burn efficiency for different water contents of the emulsions predicted by the model is similar to the trend observed experimentally. The efficiency values predicted by the model are within 36% of the experimentally measured efficiency values.

Figure 20 shows that the burn efficiency decreases with increasing water content of the emulsion. Figure 19 shows that the amount of the diesel left after the burn decreases as the water fraction in the emulsion increases. This would tend to increase the burn efficiency. However, the amount of diesel present in the emulsion decreases as the water fraction of the emulsion increases. This effect tends to decrease the burn efficiency. The net result is the decrease in the burn efficiency of the emulsion combustion as the water content of the emulsion increases.

The burn efficiency is defined as the ratio of the volume of the diesel burned during the test to the initial volume of the diesel present in the emulsion. Here it should be noted that the efficiency value is strongly dependent on the initial thickness of the emulsion, as the final thickness is governed by the heat loss mechanisms that cause the extinction of the fire. Hence, for a given emulsion type exposed to a particular heat flux, the burn efficiency will increase with increasing initial thickness. It can be argued that the total residue thickness is a better indicator of the effectiveness of the *in-situ* combustion as an oil spill clean up technique. This is because it is the total residue that needs to be removed from the ocean surface after combustion.

Figure 19 shows the variation of the diesel residue thickness with the emulsion water fraction and not the total residue thickness. Diesel residue thickness represents the thickness of the diesel present in the total residue. The variation of the total residue thickness with the emulsion water fraction is presented in figure 21. It can be seen that the total residue left increases with the increase in the water fraction of the emulsion. Thus more the extent of emulsification, the more will be the residue left after combustion when the emulsion is exposed to heat flux values equal to the threshold heat flux values.

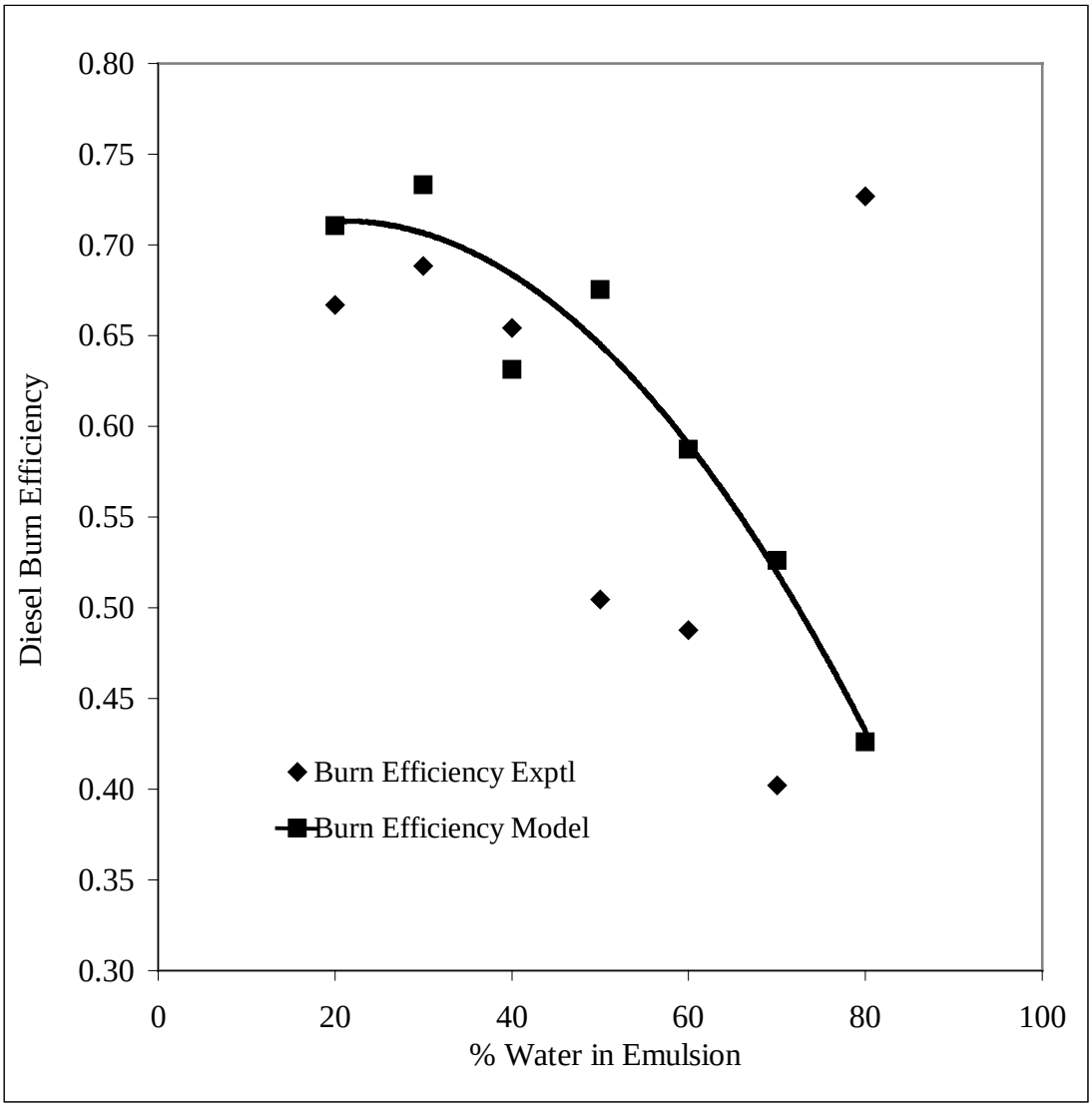

Figure 20. Comparison of the diesel burn efficiency predicted by the model with the experimentally measured diesel burn efficiency as a function of water content of the emulsion at threshold heat flux.

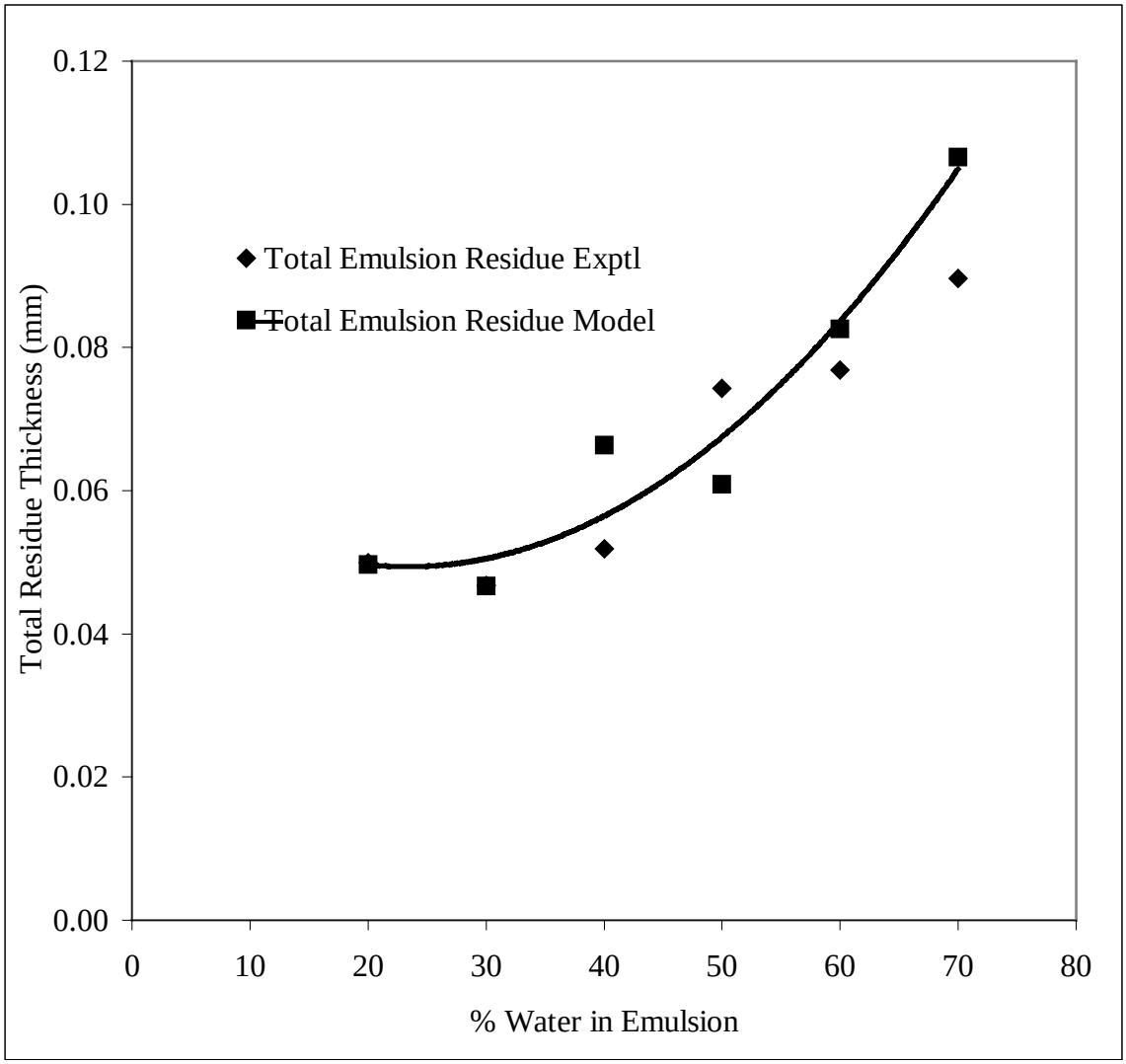

Figure 21. Comparison of the total residue thickness predicted by the model with the experimentally measured total residue thickness as a function of water content of the emulsion at threshold heat flux.

The overall uncertainty in the experimental values is best indicated by the scatter in the data. It is estimated to be about 4% for the burn time measurements, 11% for the residue thickness measurements, and 9% for the burn rate measurements. The threshold heat flux values are estimated to have an uncertainty of about ± 0.3 kW/m^2 in addition to a non-uniformity of ± 5% around the mean values reported.

6.5 Conclusions from the Diesel-Water Emulsion Tests

The laboratory scale burn tests performed using the diesel-water emulsions have shown that *there exists a minimum value of heat flux such that the emulsion layer, when exposed to heat flux levels below such threshold heat flux will not ignite and sustain fire.* However, when the same emulsion is incident with a heat flux higher than or equal to the threshold heat flux value, it will ignite and sustain combustion. One of the factors that threshold heat flux value depends on is the water content of the emulsion. The results for the diesel-water emulsion burn tests performed at laboratory scales show that the threshold heat flux value increases with an increase in water fraction of the emulsion.

Comparisons between different parameters of diesel-water emulsion pool fires predicted by the model and those measured experimentally are presented in this chapter. Analyses of the trends shown by these parameters for increasing water contents of the emulsion and the reasons behind the observed deviations of the model predictions from the experimental measurements are also provided.

It was found that the time for emulsion separation increases with increasing water fraction of the emulsion at a given constant heat flux value. The average diesel burning rate, total duration of the burn, the volume of diesel remaining as residue, and the diesel burning efficiency, all decrease with increasing water content of the emulsion. The total residue thickness, however, was seen to increase with increasing water fraction in the emulsion.

The development of the model involved use of approximations, e.g. approximating the heat feedback from the fire by a constant radiant heat flux, and assumptions, e.g. modeling the separation of emulsion into water and oil as a process occurring at a constant temperature. These approximations and assumptions made the model mathematically tractable. The input data to the model also involved certain

approximation due to lack of availability of the property data values for the commercial diesel oil. However, the comparisons of the model predictions with the experimental observations show that the model has captured the description of significant processes involved in emulsion combustion, and thus is able to describe the experimental observations with sufficient accuracy. In all the comparisons, the trends shown by the experimental observations were similar to the trends predicted by the model. Hence it can be concluded that the model can be used to predict the important emulsion pool fire characteristics.

The next chapter presents the experimental data for burn tests involving emulsions of two crude oil samples and the model predictions of the pool fire characteristics for the emulsions.

Chapter 7

CRUDE OIL EMULSION TESTS AND THE MODEL PREDICTIONS

7.1 Objectives of the Crude Oil-Water Emulsion Tests

The diesel-water emulsion tests were conducted to verify the existence of threshold heat flux and to study the effects of water content of emulsion on the threshold heat flux. However, most of the oil spills on the ocean involve the spillage of crude oils that are being transported, rather than diesel. Hence, it was necessary to verify the concept of existence of threshold heat flux for the crude oil emulsions with water. Also in case of crude oils, the evaporation of different components of the oil affects the oil properties and hence, the threshold heat flux values. The objectives in conducting the laboratory scale tests with the emulsions of crude oils with water were as follows:

1. To verify the concept of the existence of the threshold heat flux for the crude oil-water emulsions.
2. To generate data of the threshold heat flux values for emulsions of some common crude oils, and to investigate the effects of water content of the emulsion and weathering of crude oil on the threshold heat flux values.
3. To use the model predictions to study the effects of water content of emulsion and crude oil evaporation on various emulsion pool fire characteristics, such as the average oil burning rate, the total burn time, the burn efficiency, and the amount of residue left.

Milne Point (MPU) and Alaska North Slope (ANS) crude oils were used for the laboratory scale burn tests to serve the above-mentioned objectives. These two oils were selected primarily as the same two oils were tested by Buist and McCourt, (1998) in similar types of experiments but without the application of the external heat flux. Observations from the emulsion pool fires of MPU and ANS are presented in this chapter. The model predictions using the threshold heat flux data obtained from the laboratory experiments are also presented. Twenty gallons of each of Milne Point crude

oil (MPU) and Alaska North Slope crude oil were obtained from oil wells in Alaska. The oils were shipped in closed steel containers of 5 gallons capacity. The closed containers ensured that there was negligible weathering of the crude oils during the transit. After receiving the crude oils, except for the oil that was in use for the experiments, the rest of the oil was stored in the same closed containers.

7.2 Emulsification and Weathering of Crude Oils

MPU was found to form emulsions quite easily with water. Stable emulsions containing up to 75% of water by volume could be made with the apparatus shown in figure 8 (Chapter 5). This was an interesting observation, as Buist and McCourt had reported that stable emulsions could not be made with fresh (unweathered) MPU. In our case, the fresh MPU emulsions could be obtained with short periods of mixing, and the emulsions were found to be stable even after standing for a period of one week. After personal communication with Mr. Buist and Mr. McCourt of S. L. Ross, Inc, it is suspected that the two samples were probably from different wells, and probably had different additives in them. This could have caused the differences in the emulsion formation properties of MPU observed.

Evaporation of crude oil is known to change properties of oil, and hence, those of the emulsions. One of the objectives of this study was to investigate the effects of evaporation on the threshold heat flux values. Hence, precise evaporation of the crude oils was carried out using the apparatus shown in figure 7 (Chapter 5). The degree of weathering was determined by measuring the volume of oil that was evaporated. For MPU it was found that the degree of evaporation did not exceed 15%, even after bubbling air through the sample for a period of 2 weeks. Though Buist and McCourt (1998) have reported degree of evaporation for MPU as high as 41%, their method of weathering the oil involved heating the oil in water baths to increase the rate of evaporation.

ANS was found not to form emulsions easily with water. Stable emulsions could not be formed with Fresh ANS (unweathered). The oil and water would separate out within a very short time (in the order of few minutes) after the mixing process was stopped. Attempts of aiding the emulsification by adding a small fraction of motor oil also did not yield stable emulsions. Hence, the emulsions of the fresh ANS could be

burned without any external heat flux. Somewhat stable emulsions containing up to 50% of water by volume could be made with a minimum of 15 % weathering of the ANS. This observation was consistent with the data reported by Buist and McCourt (1998) for ANS.

For ANS it was found that the degree of evaporation did not exceed beyond 29% even after bubbling air through the sample for a period of 2 weeks. This is the maximum weathering percentage reported by Buist and McCourt (1998) for ANS.

7.3 Threshold Heat Flux Data for Crude Oil Emulsions

7.3.1 Milne Point Crude Oil-Water Emulsions

Table 9 shows a summary of the tests conducted with the emulsions of MPU-water. In addition to the fresh (i.e. unweathered) MPU, two more levels of evaporation were selected to study the effects of weathering. For all the levels of evaporation, MPU formed stable emulsions with water for all the water fractions in the emulsion.

In comparison to diesel, fires from burning of MPU emulsions produced lesser amounts of soot. For all weathering levels, the emulsions seemed to separate into water and oil between 100 °C and 110 °C. For all the emulsion types involving MPU, the emulsions were seen to be bubbling prior to ignition, as the lighter components of the oil evaporated with increased temperature. As the lighter components were evaporating out of the emulsion layer, the flashing phenomenon was observed for almost all the heat flux levels, even when the heat flux was not sufficient to cause sustained burning. The flashing of flames over the emulsion pool would stop quickly after the pilot flame was turned off. It can be argued that when exposed to the threshold heat flux, the evaporation of the components of MPU occurs at a rate high enough to sustain the fire. Therefore, the cases in which the flashing lasted for at least two minutes after the pilot flame was turned off were considered as successful burn cases. Table 9 clearly verifies the existence of threshold heat flux for the MPU-water emulsions.

Buist and McCourt (1998) have observed that the emulsions of 40.7% weathered MPU containing 60% water by volume could be burned without any external heat flux. However, our lab tests showed that even 10 % weathered unemulsified MPU could not be ignited without imposing external heat flux.

Table 9. Summary of the MPU-Water Emulsion Tests to Establish the Threshold Heat Flux Values for Varying Water Content of the Emulsion

Emulsion Composition, % by Volume		Degree of Evaporation %	Radiant Heat Flux (kW/m^2)	Ignition Result
Water	MPU			
0	100	0	**0.0**	**Ignition**
25	75	0	0	No Ignition
			2.06	No Ignition.
			2.97	No Ignition
			8.12	No Ignition
			9.23	No Ignition
			10.34	**Ignition**
30	70	0	10.34	No Ignition
			11.47	**Ignition**
35	65	0	10.34	No Ignition
			11.47	No Ignition
			13.70	**Ignition**
			15.89	**Ignition**
			16.95	**Ignition**
			18.96	**Ignition**
40	60	0	14.81	No Ignition
			15.89	No Ignition
			17.97	No Ignition
			19.90	No Ignition
			20.79	No Ignition
45	55	0	16.95	No Ignition
			18.96	No Ignition
			20.79	No Ignition
75	25	0	20.79	No Ignition

Table 9 (continued). Summary of the MPU-Water Emulsion Tests to Establish the Threshold Heat Flux Values for Varying Water Content of the Emulsion

Emulsion Composition, % by Volume		Degree of Evaporation %	Radiant Heat Flux (kW/m^2)	Ignition Result
Water	MPU			
0	100	10	0	No Ignition
			4.93	No Ignition
			5.97	No Ignition
			7.03	**Ignition**
			8.12	**Ignition**
			10.34	**Ignition**
25	75	10	10.34	No Ignition
			13.74	No Ignition
			14.81	**Ignition**
			15.89	**Ignition**
30	70	10	17.97	No Ignition
			19.90	**Ignition**
			20.79	**Ignition**
35	65	10	20.79	No Ignition
0	100	15	0	No Ignition
			4.93	No Ignition
			9.23	No Ignition
			10.34	**Ignition**
			15.89	**Ignition**
25	75	15	4.93	No Ignition
			10.34	No Ignition
			15.89	No Ignition
			17.97	No Ignition
			17.97	No Ignition
			18.96	**Ignition**

Table 9 (continued). Summary of the MPU-Water Emulsion Tests to Establish the Threshold Heat Flux Values for Varying Water Content of the Emulsion

Emulsion Composition, % by Volume		Degree of Evaporation %	Radiant Heat Flux (kW/m^2)	Ignition Result
Water	MPU			
30	70	15	15.89	No Ignition
			18.96	No ignition
			20.79	No Ignition

Two main factors could be responsible for these observed differences. First, as described earlier, the two oil samples tested may be quite different, as they may be from different oil wells and may have different additives in them. Thus, in the case of Buist and McCourt (1998), since the MPU had very low emulsion stability, the emulsions might have separated very easily during the burn tests, thus making it possible to burn the emulsions containing up to 60% of water. Another reason that may have possibly contributed to the observed differences is the difference in the types of the igniters used in the two studies. In the studies by Buist and McCourt (1998), the igniter used was gelled gasoline, whose amount varied from 500 ml for fresh oil burns to 3.75 liter for emulsion burns. These igniters themselves might have provided the required threshold heat flux on the emulsion surface to initiate combustion. In our studies, the igniter used was a pilot flame of propane gas that imposed negligible heat flux at the point of contact on the emulsion surface.

One of the limitations of the present set up is that the maximum heat flux that can be imposed on the emulsion pool surface is 20.8 kW/m^2. Hence the emulsions that require heat flux higher than 20.8 kW/m^2 could not be burned in the present set up. Due to this limitation, emulsions of the fresh MPU with more than 35% water, emulsions of 10% weathered MPU with more than 30% water, and emulsions of 15% weathered MPU with more than 25% water could not be burned in the present set up. Figure 22 shows the variation of the threshold heat flux values for MPU-water emulsions with water content of the emulsions at different degrees of weathering. The threshold heat flux value increases with an increase in water fraction of the MPU-water emulsion. As the water content of the emulsion increases, the rate at which the oil is released from the emulsion decreases at a fixed heat flux. Hence, to maintain a sufficient rate of oil removal from the emulsion to sustain combustion, the required heat flux increases. Therefore, the threshold heat flux increases with increasing water fraction of the emulsion.

Figure 22 shows that the threshold heat flux value increases with the increase in the degree of evaporation of the crude oil. With increased evaporation of the lighter fractions of the crude oil, the density and the viscosity of the crude oil increases. As the lighter components of the crude oil evaporate out, the impurities like the asphaltenes and the waxes that are soluble in these lighter components precipitate out.

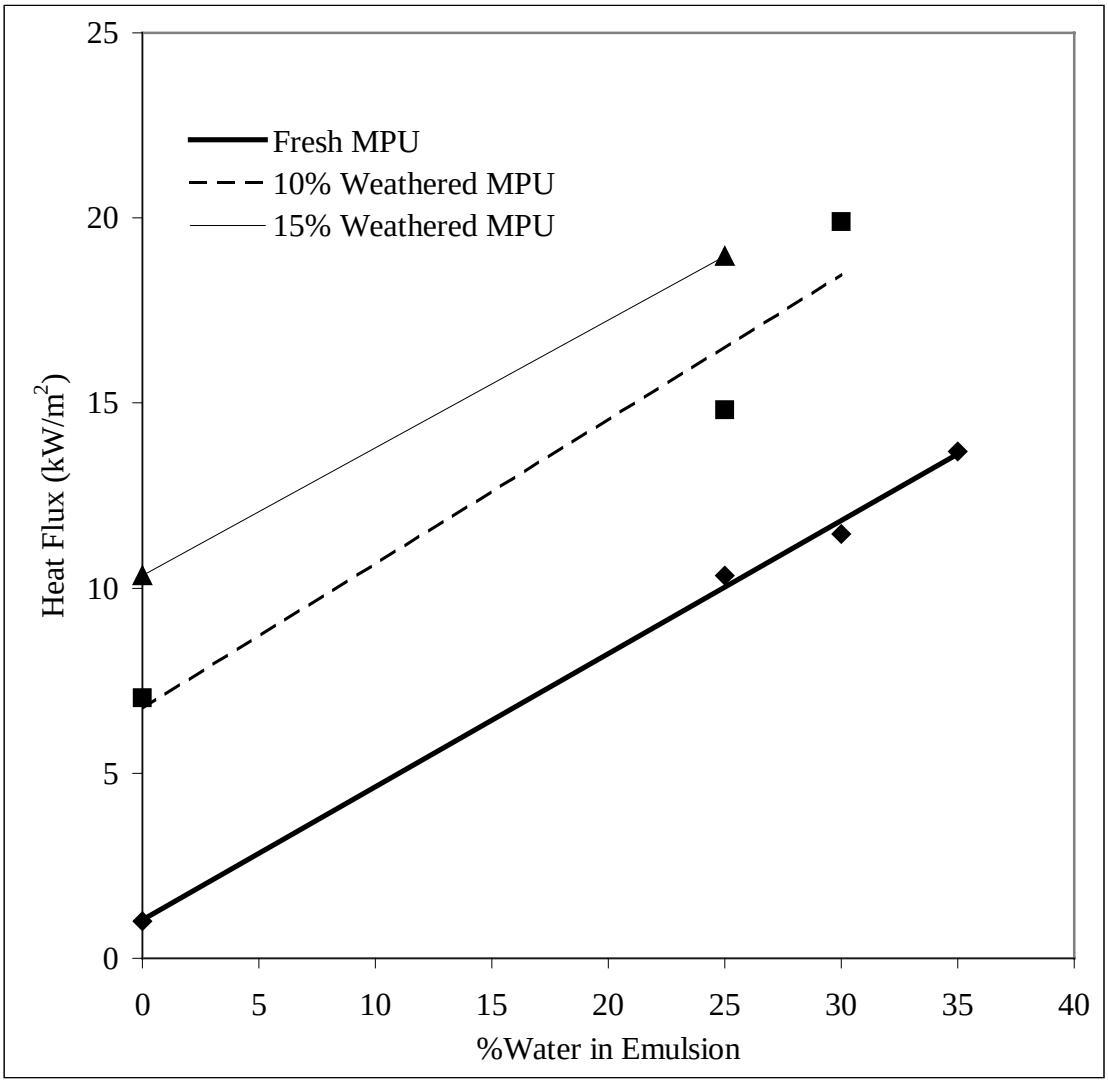

Figure 22. Threshold heat flux required to create a sustained fire as a function of water content of MPU-water emulsion at different degrees of weathering of MPU.

Since, these impurities act as emulsifying agents, the emulsions of the crude oils that have higher degree of weathering are harder to separate. In order to maintain the rate of release of oil from such emulsions enough to sustain the fire, more external heat flux is required to be imposed. The above data verify the concept of the existence of threshold heat flux for the emulsions of MPU with water.

7.3.2 Alaska North Slope Crude Oil-Water Emulsions

Table 10 shows a summary of the tests conducted with the emulsions of ANS-water. Three levels of degree of evaporation were selected to study the effects of weathering. The tests were conducted within a few hours of stopping the mixing of the emulsions. The fires from burning of ANS emulsions produced substantial amounts of soot. The fires were the tallest among the three oils, ANS, MPU and diesel, tested. For all weathering levels, the emulsions seemed to separate into water and oil between 90 °C and 97 °C. For all the emulsion types involving ANS, vapors of oil leaving the surface of the emulsion were visible, as the lighter components of the oil evaporated with increased temperature. However, unlike the MPU emulsions, no bubbling was observed. Table 10 clearly verifies the existence of threshold heat flux for the ANS-water emulsions

Buist and McCourt (1998) have observed that the emulsions of 29% weathered ANS containing a maximum of 25% water by volume could be burned without any external heat flux. However, our lab tests showed that even 20% weathered unemulsified ANS could not be ignited with out imposing external heat flux. A reason that may have possibly contributed to the observed differences is the difference in the types of the igniters used in the two studies. In the studies by Buist and McCourt (1998), a sequence of igniters was used, starting from a 10-second exposure to finally adding 2 mm layer of fresh crude oil on top of the emulsion slick layer and igniting it with a propane torch. These ignition approaches themselves might have provided the required threshold heat flux on the emulsion surface to initiate combustion. In our studies, the igniter used was a pilot flame of propane gas that imposed negligible heat flux at the point of contact on the emulsion surface.

Table 10. Summary of the ANS-Water Emulsion Tests to Establish the Threshold Heat Flux Values for Varying Water Content of the Emulsion.

Emulsion Composition, % by Volume		Degree of Evaporation %	Radiant Heat Flux (kW/m^2)	Ignition Result
Water	ANS			
0	100	0	**0.0**	**Ignition**
35	65	0	**0.0**	**Ignition**
0	100	15	**0.0**	**Ignition**
25	75	15	0.0	No Ignition
			1.2	**Ignition**
40	60	15	0.0	No Ignition
			1.2	**Ignition**
50	50	15	0.0	No Ignition
			1.2	**Ignition**
			2.06	**Ignition**
60	40	15	0.0	Ignition, Emulsion Unstable.
0	100	20	0.0	No Ignition
			1.2	No Ignition
			2.06	**Ignition**
25	75	20	0.0	No Ignition
			2.06	No Ignition
			2.97	**Ignition**
40	60	20	0.0	No Ignition
			2.97	No Ignition
			3.93	**Ignition**
			4.93	**Ignition**
50	50	20	0.0	No Ignition
			2.97	No Ignition
			3.93	**Ignition**

Table 10 (continued). Summary of the ANS-Water Emulsion Tests to Establish the Threshold Heat Flux Values for Varying Water Content of the Emulsion.

Emulsion Composition, % by Volume		Degree of Evaporation %	Radiant Heat Flux (kW/m^2)	Ignition Result
Water	ANS			
0	100	26	0.0	No Ignition
			2.06	No Ignition
			2.97	**Ignition**
			4.93	**Ignition**
25	75	26	0.0	No Ignition
			2.97	No Ignition
			3.93	No Ignition
			4.93	**Ignition**
			7.03	**Ignition**
40	60	26	0.0	No Ignition
			5.97	No Ignition
			7.03	**Ignition**
			8.12	**Ignition**
			15.89	**Ignition**
50	50	26	0	No Ignition
			8.12	No Ignition
			9.23	**Ignition**
			10.34	**Ignition**
60	40	26	**7.03**	**Ignition, Emulsion Unstable**
			9.23	

Figure 23 shows the variation of the threshold heat flux values for ANS-water emulsions with water content of the emulsions at different degrees of weathering. The threshold heat flux value increases with an increase in water fraction of the ANS-water emulsion with the increase in the degree of evaporation of the crude oil. These trends are similar to the trends observed for the MPU-water emulsions in figure 22. The reasons for these observed trends are discussed in 7.3.1. The data from the ANS-water emulsion burn tests verify the concept of existence of threshold heat flux for the emulsions of ANS with water.

7.4 Input Data for Model Predictions for the Crude Oil-Water Emulsions

The property value data as input to the model such as the thermal conductivity, specific heat capacity, latent heat of vaporization, and the heat combustion were obtained from Cragoe (1929). These data were provided for crude oil as a function of the crude oil density *(ρ)* in g/cm^3 and temperature *(T)* in °C for all the properties except for the heat of combustion, for which the values depend only on the density. A constant temperature of 15 °C was used to evaluate the properties. Sensitivity analysis showed that changing the temperature from 15 °C to 25 °C changed the property values by less than 4%. Following equations show the functional relationships used to calculate the values:

$$Heat\ of\ Combustion\ (J/kg) = 51.8816\times10^{6} - 8.7864\times10^{6}\times\rho^{2} \quad (48)$$

$$Thermal\ Conductivity\ (W/m^{\circ}C) = \frac{0.1172}{\rho}(1-0.00054\times T) \quad (49)$$

$$Specific\ Heat\ Capacity\ (J/kg^{\circ}C) = \frac{4184}{\sqrt{\rho}}(0.403+0.00081\times T) \quad (50)$$

$$Latent\ Heat\ of\ Vaporization\ (J/kg) = \frac{4184}{\rho}(60-0.09\times T) \quad (51)$$

The density values required as input to the above equation were measured for MPU and ANS in the laboratory. Volume measurements of samples of MPU and ANS with varying degrees of evaporation were made, using a graduated cylinder. Mass of the samples of known volume were then measured, using an electronic balance with accuracy of 0.1 g. Tables 11 and 12 show the density measurements for MPU and ANS respectively, and the respective property values obtained using equations 48-51.

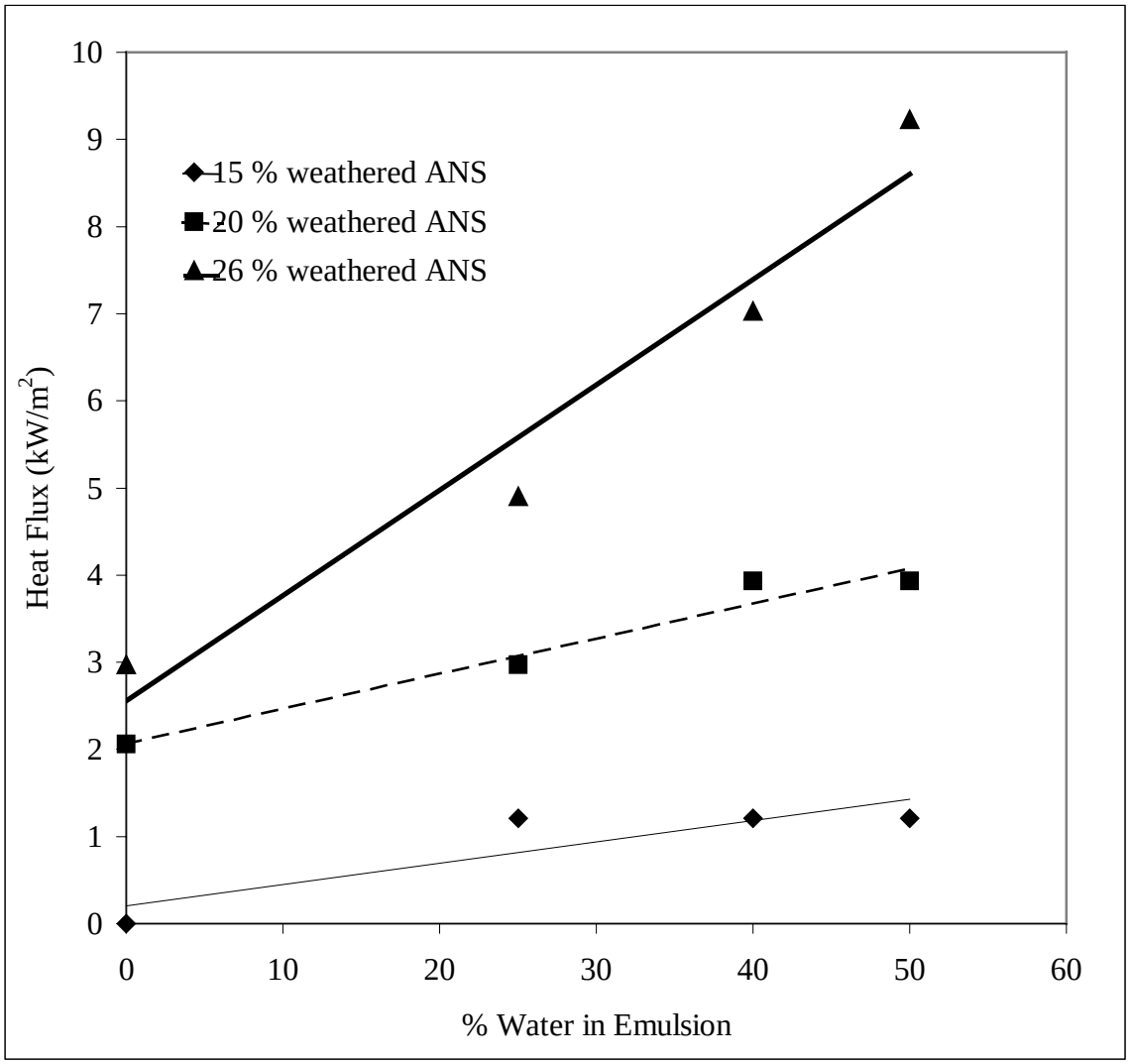

Figure 23. Threshold heat flux required to create a sustained fire as a function of water content of ANS-water emulsion at different degrees of weathering of ANS.

Table 11. Thermo-physical Properties for MPU

Degree of Evaporation	Density	Heat of Combustion	Thermal Conductivity	Specific Heat Capacity	Latent Heat of Vaporization
(%)	(kg/m^3)	(J / kg)	(W / m °C)	(J / kg °C)	(J / kg)
0	931.83	$4.43x10^7$	0.125	1799.40	$2.63x10^5$
10	950.13	$4.40x10^7$	0.122	1781.99	$2.58x10^5$
15	956.78	$4.38x10^7$	0.122	1775.79	$2.57x10^5$

Table 12. Thermo-physical Properties for ANS

Degree of Evaporation	Density	Heat of Combustion	Thermal Conductivity	Specific Heat Capacity	Latent Heat of Vaporization
(%)	(kg / m^3)	(J / kg)	(W / m °C)	(J / kg °C)	(J / kg)
15	901.01	$4.48x10^7$	0.129	1829.92	$2.72x10^5$
20	901.35	$4.47x10^7$	0.129	1829.57	$2.72x10^5$
26	916.75	$4.45x10^7$	0.127	1814.14	$2.68x10^5$

In addition to the input properties listed in tables 11 and 12, the model requires the emulsion breaking temperature and the oil vaporization temperature as input data. Both of these were approximated from the observations made during the laboratory tests. For MPU, the emulsion breaking temperature was between 92 °C and 97 °C, whereas the oil vaporization temperature was approximated to be between 102 °C and 107 °C, depending on the degree of evaporation the oil had undergone. For ANS, the emulsion breaking temperature was between 90 °C and 97 °C, whereas the oil vaporization temperature was approximated to be between 100 °C and 107 °C, depending on the degree of evaporation the oil had undergone.

The threshold heat flux values were used as the external heat flux values for the respective emulsion types. For the case of fresh (unweathered) MPU oil (unemulsified) the initial incident heat flux was kept to 1 kW/m^2, as the model could not proceed with zero heat flux. Similarly, for the case of 15% weathered ANS oil (unemulsified), the initial incident heat flux was kept to 1 kW/m^2, although the experimental observations showed that the oil could be ignited without any external heat flux.

For the MPU-water emulsion model predictions, the maximum net absorbed heat flux value was approximated to be 12 kW/m^2. For the diesel-water emulsion case, the value of maximum net absorbed heat flux was approximated to be 8 kW/m^2. In case of MPU emulsion fires, the soot production was not as high as the diesel-water emulsion fires. Hence, in addition to the heat feedback from the fire, a fraction of the heat flux from the heater panels may also have reached the emulsion surface. The maximum net absorbed heat flux value was approximated to be 5 kW/m^2 for the ANS-water emulsion model predictions. Test cases, one for each MPU and ANS, yielded average burn rates values with the use of above-mentioned $\dot{q}''_{\max}$ values that were comparable to the experimentally observed burn rates. Hence, the same values were used consistently for all cases of the respective oils.

The optical depth of 2.25 mm reported by Inamura *et al.,* (1992) for the Alberta Sweet crude oil was used. A convective heat transfer coefficient of 10 W/m^2 K and absorptivity and emissivity between 0.90 and 0.99 were used.

7.5 Comparison of Model Predictions for the Crude Oil-Water Emulsions with Data from Literature

The mathematical model described in chapter 4 was used with the input data described above, to predict the emulsion pool fire characteristics, such as average oil burn rate, time of burn, thickness of oil residue left, and efficiency of the burn. The model was validated in the previous chapter using the experimental data from the diesel-water emulsion tests. Comparisons of some of the model predictions with the published data for burn tests performed under different conditions are presented next.

Figure 24 and figure 25 show a comparison of the model predictions with the data presented by Buist and McCourt (1998) for the fresh MPU with no external heat flux imposed. The model predictions are similar in magnitude to the data from Buist and McCourt (1998).

As discussed earlier, the Milne Point crude oil tested by Buist and McCourt at S. L. Ross, Inc, in Ottawa had quite different properties compared to those obtained at Penn State. They have reported that the sample of MPU they tested had very low emulsion formation tendency and very low emulsion stability. The sample of MPU tested in our lab, however, would form emulsions readily and these emulsions would be extremely stable. As the sample source well changes, the oil properties are believed to change. Oil properties are also dependent on the additives that are added to the crude oil to facilitate its transportation. Thus, although the values presented here are valid for the sample of the oil tested, extending the same data to cover MPU from different wells obtained at different times may be difficult.

Figure 26 and figure 27 show a comparison of the model predictions with the data presented by Buist *et al.,* (1995) for weathered ANS with no external heat flux imposed. While the model predictions are similar in magnitude to the data from Buist *et al.,* (1995), the tests conducted by Buist *et al.,* (1995) were under different conditions.

With the comparisons discussed above and the model validation presented in chapter 6, it can be seen that the model can predict various characteristics of emulsion pool fire with adequate accuracy. In the next section the model predictions are used to study the effects of emulsification and oil weathering on such pool fire characteristics.

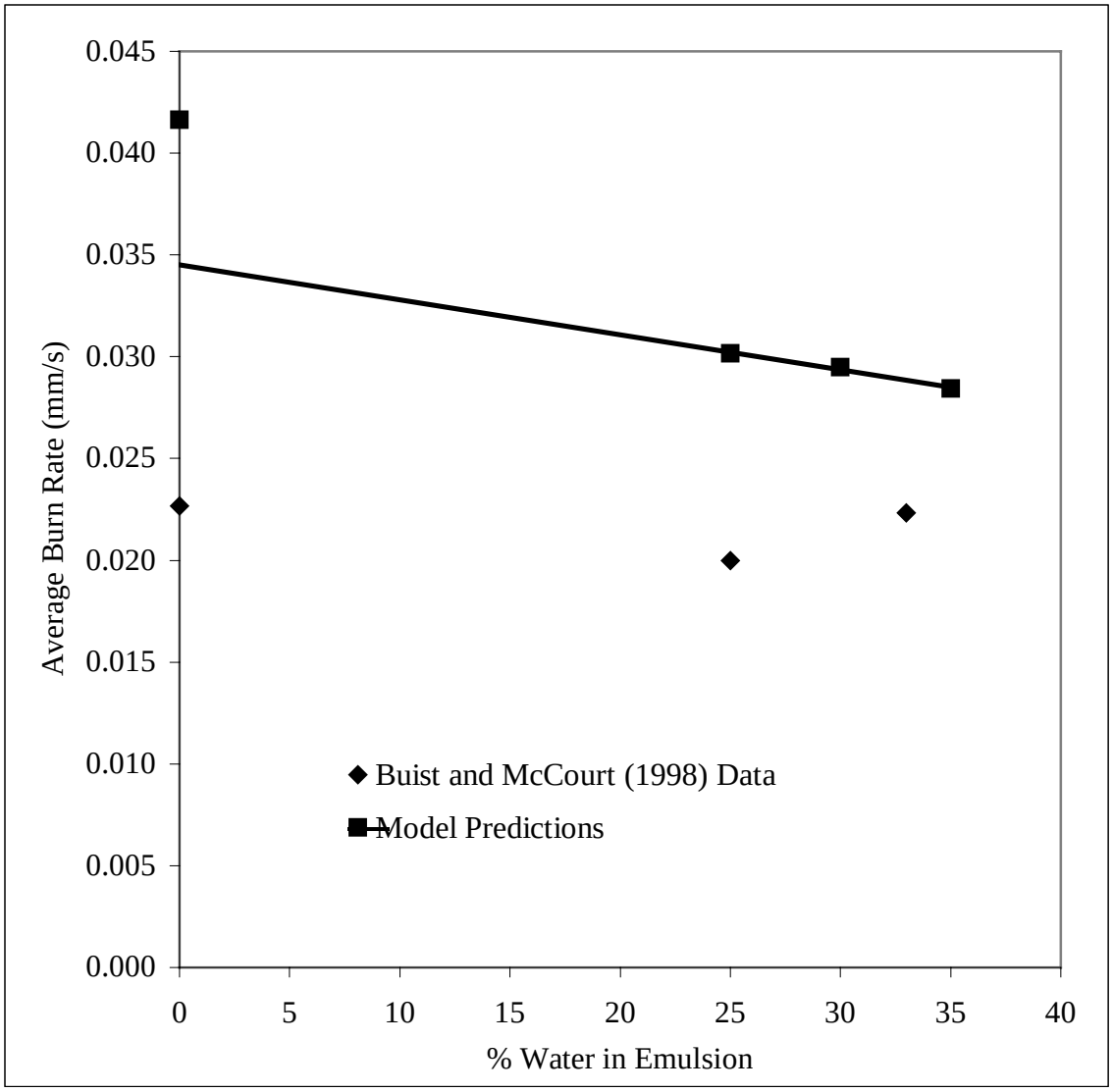

Figure 24. Comparison of the average oil burn rate for fresh MPU burn tests from Buist and McCourt (1998) with the model predictions for different water fractions in emulsion.

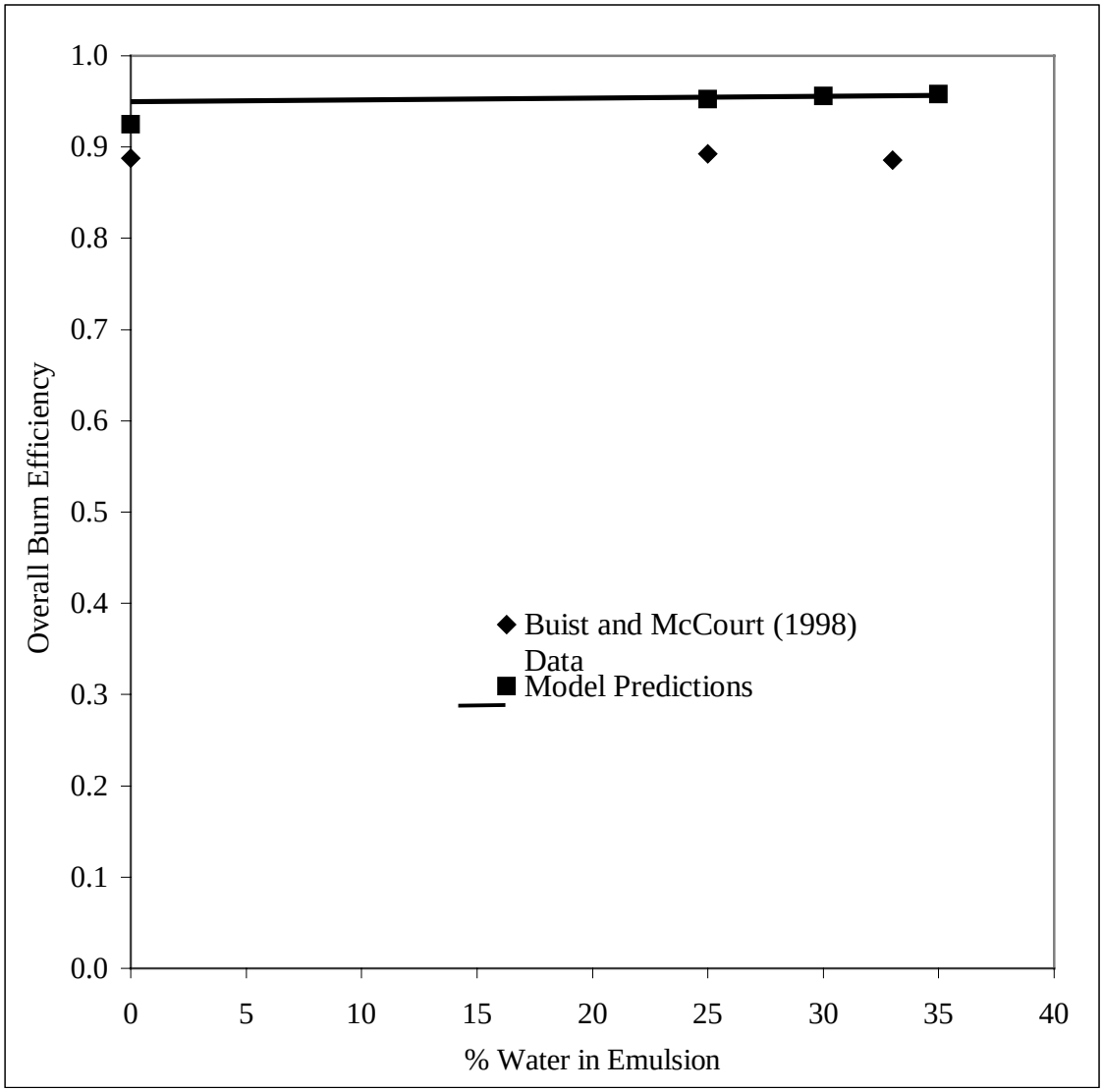

Figure 25. Comparison of the overall burn efficiency for fresh MPU burn tests from Buist and McCourt (1998) with the model predictions for different water fractions in emulsion.

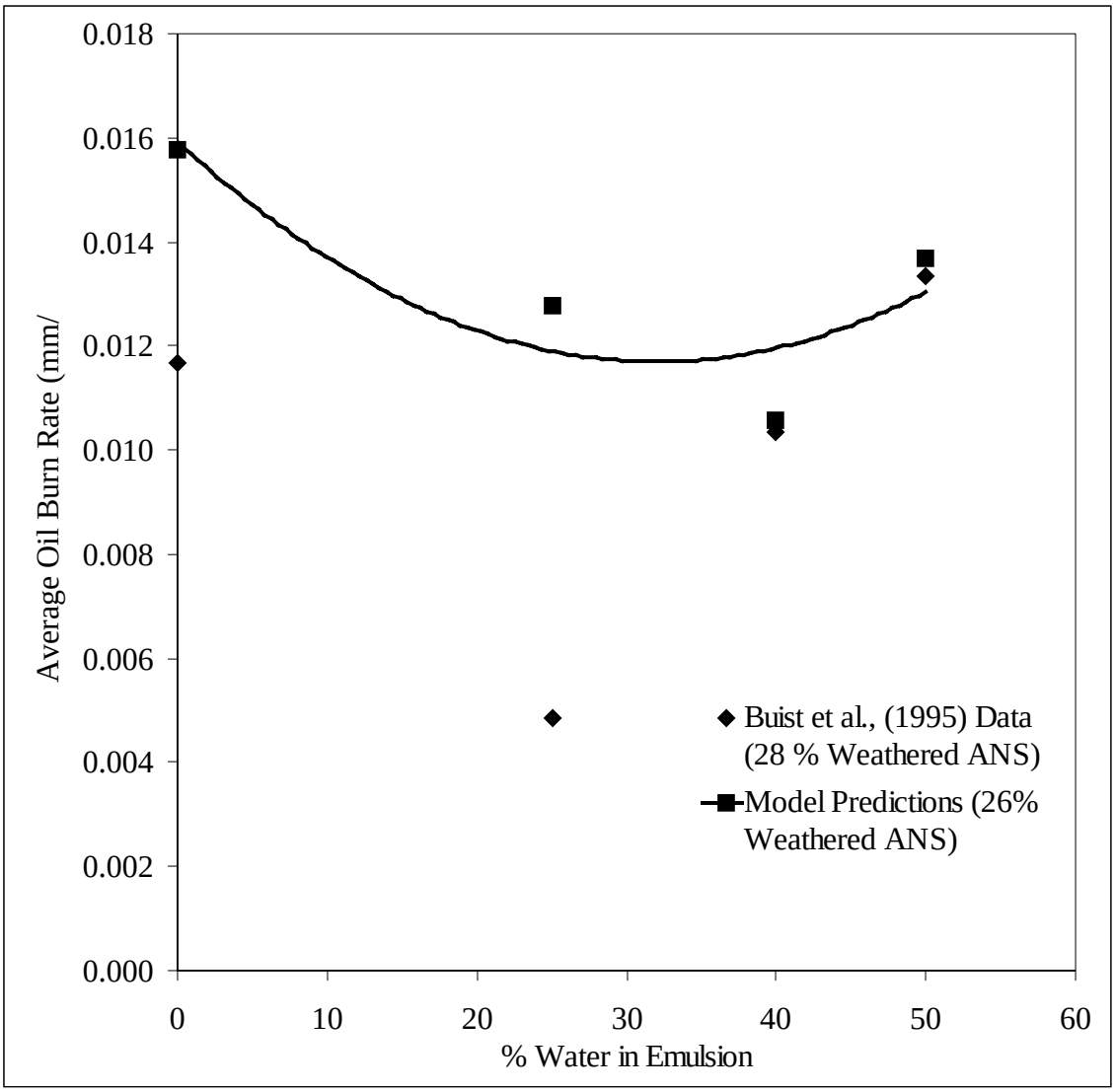

Figure 26 Comparison of the average oil burn rate for ANS burn tests from Buist *et al.*, (1995) with the model predictions for different water fractions in emulsion.

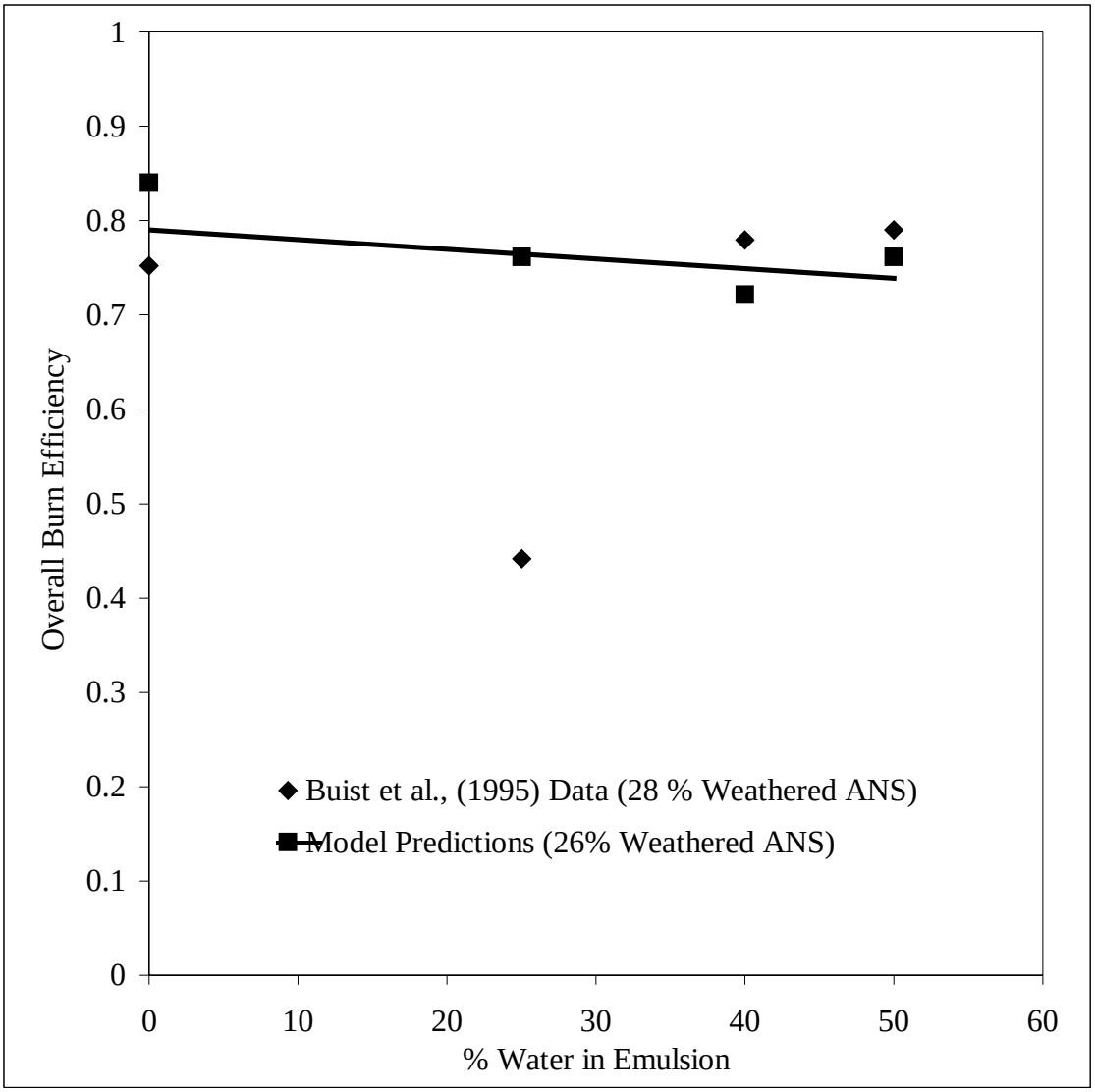

Figure 27. Comparison of the overall burn efficiency for ANS burn tests from Buist *et al.*, (1995) with the model predictions for different water fractions in emulsion.

7.6 Model Predictions for the Crude Oil-Water Emulsions

The results from the model for MPU-water and ANS-water emulsions are summarized in table 13. The results are also represented graphically in figures 28-33.

Figure 28 and figure 29 show the dependence of the average burning rate of oil predicted by the mathematical model on the water content of the emulsion for the MPU-water and ANS-water emulsions respectively, at the threshold heat flux values.

As was observed in the case of the diesel-water emulsions, the burning rate of oil is seen to be decreasing with the increased water fraction in the emulsion and with increased weathering of the oil. As the water content of the emulsion increases, there is less oil separated from the same amount of emulsion. As the maximum heat flux that the emulsion is exposed to during burning is the same for all the emulsion types, the rate at which the emulsion separates remains the same. With the rate of emulsion separation remaining the same, the rate at which oil is produced decreases with an increase in water content of the emulsion. Thus, the burning rate of oil decreases with increase in water fraction of the emulsion for both MPU and ANS emulsions.

With the increase in the weathering of the oil, the temperature at which the emulsions separate and the oil vaporization temperature increase. Thus, the rate at which the emulsion is broken decreases with an increasing degree of evaporation. Hence increase in weathering causes the decrease in the average burning rate of oil. This is observed consistently for MPU. The average burning rates of oil for the emulsions of 26% weathered ANS are also smaller than the average oil burning rates for emulsions of 15% and 20% weathered ANS.

The model predictions for the fresh, unemulsified MPU were not considered when fitting the best curve through the data, as the use of near zero initial heat flux value (1 kW/m^2) seems to have caused errors in model predictions.

Low threshold heat flux values (about 1 kW/m^2) make the initial and the intermediate regimes of the model unrealistically long. This causes unrealistic heating of the emulsion layer prior to ignition and thus results in incorrect model predictions. Inability of the mathematical model to handle the low threshold heat flux cases is one of the limitations of the model.

Table 13. Model Predictions of Characteristics of the Crude Oil Emulsion Pool Fires.

Oil Type	% Weathering	% Water	Average Oil Burn Rate (mm/s) $\times 10^2$	Oil Residue Thickness (mm)	Overall Burn Efficiency
MPU	0	0*	4.17	0.753	0.92
		25	3.02	0.354	0.95
		30	2.95	0.308	0.96
		35	2.84	0.273	0.96
	10	0	3.18	0.659	0.93
		25	2.83	0.678	0.91
		30	2.68	0.728	0.90
	15	0	3.09	0.708	0.93
		25	2.69	0.960	0.87
ANS	15	0*	1.55	2.82	0.72
		25*	1.50	2.67	0.64
		40*	1.49	2.70	0.55
		50*	1.53	2.56	0.49
	20	0	1.73	1.69	0.83
		25	1.61	1.28	0.83
		40	1.43	1.19	0.80
		50	1.45	1.06	0.79
	26	0	1.58	1.60	0.84
		25	1.28	1.79	0.76
		40	1.06	1.67	0.72
		50	1.37	1.19	0.76

*Model predictions are affected by low threshold heat flux values. Inability of the model to handle the low threshold heat flux cases is one of the drawbacks of the model. Please see page 111 for discussion.

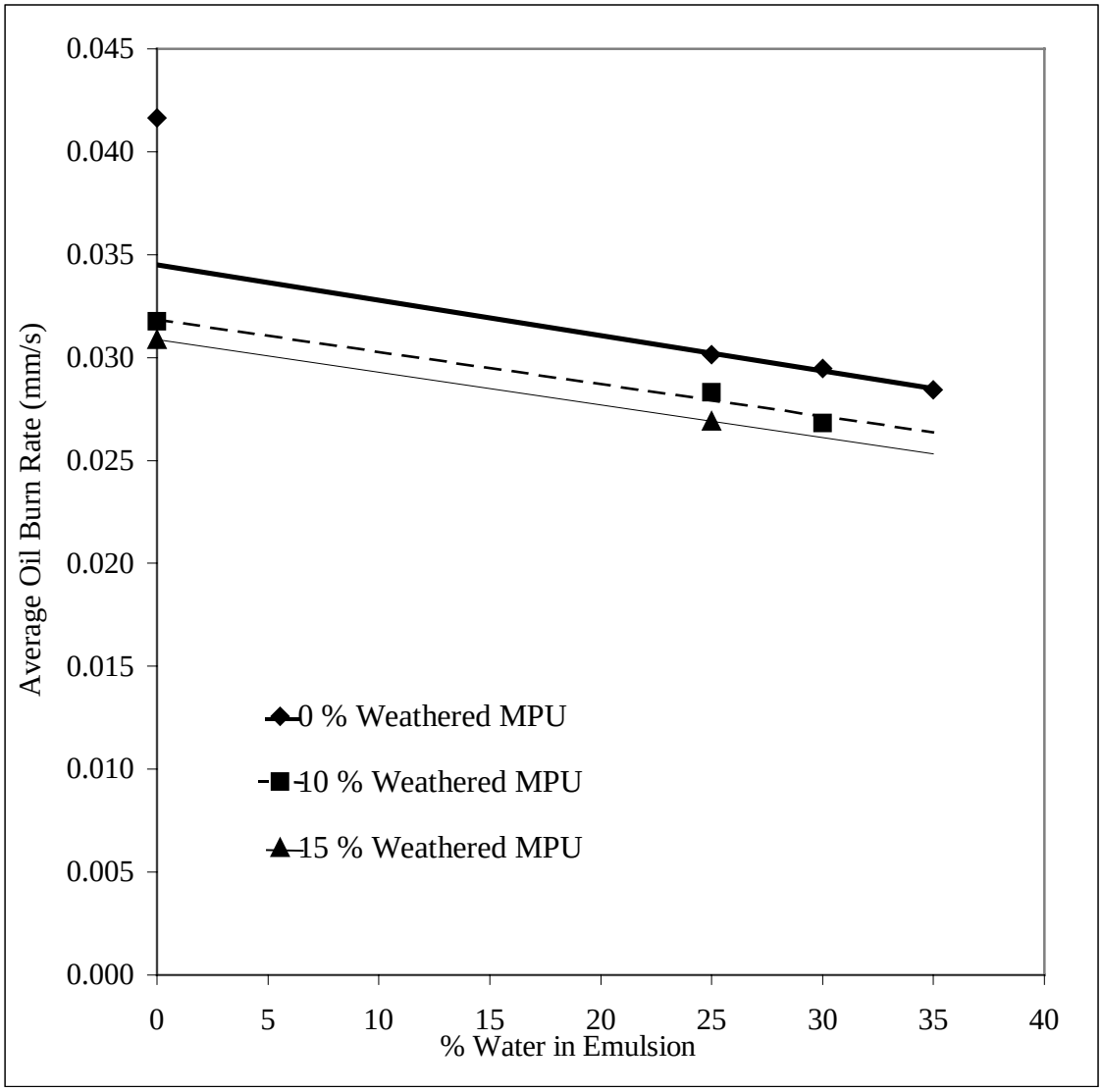

Figure 28. Average oil burning rate predictions by the mathematical model for the MPU-water emulsions as a function of the water content of the emulsion at the threshold heat flux for different weathering levels of the crude oil.

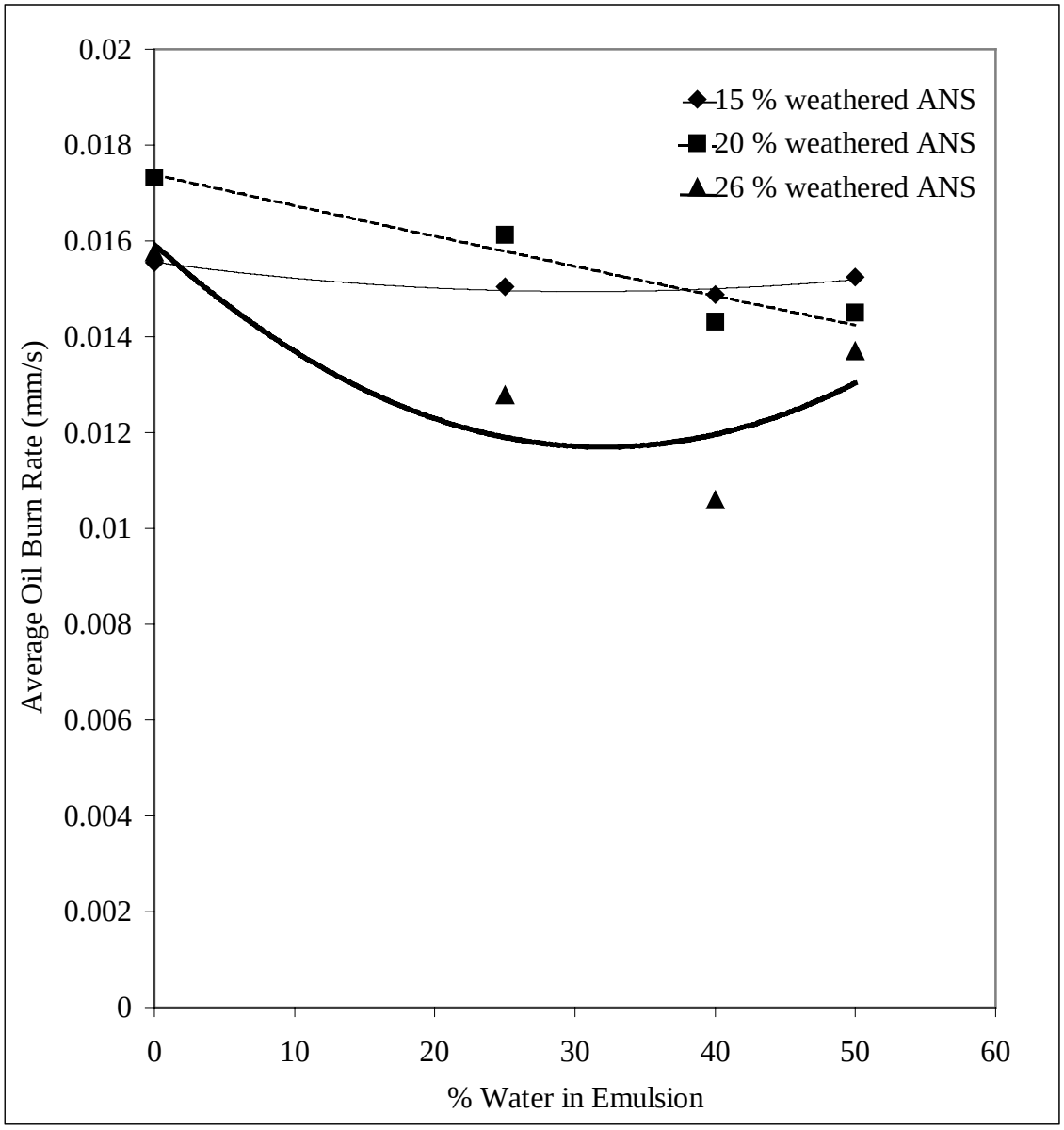

Figure 29. Average oil burning rate predictions by the mathematical model for the ANS-water emulsions as a function of the water content of the emulsion at the threshold heat flux for different weathering levels of the crude oil.

Figure 30 and figure 31 show the dependence of the oil residue thickness predicted by the mathematical model on the water content of the emulsion for the MPU-water and ANS-water emulsions respectively, at the threshold heat flux values.

A factor that affects the extinction of the emulsion combustion is the initial heating of the emulsion layer and oil layer prior to ignition. With the increasing threshold heat flux as the water content of the emulsion increases, the average temperature of the oil prior to ignition also increases. With increasing water content of emulsion, more of the oil is now at a temperature close to the vaporization temperature of oil. Hence, more of the oil is burned away. Thus, the residue thickness decreases with increasing water content of the emulsion, as seen for the case of unweathered (0% weathered) MPU in figure 30 and for all weathering levels of ANS in figure 31.

With the increase in the emulsion separation temperature for more weathered oil, less amount of oil is separated from the emulsion prior to the ignition. Thus, this factor becomes less effective. Now, more of the emulsion layer is still un-separated as the ignition occurs. The thickness of the residue is determined by the heat loss to the water through the emulsion layer. The rate at which the heat is transferred into the water is dependent on the diffusivity of the emulsion layer. As the water content of the emulsion increases, the diffusivity of the emulsion layer increases. With increased thermal diffusivity, the emulsion layer passes more of the heat that it receives to the water underneath. The heat loss to the water increases with increasing water content of the emulsion, thereby causing early extinction of the fire and hence, the thicker residue is observed for the emulsions of 10% and 15 % weathered MPU in figure 30. This effect is more prominent in emulsions of MPU, since MPU forms more stable emulsions than ANS.

For a given water fraction of the emulsion, the residue thickness increases with increased weathering for all weathering levels of MPU and for increase in weathering from 20% to 26% for ANS. This is observed because with increased weathering, the emulsion separation temperature and the oil vaporization temperature increase. It is more difficult to continue the combustion with increased weathering of the oil. Therefore, extinction occurs at a higher thickness of the oil layer. For the 15 % weathered ANS emulsions, the behavior seems to be governed by low threshold heat flux value.

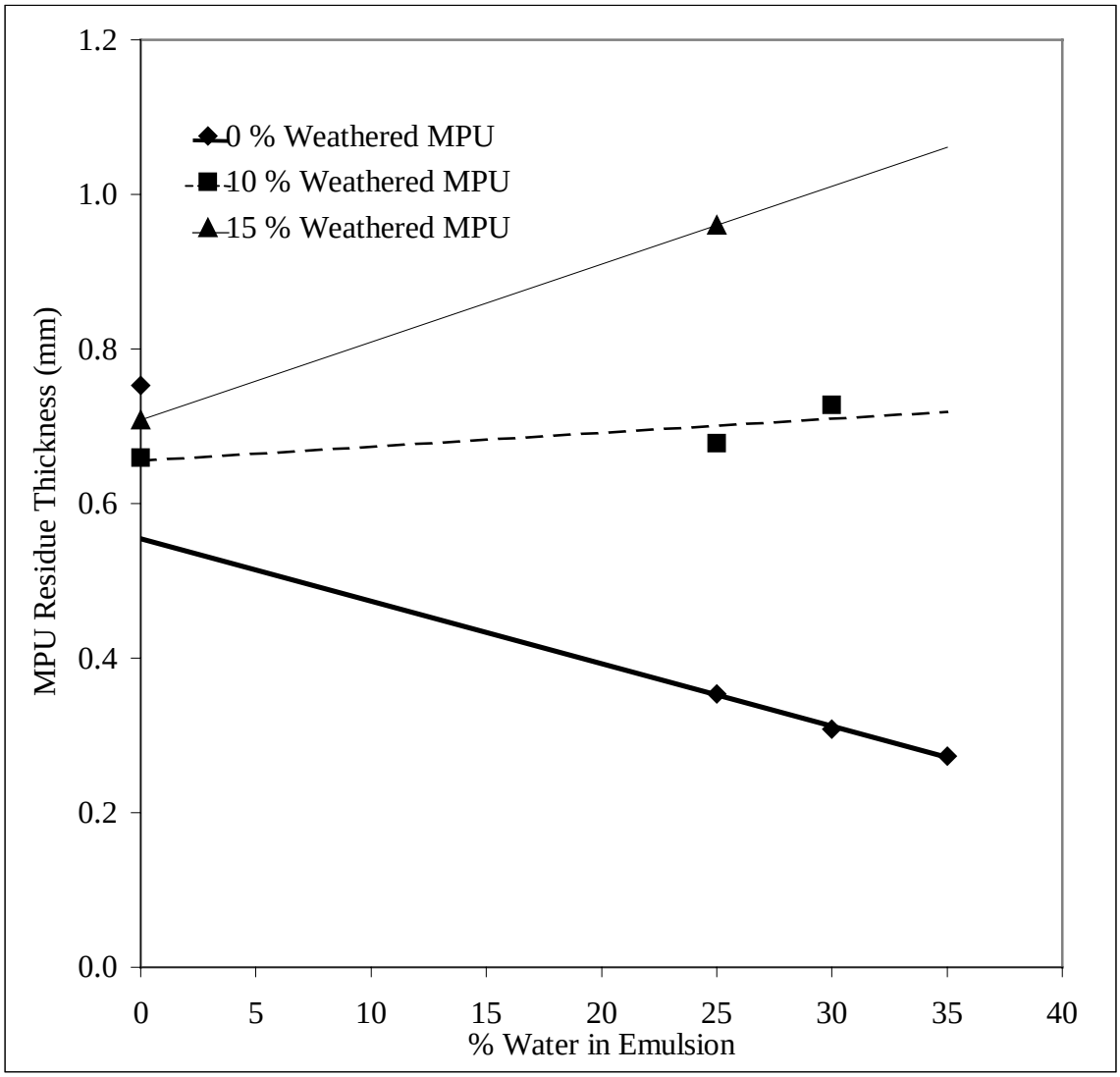

Figure 30. Oil residue thickness predictions by the mathematical model for the MPU-water emulsions as a function of the water content of the emulsion at the threshold heat flux for different weathering levels of the crude oil.

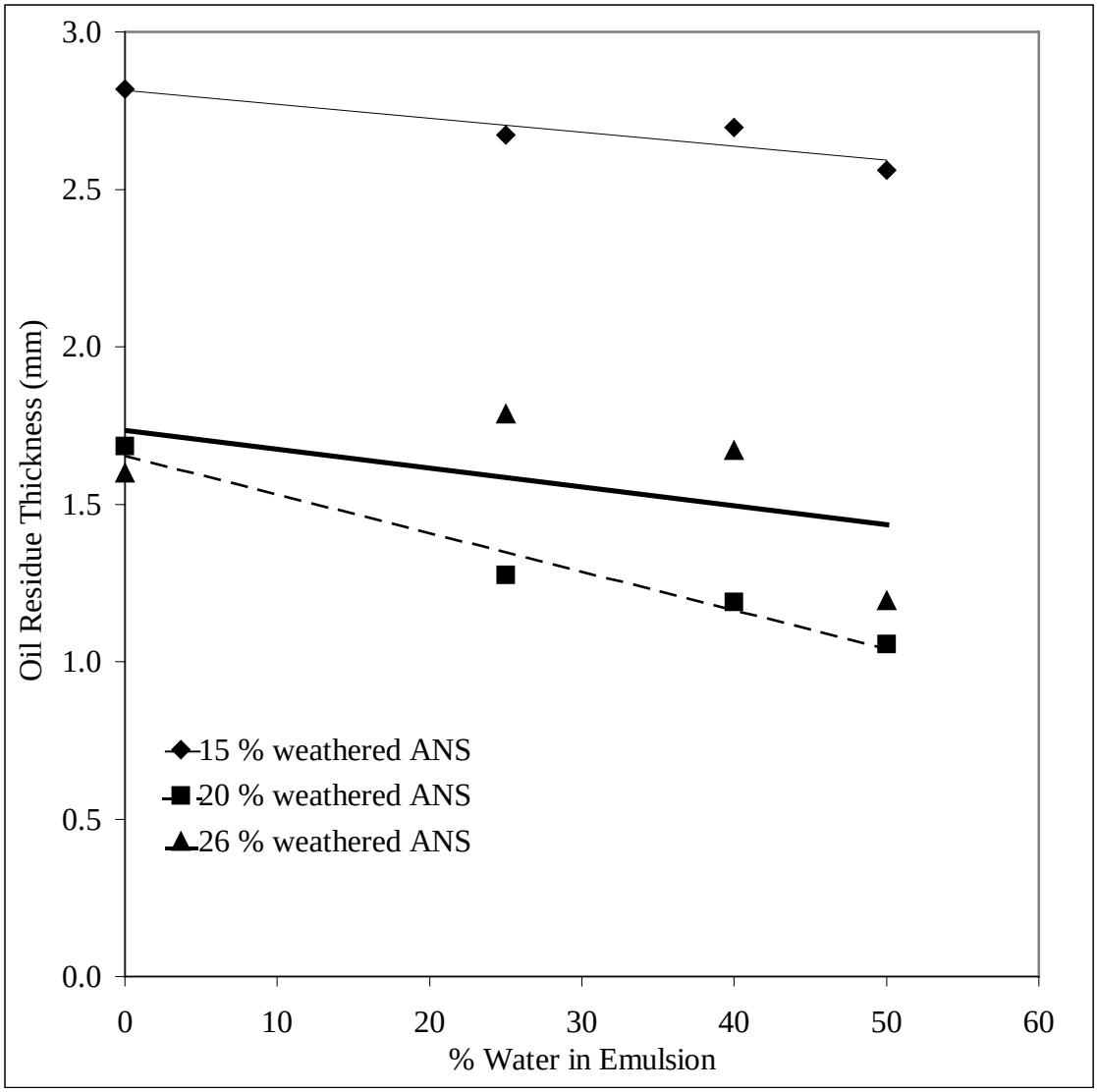

Figure 31. Oil residue thickness predictions by the mathematical model for the ANS-water emulsions as a function of the water content of the emulsion at the threshold heat flux for different weathering levels of the crude oil.

Figure 32 and figure 33 show the dependence of the overall oil burning efficiency predicted by the mathematical model on the water content of the emulsion for the MPU-water and ANS-water emulsions respectively at the threshold heat flux values. The oil burning efficiency represents the fraction of the initial oil volume that is removed by combustion. The efficiency depends on the thickness of the oil residue and initial volume of the oil present in the emulsion.

With the initial emulsion layer thickness remaining constant, the initial volume of the oil decreases with increasing water content of the emulsion. This tends to decrease the efficiency of oil removal, if the extinction thickness were to remain constant.

For the fresh unweathered MPU and for all levels of weathering of ANS, an increase of water content in emulsion causes the decrease in the extinction thickness, which tends to increase the oil burning efficiency. The two effects almost cancel each other and the oil burning efficiency remains almost constant with increasing water content of the emulsion for the unweathered MPU emulsions. In case of the ANS emulsions, the effect of the decrease in initial oil volume with the increase in water content of the emulsion dominates the trend shown by the efficiency and the efficiency is seen to be decreasing with increasing water content of the emulsion.

For the 10% and 15% weathered MPU, the increase in water content of the emulsion tends to increase the residue thickness and thus, a decrease the oil removal efficiency. Here the two effects add to each other and the net trend is decrease in overall burn efficiency with an increase in water content of the emulsion.

The burn efficiency decreases with the increased weathering of the oil for a given emulsion composition. This is because with increased weathering, the residue thickness increases as shown in figures 30 and 31. Therefore, less of the oil is burned away resulting in the lower burn efficiency.

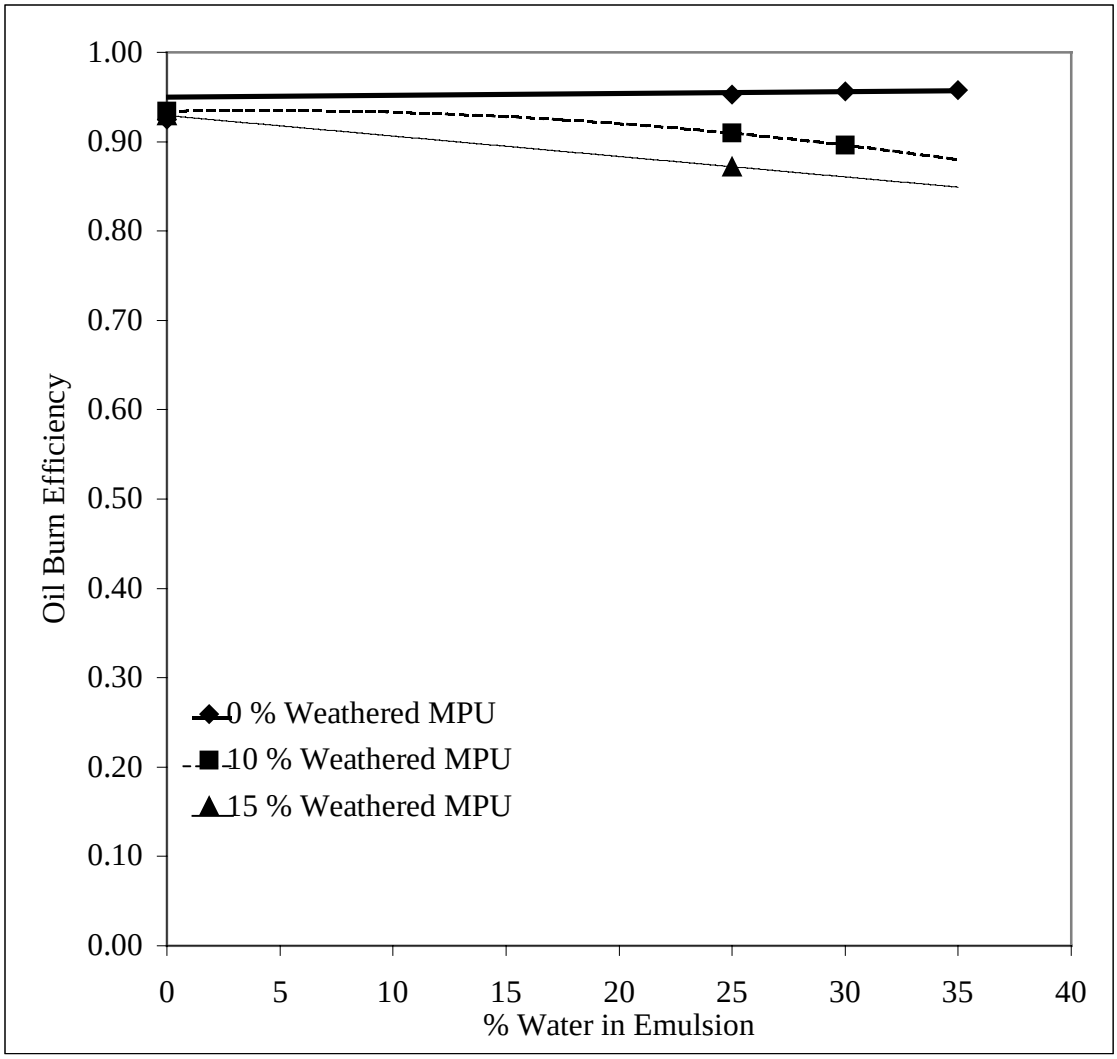

Figure 32. Oil burn efficiency predictions by the mathematical model for the MPU-water emulsions as a function of the water content of the emulsion at the threshold heat flux for different weathering levels of the crude oil.

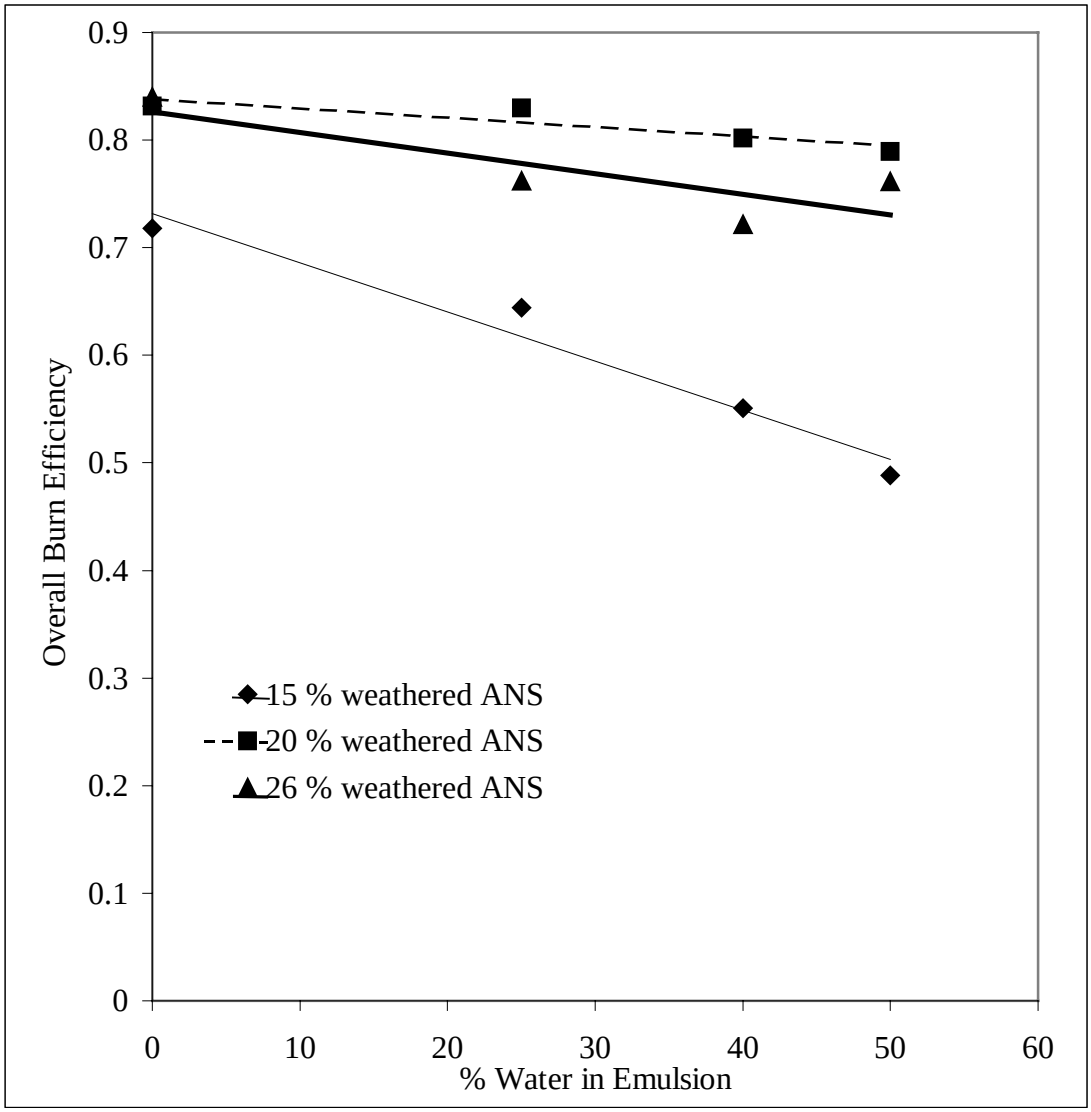

Figure 33. Oil burn efficiency predictions by the mathematical model for the ANS-water emulsions as a function of the water content of the emulsion at the threshold heat flux for different weathering levels of the crude oil.

7.7 Conclusions from Crude Oil Emulsion Tests

The laboratory scale burn tests of the crude oil-water emulsions were conducted to verify the concept of existence of threshold heat flux for the crude oil water emulsions. The tests were also conducted to investigate the effects of evaporation of lighter fractions (weathering) of the crude oil on the threshold heat flux value.

The data from the laboratory scale burn tests of the crude oil-water emulsions clearly verify the concept of existence of the threshold heat flux for the crude oil-water emulsions. The threshold heat flux data for the crude oils tested also show that the threshold heat flux values depend on the weathering level of the crude oil and the water content of the emulsion. The threshold heat flux values increase with an increase in the weathering level of the crude oil. Results from literature for the burn tests on the crude oils with the same brand names as the ones tested in the present study suggest that some of the current ignition methods may successfully impose the threshold heat flux on the emulsion surface in some cases. However, with precise data on the threshold heat flux values for emulsions of different oils, with different levels of weathering and different water contents, the *in-situ* combustion technique can be used very effectively to achieve efficient removal of spilled oil from the ocean surface.

From the point of view of applying these data in expanding the window of opportunity for application of *in-situ* burning as an oil spill clean up technique, these results suggest that the longer the crude oil stays on the ocean surface prior to attempting the *in-situ* burning, the higher will be threshold heat flux required to achieve a successful burn.

The threshold heat flux values for the emulsions tested ranged from 0 kW/m^2 to 21 kW/m^2. The proposed technique of imposing external heat flux equal to, or more than, the threshold heat flux can be used to enhance the window of opportunity for application of the in-situ burning technique for oil spill clean up. The heat flux can be obtained from an adjacent pool fire of sufficient size. This pool fire of the desired size can be created by intentionally starting a fresh oil pool fire. However, to achieve successful ignition, a correlation between base fire size and the heat feedback from the fire to the surrounding area is required. Such a correlation will depend on the type of the oil, and surrounding

conditions such as direction if wind, intensity of the wind and ocean turbulence, etc. Figure 34 shows the heat flux distribution from pool fires of Heptane with 30 cm base diameter and 100 cm base diameter as a function of distance from the pool periphery from the data from Klassen and Gore (1992). It can be seen that the pool fire of Heptane with 100 cm base diameter can easily impose heat fluxes in the range of 30 kW/m^2 up to about 20 cm away from the pool periphery. A smaller diameter pool has a smaller heat flux distribution. Thus it can be seen that the range of threshold heat flux values for the emulsions tested can be obtained on ocean surface with reasonable sized pool fires.

The crude oil properties vary with changes in the source well that the samples are taken from, and with different additives that may be added at different times. Cragoe (1929) has reported that many of the thermodynamic properties of the crude oils are not seriously affected by considerable changes in composition. However, many of these properties are closely related to the density of the oil. Therefore, rather than relating the threshold heat flux values to the generic names of the crude oils, a more useful parameter for correlating the threshold heat flux values to may be the density of the crude oils. Figure 35 shows the threshold heat flux values plotted as a function of water content of emulsion with the density of the oil as a parameter. It can be seen that with an increase in the density, the threshold heat flux value increases. Higher density crude oils can be looked up on as mixtures of heavier hydrocarbons that are more difficult to ignite.

Threshold heat flux data for the diesel-water emulsions are not included in figure 35. There are two reasons for not including the threshold heat flux data for diesel-water emulsions. First reason is that all the diesel-water emulsions contained 10% by volume of the SAE 30 motor oil to aid emulsification. This makes it difficult to determine the oil density for the emulsions, as the SAE 30 oil is also combustible. Secondly, as the commercially available diesel is a refined oil, it does not contain the impurities that are present in the crude oils in addition to the hydrocarbons. Hence, comparing the diesel-water emulsion data with the crude oil-water emulsion data may not be appropriate.

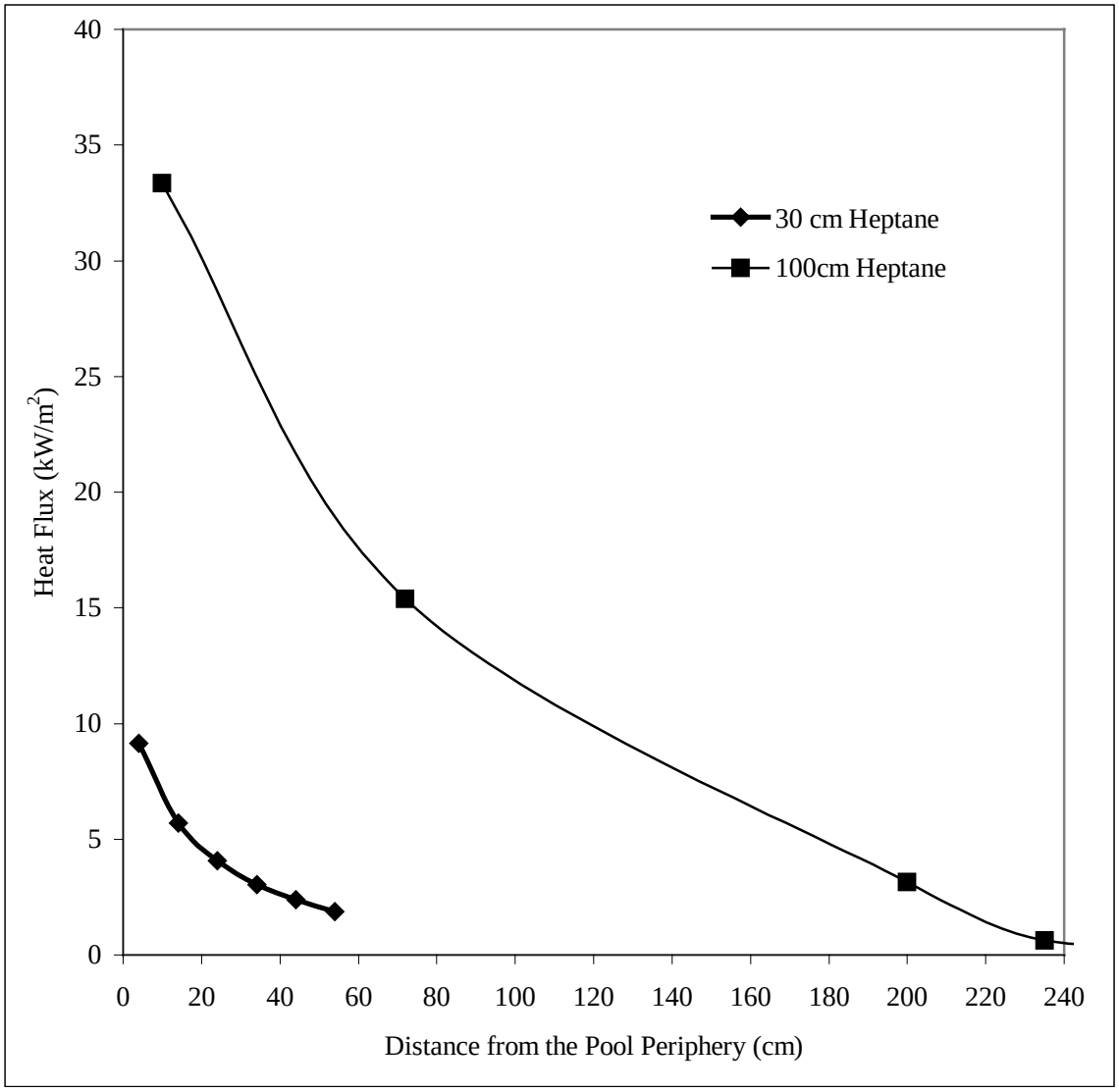

Figure 34. Heat flux distribution from Heptane pool fires of 30 cm and 100 cm base diameters as a function of the distance from the pool periphery. Plotted with data from Klassen and Gore (1992).

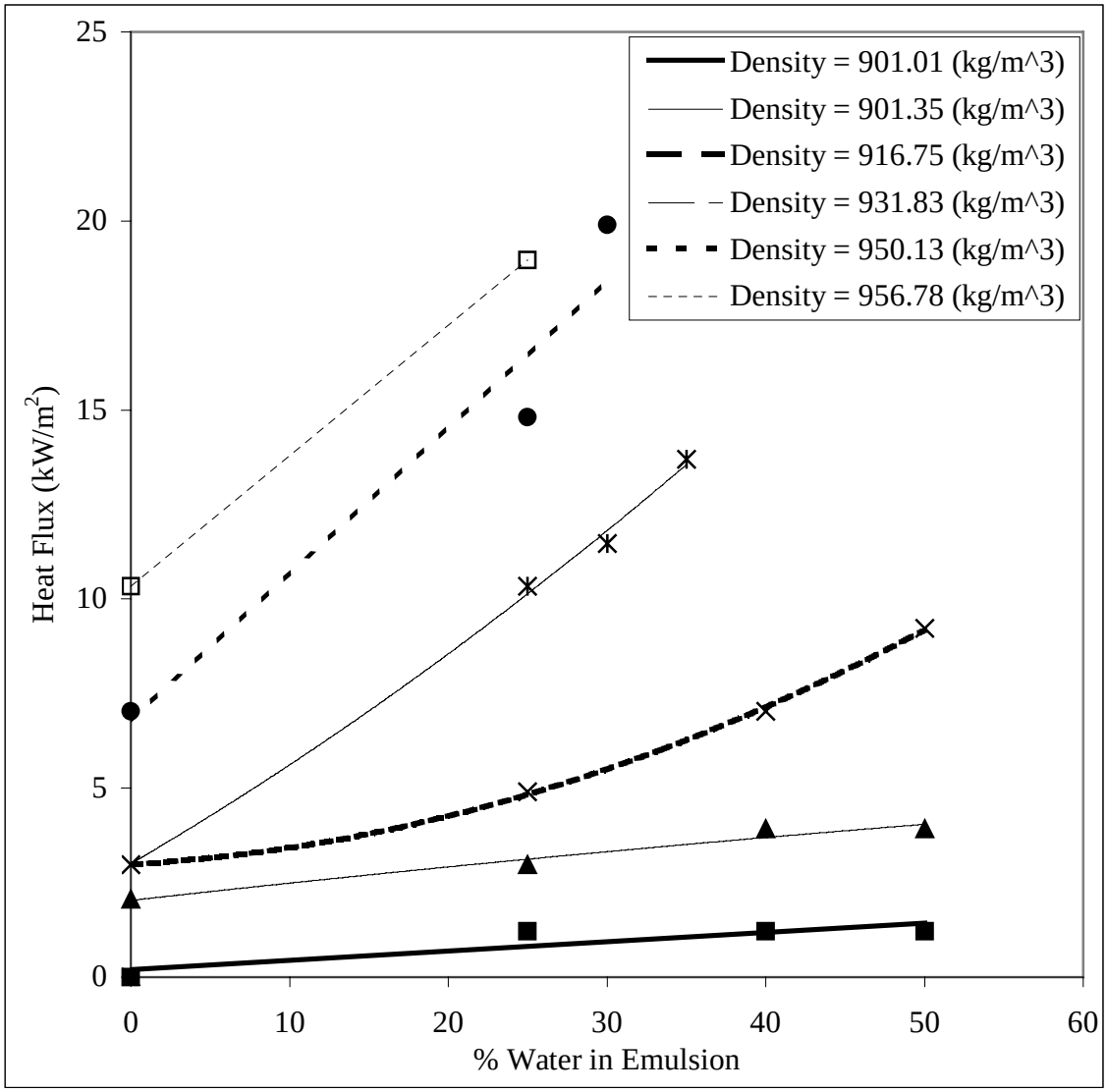

Figure 35. Threshold heat flux data from the laboratory scale pool fire data for the crude oil-water emulsions plotted with the density of the oil as a parameter. Densities from 901.01 kg/m^3 to 916.75 kg/m^3 represent ANS from 0% weathering to 26% weathering whereas densities from 931.83 kg/m^3 to 956.78 kg/m^3 represent MPU from 0% weathering to 15% weathering.

The threshold heat flux data for the crude oil emulsions presented in figure 35 are plotted in figure 36 with threshold heat flux values as parameters. An emulsion with a given water fraction and a given density of the oil will burn when exposed to a particular heat flux, if the state representing the % water in emulsion and density of the oil in figure 36 lies in the region below and to left of the curve representing the heat flux under consideration. This region increases with the increase in heat flux as can be seen in figure 36. Development of such chart can facilitate an easy decision about the external heat flux value to be incident on a given emulsion.

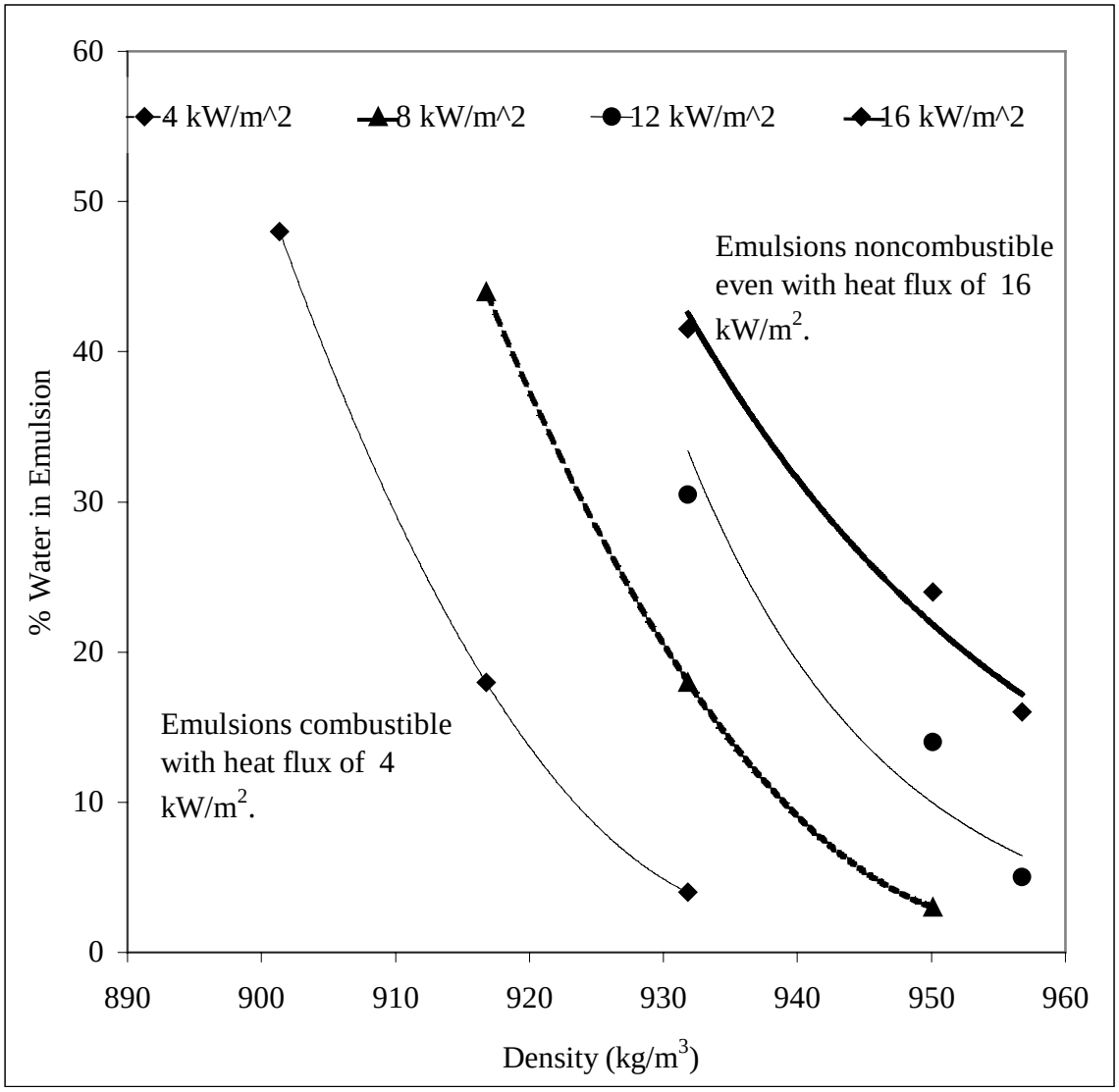

Figure 36. Threshold heat flux data from the laboratory scale pool fire data for the crude oil-water emulsions plotted with the heat flux as a parameter. Each of the curves divides the domain into combustible (below and to left of the curve) and noncombustible (above and to right of the curve) emulsion compositions.

Chapter 8

SUMMARY AND CONCLUSIONS

8.1 Summary

Burning of the spilled oil on the ocean surface is one of the techniques used in the oil spill clean up operations. With the passage of time, as the crude oil stays on the ocean surface, evaporation of the lighter components of the crude oil and mixing of water with the oil due to wind and ocean turbulence create a dense and more viscous mousse. This makes the ignition of the oil harder to achieve and reduces the window of opportunity for application of the *in-situ* burning technique for oil spill clean up. In order to expand this window of opportunity, it was proposed that the emulsions of water in oil that are considered non-combustible can be ignited, if exposed to a minimum external heat flux, called the threshold heat flux.

A test facility was designed and built to conduct laboratory scale tests of water in oil emulsions to study the threshold heat flux values for different types of emulsions. The emulsion samples can be subject to heat flux from 1.2 kW/m^2 to 21 kW/m^2 in steps of about 1 kW/m^2.

Experimental measurements of threshold heat flux values were made for emulsions of diesel, Milne Point crude oil and Alaska North Slope crude oil with water. The water fraction of the emulsion was changed from 0 % to 80% by volume. The crude oil samples were also tested for effects of evaporation of the lighter fractions from the crude oil. The concept of existence of threshold heat flux values for different emulsions was verified. The threshold heat flux data shows that a higher threshold heat flux is required to cause successful burning of emulsions with more water or emulsions of more weathered oil.

A mathematical model describing the important processes of the emulsion pool fire was developed. The model was finite differenced and solved numerically. The solution of the model was validated by the data from the diesel-water emulsions. Upon validation, the model was used to predict the emulsion pool fire characteristics, such as the average burning rate of oil, the total duration of the burn, the volume of the oil

residue and the overall oil removal efficiency. The model predictions enabled an investigation of the effects of oil type, water content of the emulsion, and degree of weathering on these characteristics.

8.2 Conclusions

Laboratory scale tests were conducted on water in oil emulsions of diesel and two crude oil samples, Alaska North Slope (ANS) crude oil and Milne Point crude (MPU) oil. The water fraction in the emulsion was changed from 0% to 80% by volume. The crude oil samples were also tested for effects of evaporation of the lighter fractions from the crude oil. Laboratory scale experiments clearly verified that there exists a threshold heat flux for each type of emulsion studied. Diesel-water emulsions containing as high as 80% water by volume could be ignited and successfully burned by applying external heat flux of 6 kW/m^2. Emulsions of fresh Milne Point crude oil containing 35% water by volume could not be ignited with external heat flux of 11 kW/m^2. But the same emulsion composition could be ignited when exposed to external heat flux of 13 kW/m^2. Milne Point crude oil that was weathered by 15% could not be burned, even in unemulsified state, without external heat flux of 10 kW/m^2. Compared to the Milne Point crude oil, emulsions of Alaska North Slope crude oil could be burned more easily. Emulsions of 26 % weathered Alaska North Slope crude oil containing 50% water by volume could be successfully burned with the help of external heat flux of 9 kW/m^2.

Previous studies have proposed that it is the oil that separates from the emulsion that burns and not the emulsion itself. Combining this idea with the results presented, it can be argued that in order to create a sustained emulsion pool fire, the emulsion must be separated into water and oil at such a rate that the rate at which the oil is separated from the emulsion must be at least equal to the rate at which the oil is consumed by combustion. The results from the study also suggest that in order to achieve flame spread, the fire must be of such size as to impose the surrounding emulsion pool with heat flux equal to or more than the threshold heat flux.

The data from the laboratory tests were used to validate the mathematical model and predict the dependence of various pool fire characteristics, such as the average oil burning rate, the total duration of the burn, the volume of the oil residue and the overall

burn efficiency on water content of the emulsion and the weathering level of the oil. Following conclusions can be drawn from the results presented in the previous two chapters:

1. There exists a threshold heat flux value for each type of emulsion, such that, when the emulsion is subjected to a heat flux lower than this threshold value, sustained combustion of a layer of the emulsion floating on top of water surface cannot be achieved. However, when the external incident heat flux value is higher than the threshold value, the emulsion layer floating on top of the water surface can be successfully burned.
2. The value of the threshold heat flux is dependent on the oil type involved, the amount of water present in the emulsion, and the extent of weathering experienced by the crude oil prior to ignition. The laboratory scale burn experiments showed that the threshold heat flux value increases with the increased amount of water present in the emulsion and with the increase in the level of weathering the oil undergoes.
3. Comparisons of the data from the laboratory scale tests with the predictions of a mathematical model have demonstrated that the model predicts important pool fire characteristics, such as the average burn rate, the total burn time, the volume of the oil residue, and the overall burn efficiency within 25% of the observed values for most of the cases. The model in unique in the way the separation of emulsion during the pool fires is treated. The model is, however, seen to be unable to handle the low threshold heat flux (about 1 kW/m^2) cases.
4. The average oil burning rate, total duration of burn, the volume of the oil residue and the burn efficiency decrease with increasing water content of the emulsion. Average oil burn rate and the overall burn efficiency decrease with increased weathering of the oil, whereas the total burn time and the volume of the oil residue increase with increased weathering of the oil.

Some of the factors such as wind, ocean turbulence, water temperature, etc. are not considered in this study. These factors are suspected to affect the emulsion pool fires

significantly. Hence there is a need to continue this work further to investigate the effects of these factors on emulsion pool fires.

8.3 Recommendations for Future Work

1. Testing at a larger scale could provide a more realistic estimate of the threshold heat flux values. Hence, tests on large scales should be conducted. The threshold heat flux values obtained in the present set up were at laboratory conditions. Establishing the threshold heat flux data at the real life operating conditions can be more useful from the point of view of implementing the proposed technique for application of *in-situ* burning method. Effects of winds and waves should also be studied.
2. A more comprehensive database of threshold heat flux values for various oils would enhance the efficient application of the *in-situ* combustion method.
3. A reliable and extensive correlation for the heat flux distribution around a pool fire based on the controlling parameters such as fuel type, the base size of the fire, etc., can be useful for implementing the proposed technique for application of *in-situ* burning method.
4. Some of the crude oil property data such as the optical depth, emissivity, absorptivity, etc., required as input to the mathematical model, need to be measured accurately.
5. One of the limitations of the current set up is that the emulsion surface can be exposed to a maximum of 21 kW/m^2 of heat flux. The MPU data shows that some of the crude oil emulsions need a threshold heat flux higher than 21 kW/m^2. Upgrading the heater panels to achieve higher values of heat flux at the emulsion surface will increase the range of emulsions for which the data can be obtained from the present set up.

REFERENCES

Allen, A. A., “Contained Controlled Burning of Spilled Oil During the Exxon Valdez Oil Spill”, *Proceedings of Thirteenth Arctic and Marine Oilspill Program,* Technical Seminar, (1990).

Allen, A. and W. Simpson, “Alaska Clean Seas and Evaluation of Fire Containment Boom”, *Proceedings of the Ninth Annual Arctic and Marine Oilspill Program,* Technical Seminar, (1986).

Arai, M., K. Saito, and R. A. Altenkirch, “Experimental Studies of Burning Liquid Fuels On Water Sub-layer”, *Symposium (International) On Combustion*, 22nd, Seattle, WA, 1-1 pp, (1988).

Arai, M., K. Saito, and R. A. Altenkirch, “A Study of Boilover in Liquid Pool Fires Supported on Water Part I: Effect of Water Pool Fires”, *Combustion Science and Technology*, 71, pp. 25-40, (1990).

Baum, H. R., K. B. McGrattan, and R. G. Rehm, “Simulation of Smoke Plumes From Large Pool Fires”, *Symposium (International) on Combustion,* 25th, (1994).

Bech, C., P. Sveum, and I. A. Buist, “*In Situ* Burning of Emulsions: The Effects of Varying Water Content and Degree of Evaporation”, *Proceedings of the Fifteenth Arctic and Marine Oilspill Program,* Technical Seminar, 547-559, (1992).

Bitting, K. R., and P. M. Coyne, “Oil Containment Tests of Fire Booms”, *Proceedings of the Twentieth Arctic and Marine Oilspill Program,* Technical Seminar, 2:735-754, (1997).

Bobra, M., “A Study of Water-In-Oil Emulsification”, pp 63, (1992).

Brehob, E. and A. K. Kulkarni, “Experimental Measurements of Upward Flame Spread on a Vertical Wall with External Radiation”, *Journal of Fire Safety Science*, vol. 31, 181-200, (1998).

Brown, H. M. and R. H. Goodman, “Initial Dynamics of the Spreading of Oil On Water”, *Proceedings of the Eighteenth Arctic and Marine Oilspill Program,* Technical Seminar, 1:61-68, (1995).

Brzustowski, T. A. and E. M. Twardus, “Study of the Burning of a Slick of Crude Oil on Water”, *Symposium (International) on Combustion*, 19th, (1982).

Buist, I. A., J. McCourt, N. Glover, C. Hutton, J. McHale, and J. Mullin, “Mid-Scale Tests of *In Situ* Burning in a New Wave Tank at Prudhoe Bay, AK”, *Proceedings of the Twenty First Arctic and Marine Oilspill Program,* Technical Seminar, 2:599-622, (1998).

Buist, I. A., and J. McCourt, “The Efficacy of *In Situ* Burning for Alaskan Risk Oils”, Final Report, S. L. Ross Environmental Research, Ltd., 1998.

Buist, I. A., “Window of Opportunity for *In Situ* Burning”, *In Situ Burning of Oil Spills Workshop Proceedings*, 21-26, (1998)

Buist, I. A., N. Glover, B. McKenzie, and R. Ranger, “*In Situ* Burning of Alaska North Slope Emulsions”, *Proceedings of the 1995 International Oil Spill Conference*, 139-146, (1995).

Chemical Week, “Swedes Solve Oil Spill”, pp 25, (April 15, 1970).

Cragoe, C. S., “Thermal Properties of Petroleum Products”, U. S. Department of Commerce, Miscellaneous Publication No. 97, (1929).

Daykin, M., A. Tang, D. Aurand, Z. Wang, G. Sergy and G. Shigenaka, "Aquatic Toxicity Resulting from *In Situ* Burning of Oil-On-Water", *Proceedings of the Eighteenth Arctic and Marine Oilspill Program,* Technical Seminar, 2:1165-1193, (1995).

Evans, D. D., and W. D. Walton, "Burning of Oil Spills", *U. S./Japan Government Cooperative Program on Natural Resources (UJNR),* Fire Research and Safety, 11th Joint Panel Meeting, (1989).

Exxon Valdez Oil-Spill Restoration Web-Page, On World Wide Web at the address: http://www.oilspill.state.ak.us/nwhistory.html.

Fay, J. A., "The Spread of Oil Slick on a Calm Sea", *Oil on The Sea,* Plenum Press, New York, 53:63, (1969).

Fingas, M. F., B. Fieldhouse, J. Lane, and J. V. Mullin, "Studies of Water-in-Oil Emulsions: Long-Term Stability, Oil Properties, and Emulsions Formed at Sea", *Proceedings of the Twenty Third Arctic and Marine Oilspill Program,* Technical Seminar, 1:145-160, (2000a).

Fingas, M. F., B. Fieldhouse, J. Lane, and J. V. Mullin, "Studies of Water-in-Oil Emulsions: Energy and Work Threshold for Emulsion Formation", *Proceedings of the Twenty Third Arctic and Marine Oilspill Program,* Technical Seminar, 1:19-36, (2000b).

Fingas, M. F., Z. Wang, P. Lambert, F. Ackerman, K. Li, M. Goldthrop, S. Whiticar, R. Nelson, P. Campagna, R. Turpin, R. Nadeau, S. Schuetz, M. Morganti, and R. A. Hiltabrand, "Emissions from Mesoscale *In Situ* Oil (Diesel) Fires: Emissions from the Mobile 1998 Experiments", *Proceedings of the Twenty Third Arctic and Marine Oilspill Program,* Technical Seminar, 2:857-902, (2000c).

Fingas, M. F., B. Fieldhouse, and J. V. Mullin, "Studies of Water-in-Oil Emulsions: Stability and Oil Properties", *Proceedings of the Twenty First Arctic and Marine Oilspill Program,* Technical Seminar, 1:1-26, (1998).

Fingas, M. F., "*In Situ* Burning of Oil Spills: A Historical Perspective", *In Situ Burning of Oil Spills Workshop Proceedings*, 55-65, (1998)

Fingas, M. F., F. Ackerman, P. Lambert, K. Li, Z. Wang, R. Nelson, M. Goldthrop, J. Mullin, L. Hannon, D. Wang, A. Steenkammer, S. Schuetz, R. Turpin, P. Campagna, L. Graham, and R. Hiltabrand, "Emissions from Mesoscale *In Situ* Oil (Diesel) Fires: The Mobile 1994 Experiments", *Proceedings of the Nineteenth Arctic and Marine Oilspill Program,* Technical Seminar, 2:907-978, (1996).

Fingas, M. F., "The evaporation of Oil Spills: Variation with Temperature and Correlation with Distillation Data", *Proceedings of the Nineteenth Arctic and Marine Oilspill Program*, Technical Seminar, 1:29-72, (1996).

Fingas, M. F., G. Halley, F. Ackerman, R. Nelson, M. Bissonnette, N. Laroche, Z. Wang, P. Lambert, K. Li, P. Jokuty, G. Sergy, E. J. Tennyson, J. Mullin, L. Hannon, W. Halley, J. Latour, R. Galarneau, B. Ryan, R. Turpin, P. Campagna, D.V. Aurand, and R. R. Hiltabrand, "The Newfoundland Offshore Burn Experiment -- NOBE", *1995 Oil Spill Conference*, 123-132, (1995).

Fingas, M., "Studies on the Evaporation of Oil Spills", *Proceedings of the Seventeenth Arctic and Marine Oilspill Program,* Technical Seminar, 189-212, (1994).

Fingas, M. F., G. Halley, F. Ackerman, N. Vanderkooy, R. Nelson, M. C. Bissonnette, N. Laroche, P. Lambert, P. Jokuty, K. Li, W. Halley, G. Warbanski, P. R. Campagna, R. D. Turpin, M. J. Trespalcios, D. Dickins, E. J. Tennyson, D. Aurand, and R. Hiltabrand, "Newfoundland Offshore Burn Experiment (NOBE): Experimental Design and

Overview", *Proceedings of Seventeenth Arctic and Marine Oilspill Program,* Technical Seminar, 2 (1994).

Fingas, M. and N. Laroche, "Introduction to *In Situ* Burning of Oil Spills", *Spill Technology Newsletter,* (December, 1990).

Fraser, J., I. Buist, and J. V. Mullin, "A Review of the Literature on Soot Production during *In Situ* Burning of Oil", *Proceedings of the Twentieth Arctic and Marine Oilspill Program,* Technical Seminar, 2:1365-1406, (1997).

Fuji, T., "Research and Study on Burning Disposal for Emulsified Oil", *Second International Oil Spill Conference,* 472-478, London, (1995).

Galt, J. A., "Trajectory Analysis for Oil Spills", *Journal of Advanced Mar. Tech. Conf.*, vol 11, 91-126, (1994).

Garcia-Martinez, R., L. J. Mata, and H. Flores-Tovar, "A Correction to Mackay Oil Spreading Formulation", *Proceedings of the Nineteenth Arctic and Marine Oilspill Program,* Technical Seminar, 2:1627-1635, (1996).

Garo, J. P., J. P. Vantelon and A. C. Fernandez-Pello, "Experimental Study of the Burning of a Liquid Fuel Spilled on Water", *Twenty-fifth Symposium (International) on Combustion,* The Combustion Institute, pp. 1481-1488, (1994).

Gonzalez, M. F. and G. A. Lugo, "Texas Marsh Burn: Removing Oil From a Salt Marsh Using In-situ Burning", National Institute of Standards and Technology and Minerals Management Service, *In-situ Burning Oil Spill, Proceedings,* (1994).

Guenette, C., and J. Thornborough, “An Assessment of Two Off-shore Igniter Concepts”, *Proceedings of the Twentieth Arctic and Marine Oilspill Program,* Technical Seminar, 2:795-1364, (1997).

Guenette, C. C., P. Sveum, C. Bech and I. Buist, “Studies of In-situ Burning of Emulsions in Norway”, *Oil Spill Conference,* 115-122, (1995a).

Guenette, C., and P. Sveum, “Emulsion Breaking Igniters: Recent Developments in Oil Spill Igniter Concepts”, *Proceedings of the Eighteenth Arctic and Marine Oilspill Program,* Technical Seminar, 2:1011-1026, (1995).

Guenette, C., P. Sveum, I. Buist, T. Aunaas, and L. Godal, “In-Situ Burning of Water-In-Oil Emulsions”, SINTEF Report STF21 A94053, Reprinted as MSRC Technical Report Series 94-001, 139, (1994).

Hamins, A., M. E. Klassen, J. P. Gore, S. J. Fischer, and T. Kashiwagi, “Heat Feedback to the Fuel Surface in Pool Fires”, *Combustion Science and Technology* 97:37-62, (1994).

Hokstad, J. N., P. S. Daling, A. Lewis, and T. Stϕm-Kristiansen, “Methodology for Testing Water-in-Oil Emulsions and Demulsifiers. Description of Laboratory Procedures”, *Formation and Breaking of Water-in-Oil Emulsions: Workshop Proceedings*, Technical Report Series, 93-018, 223-253, (1995).

Holen, J., M. Brostrom, and B. F. Magnussen, “Finite Difference Calculation of Pool Fires”, *Proceedings of Twenty-Third Symposium (International) on Combustion*, The Combustion Institute, 1677-1683, (1990).

Inamura, T., K. Saito, and K. A. Tagavi, “A Study of Boilover in Liquid Pool Fires Supported on Water, Part II: Effects of In-depth Absorption”, *Combustion Science and Technology*, 86:105-119, (1992).

Incropera, F. P., and D. P. DeWitt, “Fundamental of Heat and Mass Tranfer”, *John Wiley and Sons*, 2nd Edition, (1985).

Jones, R. K., “A Simplified Pseudo-component Oil Evaporation Model”, ”, *Proceedings of the Twentieth Arctic and Marine Oilspill Program,* Technical Seminar, 1:43-62, (1997).

Khater, H. A., A. K. Khalil, A. A. Rizk, and G. Mahrous, “Analysis of the Role of Thermal Radiation from Liquified Petroleum Gas Pool Fires”, *ASME/HTD Heat and Mass Transfer in Fires, AIAA/ASME Thermophysics and Heat Transfer Conference*, 23-29 (1990).

Klassen, M., and J. P. Gore, “Structure and Radiation Properties of Pool Fires”, Final Report to Center for Fire Rsearch of the Building and Fire Research Laboratory of the National Institute of Standard and Technology, August, 1992, (1992).

Lewis, A. and M. Walker, “A Review of the Processes of Emulsification and Demulsification”, *Formation and Breaking of Water-in-Oil Emulsions: Workshop Proceedings*, Technical Report Series, 93-018, 223-253, (1995).

Mackay, D., I. Buist, R. Mascarenhas, and S. Paterson, “Oil Spills; Processes and Models”, *Environment Canada*, Ottawa, Ontario, (1980).

McCourt, J., I. Buist, B. Pratte, W. Jamieson, and J. V. Mullin, “Testing Fire Resistant Boom in Waves and Flames”, ”, *Proceedings of the Twentieth Arctic and Marine Oilspill Program,* Technical Seminar, 2:823-840, (1997).

McGrattan, K. B., H. R. Baum, and R. G. Rehm, "Smoke Plume Trajectory From In-situ Burning of Crude Oil in Alaska", *Proceedings of the Seventeenth Arctic and Marine Oil Spill Program,* Technical Seminar, 1:725, (1994).

O'Rourke, C., "Oil Spill Cleanup in the Beaufort Sea", *Spill Technology Newsletter*, I(6):12, (1976).

Pisarchik, M., D. Kocis, A. Walavalkar, and A. K. Kulkarni, "Effect of Temperature on Breaking of Water-in-Oil Emulsions", *Proceedings of the Twentieth Arctic and Marine Oilspill Program*, Technical Seminar, 2:809-822, (1997).

Putorti, A. D., Jr., "Application of the Critical Radiative Ignition Flux Methodology to High Viscosity Petroleum Fractions", MS Thesis, Worcester Polytechnic Institute, 68 p., (1994).

Putorti, A. D., Jr. and D. Evans, "Ignition of Weathered and Emulsified Oils", *Proceedings of the Seventeenth Arctic and Marine Oil Spill Program*, Technical Seminar, 1:657-667, (1994).

Quintere, J., "A Simplified Theory for Generalizing Results from Radiant Panel Rate of Flame Spread Apparatus", *Fire and Materials*, 5, 2, pp. 52-60, (1981).

Stiver, W., and D. Mackay, "Evaporation Rate of Spills of Hydrocarbons and Petroleum Mixtures", *Environmental Science and Technology*, vol 18, No 11, 834-840, (1984).

Strøm-Kristiansen, T., A. Lewis, P. S. Daling, and A. B. Nordvik, "Demulsification by Use of Heat and Emulsion Breaker", *Proceedings of the Eighteenth Arctic and Marine Oil spill Program,* Technical Seminar, 1:367-384, (1995).

Tennyson, E. J., "In-situ Burning Overview", National Institute of Standards and Technology and Minerals Management Service, *In-situ Burning Oil Spill. Proceedings*, (1994).

Thompson, C. H., G. W. Dawson, and G. L. Goodier, "Combustion: An Oil Spill Mitigation Tool", US Department of Energy, Washington, DC, 53 p., (1979).

Tien, C. L., "Radiative Modeling of Pool Fires," *Summaries of center for Fire Reseach Grants and In-House Programs – 1986*, National Institute of Standards and Technology, Gaithersburg, MD, (1986).

Vargaftik, N. B., "Tables on the Thermophysical Properties of Liquids and Gases", *Hemisphere Publication Corporation, 2nd Edition*, p. 695, (1975).

Walton, W. D., "Status of Fire Boom Performance Testing", *In Situ Burning of Oil Spills Workshop Proceedings*, 31-38, (1998)

Walton, W. D., D. D. Evans, K. B. McGrattan, H. R. Baum, W. H. Twilley, D. Madrzykowski, A. D. Putorti, Jr., R. G. Rehm, H. Koseki, and E. J. Tennyson, "In-situ Burning of Oil Spills: Mesoscale Experiments and Analysis", *Proceedings of Sixteenth Arctic and Marine Oil spill Program*, Technical Seminar, 2,(1993).

Walton, W. D., J. A.McElroy, W. H.Twilley, and R. R. Hiltabrand, "Smoke Measurements Using a Helicopter Transported Sampling Package", *Proceedings of Seventeenth Arctic and Marine Oil spill Program,* Technical Seminar, (1994a).

Walton, W. D., W. H.Twilley, J. A.McElroy, D. D. Evans, and E. J. Tennyson, "Smoke Measurements Using a Tethered Miniblimp at Newfoundland Offshore Burn Experiment", *Proceedings of Seventeenth Arctic and Marine Oil spill Program*, Technical Seminar, 2, pp 1083-1089, (1994b).

Wu, N., M. Baker, G. Kolb, and J. L. Torero, “Ignition, Flame Spread and Mass Burning Characteristics of Liquid Fuels on a Water Bed”, *Proceedings of Twentieth Arctic and Marine Oil spill Program*, Technical Seminar, 2, pp 769-793, (1997).

Yamaguchi, T. and Wasaka, K., “Oil Pool Fire Experiment,” *Fire Safety Science - Proceedings of the First International Symposium*, p 911, (1986).

Appendix A

Finite Differencing

Finite Differencing for the Interior Nodes

A general partial differential equation selected for finite differencing can be represented as

$$\frac{\partial T}{\partial \tau}+\frac{\partial T}{\partial t}=\alpha C_{t1}\frac{\partial^2 T}{\partial x^2}+C_{t2}\frac{\partial T}{\partial x}+\frac{aC_0\dot{q}''\beta e^{-\beta(L-x)}}{\rho_o C_{po}} \qquad (A_1)$$

where, $C_{t1} = C^2(1 - x)^4$ and $C_{t2} = -4\alpha_w C^2(1 - x)^3$ for water base and $C_{t1} = 1$ and $C_{t2} = 0$ for oil and emulsion layers. Also, $a = 1$ for oil layer to account for the in-depth radiation absorption and $a = 0$ for emulsion and water layers. The pseudo time (τ) derivative added to the governing equation is driven to zero by attaining steady state in pseudo time, for each time step in real time (t) thus assuring a converged solution. Two-point difference in time and central difference in space is used.

In the finite differencing presented here, the subscript "i" represents the spatial location index. The superscript "m" represents the time index and the superscript "k" represents pseudo time index.

Finite differencing of equation A_1 is presented below.

$$\left(\frac{T_i^{k+1}-T_i^{k}}{\Delta\tau}\right)+\left(\frac{T_i^{k+1}-T_i^{m}}{\Delta t}\right)=\alpha C_{t1}\left(\frac{T_{i+1}^{m}+T_{i-1}^{m}-2T_i^{m}}{2\Delta x^2}\right)+C_{t2}\left(\frac{T_i^{m}-T_{i-1}^{m}}{\Delta x}\right)+f(x)$$

where $f(x)=\dfrac{aC_0\dot{q}''\beta e^{-\beta(L-x)}}{\rho_o c_{po}}$.

Thus solving for T_i^{k+1},

$$T_i^{k+1}=\frac{1}{\left(\frac{1}{\Delta\tau}+\frac{1}{\Delta t}\right)}\left\{\frac{T_i^{k}}{\Delta\tau}+\frac{T_i^{k}}{\Delta t}+\frac{\alpha C_{t1}}{\Delta x^2}\left(\frac{T_{i+1}^{m}+T_{i-1}^{m}-2T_i^{m}}{2\Delta x^2}\right)+\frac{C_{t2}}{\Delta x}\left(\frac{T_i^{m}-T_{i-1}^{m}}{\Delta x}\right)+f(x)\right\} \qquad (A_2)$$

The above finite differencing was used for all the interior nodes in all the three regions *viz.* oil, emulsion and water with appropriate values of C_{t1}, C_{t2} and a.

Finite Differencing for the Emulsion-Water Interface Node

The representation of the grid at the emulsion-water interface is shown in figure A.

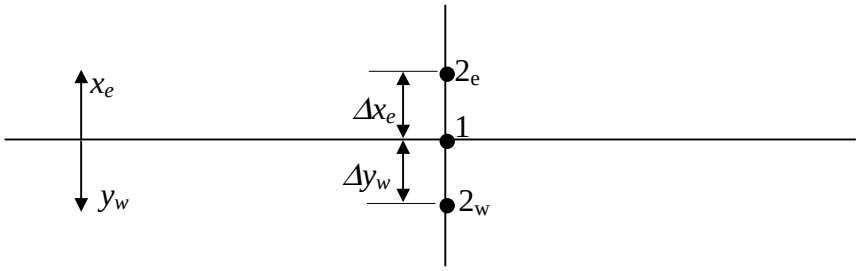

Figure A.

At node number 1, the governing equation for emulsion region, the governing equation for the water region and the boundary condition stating the continuation of heat flux need to be satisfied.

Governing equation for the emulsion region,

$$\frac{\partial T_1}{\partial \tau} + \frac{\partial T_1}{\partial t} = \alpha_e \left. \frac{\partial^2 T_e}{\partial x_e^2} \right|_1 \qquad (A_3)$$

Applying the Taylor series expansion for temperature at node 2_e.

$$T_{2e} = T_1 + \Delta x_e \left. \frac{\partial T_e}{\partial x_e} \right|_1 + \frac{\Delta x_e^2}{2} \left. \frac{\partial^2 T_e}{\partial x_e^2} \right|_1$$

Hence,

$$\left. \frac{\partial^2 T_e}{\partial x_e^2} \right|_1 = \frac{2}{\Delta x_e^2} \left(T_{2e} - T_1 - \Delta x_e \left. \frac{\partial T_e}{\partial x_e} \right|_1 \right) \qquad (A_4)$$

Substituting A_4 in A_3,

$$\frac{\partial T_1}{\partial \tau} + \frac{\partial T_1}{\partial t} = \frac{2\alpha_e}{\Delta x_e^2} \left(T_{2e} - T_1 - \Delta x_e \left. \frac{\partial T_e}{\partial x_e} \right|_1 \right) \qquad (A_5)$$

Rearranging the terms in equation A_5

$$\frac{\Delta x_e}{2\alpha_e} \frac{\partial T_1}{\partial \tau} + \frac{\Delta x_e}{2\alpha_e} \frac{\partial T_1}{\partial t} = \frac{1}{\Delta x_e} (T_{2e} - T_1) - \left. \frac{\partial T_e}{\partial x_e} \right|_1 \qquad (A_6)$$

Governing equation for the water region,

$$\frac{\partial T_1}{\partial \tau}+\frac{\partial T_1}{\partial t}=\alpha_w C^2(1-y_w)^4\frac{\partial^2 T_w}{\partial y_w^2}\bigg|_1-4\alpha_w C^2(1-y_w)^3\frac{\partial T_w}{\partial y_w}\bigg|_1 \qquad (A_7)$$

Applying the Taylor series expansion for temperature at node 2_w.

$$T_{2w}=T_1+\Delta y_w\frac{\partial T_w}{\partial y_w}\bigg|_1+\frac{\Delta y_w^2}{2}\frac{\partial^2 T_w}{\partial y_w^2}\bigg|_1$$

Hence,

$$\frac{\partial^2 T_w}{\partial y_w^2}\bigg|_1=\frac{2}{\Delta y_w^2}\left(T_{2w}-T_1-\Delta y_w\frac{\partial T_w}{\partial y_w}\bigg|_1\right) \qquad (A_8)$$

Substituting A_8 in A_7

$$\frac{\partial T_1}{\partial \tau}+\frac{\partial T_1}{\partial t}=\frac{2\alpha_w C^2(1-y_w)^4}{\Delta y_w^2}(T_{2w}-T_1)-\left\{\frac{2\alpha_w C^2(1-y_w)^4}{\Delta y_w}+4\alpha_w C^2(1-y_w)^3\right\}\frac{\partial T_w}{\partial y_w}\bigg|_1 \qquad (A_9)$$

The boundary condition at the emulsion water interface is given by

$$k_e\frac{\partial T_e}{\partial x_e}\bigg|_1=-k_w C(1-y_w)^2\frac{\partial T_w}{\partial y_w}\bigg|_1 \qquad (A_{10})$$

Hence,

$$\frac{\partial T_w}{\partial y_w}\bigg|_1=\frac{-k_e}{k_w C(1-y_w)^2}\frac{\partial T_e}{\partial x_e}\bigg|_1 \qquad (A_{11})$$

Substituting using equation A_{11} in equation A_9

$$\frac{\partial T_1}{\partial \tau}+\frac{\partial T_1}{\partial t}=\frac{2\alpha_w C^2(1-y_w)^4}{\Delta y_w^2}(T_{2w}-T_1)-\left\{\frac{2k_e\alpha_w C^2(1-y_w)^2}{k_w\Delta y_w}+\frac{4k_e\alpha_w C^2(1-y_w)}{k_w}\right\}\frac{\partial T_e}{\partial x_e}\bigg|_1 \qquad (A_{12})$$

Equation A12 is rewritten as

$$\frac{\partial T_1}{\partial \tau}+\frac{\partial T_1}{\partial t}=P(T_{2w}-T_1)+Q\frac{\partial T_e}{\partial x_e}\bigg|_1 \qquad (A_{13})$$

Where, $P=\dfrac{2\alpha_w C^2}{\Delta y_w^2}$ and, $Q=\left\{\dfrac{2k_e\alpha_w C^2}{k_w\Delta y_w}+\dfrac{4k_e\alpha_w C^2}{k_w}\right\}$

At the emulsion-water interface, $y_w = 0$.

Equation A_{13} can be rewritten as

$$\frac{1}{Q}\frac{\partial T_1}{\partial \tau}+\frac{1}{Q}\frac{\partial T_1}{\partial t}=\frac{P}{Q}\left(T_{2w}-T_1\right)+\left.\frac{\partial T_e}{\partial x_e}\right|_1 \qquad (A_{14})$$

Adding equations A_6 and A_{14}

$$\left(\frac{1}{Q}+\frac{\Delta x_e}{2\alpha_e}\right)\frac{\partial T_1}{\partial \tau}+\left(\frac{1}{Q}+\frac{\Delta x_e}{2\alpha_e}\right)\frac{\partial T_1}{\partial t}=\frac{P}{Q}\left(T_{2w}-T_1\right)+\frac{1}{\Delta x_e}\left(T_{2e}-T_1\right) \qquad (A_{15})$$

Finite differencing equation A_{15},

$$R\left(\frac{T_1^{k+1}-T_1^{k}}{\Delta\tau}\right)+R\left(\frac{T_1^{k+1}-T_1^{m}}{\Delta t}\right)=\frac{P}{Q}\left(T_{2w}^{m}-T_1^{m}\right)+\frac{1}{\Delta x_e}\left(T_{2e}^{m}-T_1^{m}\right) \qquad (A_{16})$$

Where, $R=\left(\frac{1}{Q}+\frac{\Delta x_e}{2\alpha_e}\right)$

Solving equation A16 for T_1^{k+1}

$$T_1^{k+1}=\frac{1}{\left(\frac{R}{\Delta\tau}+\frac{R}{\Delta t}\right)}\left\{\frac{R}{\Delta\tau}T_1^{k}+\frac{P}{Q}T_{2w}^{m}+\left(\frac{R}{\Delta t}-\frac{P}{Q}-\frac{1}{\Delta x_e}\right)T_1^{m}+\frac{1}{\Delta x_e}T_{2e}^{m}\right\} \qquad (A_{17})$$

Finite Differencing for the Emulsion Surface Node for the Initial Regime

The representation of the grid at the emulsion surface is shown in figure B.

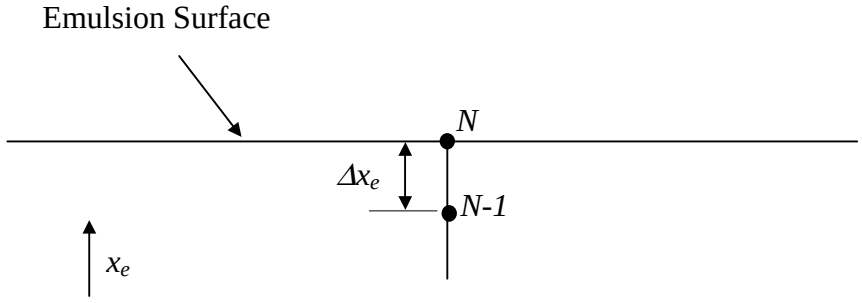

Figure B.

At node number *N* on the emulsion surface, the governing equation for emulsion region, and the boundary condition need to be satisfied.

Governing equation for the emulsion region,

$$\frac{\partial T_N}{\partial \tau} + \frac{\partial T_N}{\partial t} = \alpha_e \left. \frac{\partial^2 T_e}{\partial x_e^2} \right|_N \tag{A18}$$

Applying the Taylor series expansion for temperature at node *N-1*.

$$T_{N-1} = T_N - \Delta x_e \left. \frac{\partial T_e}{\partial x_e} \right|_N + \frac{\Delta x_e^2}{2} \left. \frac{\partial^2 T_e}{\partial x_e^2} \right|_N$$

Hence,

$$\left. \frac{\partial^2 T_e}{\partial x_e^2} \right|_N = \frac{2}{\Delta x_e^2} \left(T_{N-1} - T_N + \Delta x_e \left. \frac{\partial T_e}{\partial x_e} \right|_N \right) \tag{A19}$$

The boundary condition for the emulsion surface node during the initial regime is given by

$$k_e \left. \frac{\partial T_e}{\partial x_e} \right|_N = \dot{q}'' - h_e (T_N - T_\infty) - \sigma \varepsilon_e (T_N^4 - T_\infty^4) \tag{A20}$$

Substituting from equation A_{20} in equation A_{19}.

$$\left. \frac{\partial^2 T_e}{\partial x_e^2} \right|_N = \frac{2}{\Delta x_e^2} \left(T_{N-1} - T_N + \frac{\Delta x_e}{k_e} \left(\dot{q}'' - h_e (T_N - T_\infty) - \sigma \varepsilon_e (T_N^4 - T_\infty^4) \right) \right) \tag{A21}$$

Substituting from equation A_{21} in equation A_{18}

$$\frac{\partial T_N}{\partial \tau} + \frac{\partial T_N}{\partial t} = \frac{2\alpha_e}{\Delta x_e^2} \left(T_{N-1} - T_N + \frac{\Delta x_e}{k_e} \left(\dot{q}'' - h_e (T_N - T_\infty) - \sigma \varepsilon_e (T_N^4 - T_\infty^4) \right) \right) \tag{A22}$$

Finite differencing equation A_{22}

$$\frac{T_N^{k+1} - T_N^k}{\Delta \tau} + \frac{T_N^{k+1} - T_N^m}{\Delta t} = \frac{2\alpha_e}{\Delta x_e^2} \left(T_{N-1}^m - T_N^m + \frac{\Delta x_e}{k_e} \left(\dot{q}'' - h_e (T_N^m - T_\infty) - \sigma \varepsilon_e (T_N^{m\,4} - T_\infty^4) \right) \right) \tag{A23}$$

Solving equation A_{23} for T_N^{k+1}

$$T_N^{k+1} = \frac{\left\{ \left[\frac{T_N^k}{\Delta \tau} + \frac{T_N^m}{\Delta t} + \frac{2\alpha_e}{\Delta x_e^2} \left(T_{N-1}^m - T_N^m + \frac{\Delta x_e}{k_e} \left(\dot{q}'' - h_e (T_N^m - T_\infty) - \sigma \varepsilon_e (T_N^{m\,4} - T_\infty^4) \right) \right) \right] \right\}}{\left(\frac{1}{\Delta \tau} + \frac{1}{\Delta t} \right)} \tag{A24}$$

The same finite differenced equation can be used for surface node in the oil region during the intermediate regime by replacing the emulsion properties by the corresponding oil properties.

Finite Differencing for the Oil-Emulsion Interface Node for the Intermediate and Final Regimes

At the oil emulsion interface, the interface condition is used to calculate the temperature of the interface node. The emulsion layer that has reached temperatures above the emulsion breaking temperature is then considered to have separated and the corresponding nodes are removed from the emulsion layer and equivalent nodes are added to the oil layer at the temperature equal to the emulsion breaking temperature.

The node at the oil-emulsion interface must satisfy the governing equation in oil region, the governing equation in emulsion region and the auxiliary condition at the oil-emulsion interface.

The representation of the grid at the oil-emulsion interface is shown in figure C.

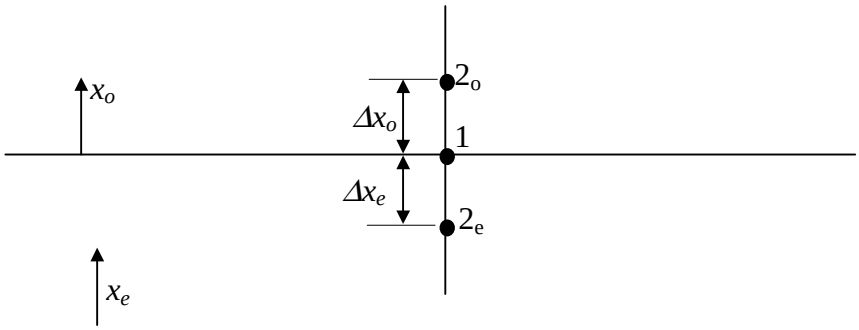

Figure C.

Governing equation for the emulsion region,

$$\frac{\partial T_1}{\partial \tau} + \frac{\partial T_1}{\partial t} = \alpha_e \frac{\partial^2 T_e}{\partial x_e^2}\bigg|_1 \qquad (A_{25})$$

Applying the Taylor series expansion for temperature at node 2_e.

$$T_{2e} = T_1 - \Delta x_e \frac{\partial T_e}{\partial x_e}\bigg|_1 + \frac{\Delta x_e^2}{2}\frac{\partial^2 T_e}{\partial x_e^2}\bigg|_1$$

Hence,

$$\left.\frac{\partial^2 T_e}{\partial x_e^2}\right|_1 = \frac{2}{\Delta x_e^2}\left(T_{2e} - T_1 + \Delta x_e \left.\frac{\partial T_e}{\partial x_e}\right|_1\right) \tag{A26}$$

Substituting A_{26} in A_{25},

$$\frac{\partial T_1}{\partial \tau} + \frac{\partial T_1}{\partial t} = \frac{2\alpha_e}{\Delta x_e^2}\left(T_{2e} - T_1 + \Delta x_e \left.\frac{\partial T_e}{\partial x_e}\right|_1\right) \tag{A27}$$

Rearranging the terms in equation A_{27} and multiplying throughout by k_e

$$\frac{k_e \Delta x_e}{2\alpha_e}\frac{\partial T_1}{\partial \tau} + \frac{k_e \Delta x_e}{2\alpha_e}\frac{\partial T_1}{\partial t} = \frac{k_e}{\Delta x_e}\left(T_{2e} - T_1\right) + k_e \left.\frac{\partial T_e}{\partial x_e}\right|_1 \tag{A28}$$

Governing equation for the oil region,

$$\frac{\partial T_1}{\partial \tau} + \frac{\partial T_1}{\partial t} = \alpha_o \frac{\partial^2 T_1}{\partial x_o^2} + \frac{C_0 \dot{q}'' \beta e^{-\beta(L - x_o)}}{\rho_o c_{po}}$$

At the interface, $x_o = 0$. Hence the governing equation is reduced to

$$\frac{\partial T_1}{\partial \tau} + \frac{\partial T_1}{\partial t} = \alpha_o \left.\frac{\partial^2 T_o}{\partial x_o^2}\right|_1 + \frac{C_0 \dot{q}'' \beta e^{-\beta L}}{\rho_o c_{po}} \tag{A29}$$

Applying the Taylor series expansion for temperature at node 2_o.

$$T_{2o} = T_1 + \Delta x_o \left.\frac{\partial T_o}{\partial x_o}\right|_1 + \frac{\Delta x_o^2}{2}\left.\frac{\partial^2 T_o}{\partial x_o^2}\right|_1$$

Hence,

$$\left.\frac{\partial^2 T_o}{\partial x_o^2}\right|_1 = \frac{2}{\Delta x_o^2}\left(T_{2o} - T_1 - \Delta x_o \left.\frac{\partial T_o}{\partial x_o}\right|_1\right) \tag{A30}$$

Substituting A_{30} in A_{29},

$$\frac{\partial T_1}{\partial \tau} + \frac{\partial T_1}{\partial t} = \frac{2\alpha_o}{\Delta x_o^2}\left(T_{2o} - T_1 - \Delta x_o \left.\frac{\partial T_o}{\partial x_o}\right|_1\right) + \frac{C_o \dot{q}'' \beta e^{-\beta L}}{\rho_o c_{po}} \tag{A31}$$

Rearranging the terms in equation A_{31} and multiplying throughout by k_o

$$\frac{k_o \Delta x_o}{2\alpha_o}\frac{\partial T_1}{\partial \tau} + \frac{k_o \Delta x_o}{2\alpha_o}\frac{\partial T_1}{\partial t} = \frac{k_o}{\Delta x_o}\left(T_{2o} - T_1\right) - k_o \left.\frac{\partial T_o}{\partial x_o}\right|_1 + \frac{k_o C_o \dot{q}'' \beta e^{-\beta L}}{\rho_o c_{po}} \tag{A32}$$

The auxiliary condition at the oil-emulsion interface is given by

$$k_o \left.\frac{\partial T_o}{\partial x_o}\right|_1 - k_e \left.\frac{\partial T_e}{\partial x_e}\right|_1 = C_o \dot{q}'' e^{-\beta L} \qquad (A_{33})$$

Adding equations A_{28} and A_{32} and substituting from equation A_{33}

$$S\left\{\left(\frac{T_1^{k+1} - T_1^k}{\Delta\tau}\right) + \left(\frac{T_1^{k+1} - T_1^m}{\Delta t}\right)\right\} = \frac{k_e\left(T_{2e}^m - T_1^m\right)}{\Delta x_e} + \frac{k_o\left(T_{2o}^m - T_1^m\right)}{\Delta x_o} + U \qquad (A_{34})$$

Where $S = \left(\frac{\Delta x_e k_e}{2\alpha_e} + \frac{\Delta x_o k_o}{2\alpha_o}\right)$ and $U = C_o \dot{q}'' e^{-\beta L}\left(\alpha_o \beta - 1\right)$.

Solving equation A_{34} for T_1^{k+1}.

$$T_1^{k+1} = \frac{\frac{S}{\Delta\tau}T_1^k + \frac{S}{\Delta t}T_1^m + \frac{k_e\left(T_{2e}^m - T_1^m\right)}{\Delta x_e} + \frac{k_o\left(T_{2o}^m - T_1^m\right)}{\Delta x_o} + U}{\left(\frac{S}{\Delta\tau} + \frac{S}{\Delta t}\right)} \qquad (A_{35})$$

Finite Differencing for the Oil Surface Node for the Final Regime

The representation of the grid at the oil surface is shown in figure D.

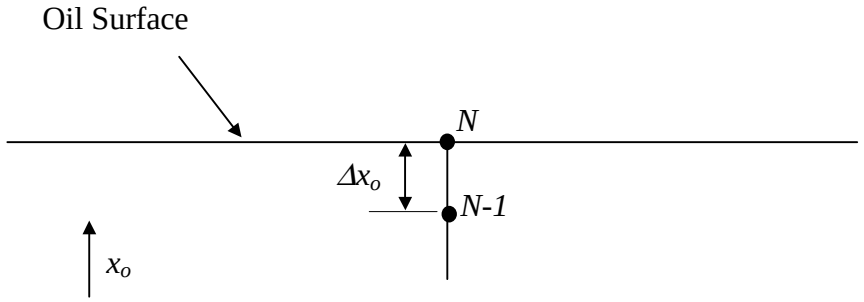

Figure D.

At node number *N* on the oil surface, the governing equation for oil region, and the boundary condition need to be satisfied. The surface temperature of the oil is equal to the oil vaporization temperature.

Governing equation for the oil region,

$$\frac{\partial T_N}{\partial \tau} + \frac{\partial T_N}{\partial t} = \alpha_o \frac{\partial^2 T_N}{\partial x_o^2} + \frac{C_0 \dot{q}'' \beta e^{-\beta(L-x_o)}}{\rho_o c_{po}}$$

At the oil surface, $x_o = L$. Hence the governing equation is reduced to

$$\frac{\partial T_N}{\partial \tau} + \frac{\partial T_N}{\partial t} = \alpha_o \left.\frac{\partial^2 T_o}{\partial x_o^2}\right|_1 + \frac{C_0 \dot{q}'' \beta}{\rho_o c_{po}} \qquad (A_{36})$$

As the temperature at the surface is constant, the terms $\frac{\partial T_N}{\partial \tau}$, and $\frac{\partial T_N}{\partial t}$ are equal to zero.

Applying the Taylor series expansion for temperature at node *N-1*.

$$T_{N-1} = T_N - \Delta x_o \left.\frac{\partial T_o}{\partial x_o}\right|_N + \frac{\Delta x_o^2}{2} \left.\frac{\partial^2 T_o}{\partial x_o^2}\right|_N$$

Hence,

$$\left.\frac{\partial^2 T_o}{\partial x_o^2}\right|_N = \frac{2}{\Delta x_o^2}\left(T_{N-1} - T_N + \Delta x_o \left.\frac{\partial T_o}{\partial x_o}\right|_N \right) \qquad (A_{37})$$

Substituting from equation A_{37} in equation A_{36} and simplifying,

$$\left.\frac{\partial T_o}{\partial x_o}\right|_N = \frac{T_N - T_{N-1}}{\Delta x_o} - \frac{\Delta x_o C_o \dot{q}'' \beta}{2\alpha_o} \qquad (A_{38})$$

The boundary condition at the oil surface is given by

$$k_o \left.\frac{\partial T_o}{\partial x_o}\right|_N = (1 - C_o)\dot{q}'' - h_o (T_N - T_\infty) - \sigma \varepsilon_o \left(T_N^4 - T_\infty^4\right) - \rho_o Q_{Lo} \frac{dL}{dt} \qquad (A_{39})$$

Substituting from equation A_{39} in equation A_{38} and solving for $\frac{dL}{dt}$.

$$\frac{dL}{dt} = \frac{(1 - C_o)\dot{q}'' - h_o (T_N - T_\infty) - \sigma \varepsilon_o \left(T_N^4 - T_\infty^4\right) + \frac{k_o}{\Delta x_o}(T_{N-1} - T_N) + \frac{k_o \Delta x_o C_o \dot{q}'' \beta}{2\alpha_o}}{\rho_o Q_{Lo}} \qquad (A_{40})$$

Equation A_{40} is used to calculate the rate at which the oil is vaporizing. Based on the thickness of the oil layer *(L)* at time *(t)*, the new thickness is calculated using equation A_{40} and the time step Δt.

During the final regime, if the emulsion layer separates before the fire is extinguished, the oil layer is now floating above the water layer. The equations for the

oil-water interface are obtained by following a procedure similar to the one used in developing the emulsion-water interface equation.

The finite difference equations presented above for the three regimes and water, oil and emulsion regions are programmed in Fortran to obtain the solution of the model. The Fortran program is presented in Appendix B.

Appendix B

Fortran Program Listings

Program for Initial Regime

```
c*********************************************************************
c
c            PROGRAM FOR PART I
c
c*********************************************************************
      implicit double precision(a-h,o-z)
      parameter (imax = 3000)
c*********************************************************************
c ho - convective heat rtansfer coefficient for oil/air
c he - convective heat rtansfer coefficient for emulsion/air
c hfgw - enthalpy of evaporation of water
c epse - emissivity of emulsion
c espo - emissivity of oil
c cone - conductivity of emulsion
c cono - conductivity of oil
c conw - conductivity of water
c dife - diffusivity of emulsion
c difo - diffusivity of oil
c difw - diffusivity of water
c stboltz - Stefan - Boltzmann Constant
c rhoe - emulsion density
c rhoo - oil density
c rhow - water density
c cpo - specific heat of oil
c co - fraction of incident heat flux not absorbed at the surface
c teb - emulsion breaking temperature
c tov - oil vaporization temperature
c beta - inverse absorption depth
c qle - latent heat of emulsion breaking
c qlo - latent heat of oil vaporization
c qcom - energy released by oil combustion
c rl - thickness of oil layer
c y - region of interest in water
c delt - time step
c delxe - grid spacing in emulsion zone
c delxw - grid spacing in water region
c tin - ambient/initial temperature
c h -  emulsion thickness
c c1 -inverse oil content of emulsion, by mass
c*********************************************************************
c Declaring Common variables for the main program as well as the
c subroutines
      common/list1/ho,epso,cono,difo,rhoo,cpo,qlo,qcom,co,tov,beta
      common/list2/conw,difw,rhow,hfgw,cpw,qmacks
      common/list3/y,delt,delxe,delxw,tin,h,c1,teb,err,deltau,q,gamma
        common/list4/epse,he
      common/list5/cone,dife,rhoe,qle
      common/list6/stboltz,delyw,rc,rl
c*********************************************************************
```

```
      namelist/list1/ho,epso,cono,difo,rhoo,cpo,qlo,qcom,co,tov,beta
      namelist/list2/conw,difw,rhow,hfgw,cpw,qmacks
      namelist/list3/y,delt,delxe,delxw,tin,h,c1,teb,err,deltau,q,
     $                   gamma
      namelist/list4/epse,he

c**********************************************************************
c The temperature in emulsion and water. First index is for space,
c second is for pseudotime tau such that 1 is for old tau and
c 2 is for new tau,and third for time t such that 1 is old time 2 is
c new time

      dimension te(imax,2,2), tw(imax,2,2)

c**********************************************************************

c**** read the oil data
      open (unit =11, file='oil.in', status = 'old')
c**** read the variables in list 1 declared above from oil property
c     input file.
      read (11, list1)
c**** save oil data
      open (unit =12, file='oil.out', status = 'unknown')
      write(12, list1)
c**** read the water data
      open (unit =13, file='water.in', status = 'old')
c**** read the variables in list 2 declared above from water property
c     input file.
      read(13, list2)
c**** save water data
      open (unit =14, file='water.out', status = 'unknown')
      write(14, list2)
c**** read the input
      open (unit =15, file='data.in', status = 'old')
c**** read the variables in list 3 declared above from data file.
      read (15,list3)
c**** save the input
      open (unit =16, file='data.out', status = 'unknown')
      write (16,list3)
c**** read the input
      open (unit =18, file='imuls.in', status = 'old')
c**** read the variables in list 4 declared above from emulsion
c      property
c     input file.
      read (18,list4)
c**** save the input
      open (unit =19, file='imuls.out', status = 'unknown')
      write (19,list4)
c**********************************************************************
c wfrpt2--> file containing water temeprature profile to be input for
c           part 2 of the model
c mandn --> file containing no of nodes in water (m) and in oil (n)
c efrpt2 --> file containing temperature profile in emulsion layer at
c            the end of part 1 for input to part2.
c tempout --> file containing a typical temp profile during part1.
c residual --> file containig residuals
```

```
      open (unit =54, file='wfrpt2', status = 'unknown')
      open (unit =55, file='mandn', status = 'unknown')
      open (unit =56, file='efrpt2', status = 'unknown')
      open (unit =57, file='tempout', status = 'unknown')
      open (unit =58, file='watin', status = 'unknown')
      open (unit =59, file='time_temp', status = 'unknown')

c*** Calculation of emulsion properties using weighted fractions
c    of oil and water in emulsion.

      qle=(1.0-(1/c1))*hfgw
      rhoe=rhow+(rhoo-rhow)/c1
      cone=conw+(cono-conw)/c1
      cpe=cpw+(cpo-cpw)/c1
      dife=cone/(rhoe*cpe)
c**********************************************************************
      stboltz=5.67e-8
c**********************************************************************
c**** Write out the emulsion properties calculated above to a file.

      open (unit =17, file='emuls.out', status = 'unknown')
      write (17,2)qle,rhoe,cone,dife,epse,he,cpe
 2    format('Qle=',e9.3,/,'Rhoe=',f9.3,/,'Cone=',e10.3,/,'Dife=',
     $           e10.3,/,'Epse=',f6.3,/,'He=',f6.3,/,'cpe=',f10.3,/)


c*** n= no of grid points in emulsion region
c*** m=no grid points in transformed water region

      n=int(h/delxe)
      n=n+1

c** y is the regoin of interest in water (typically 1m) beyond which
c   effects of heating will not be felt (or the assumption of
c   seminifite region will be valid).delxw is the grid spacing in
c   the original water region between first 2 gris points. delyw is the
c   unform graid spacing in the transformed water region. This region
c   is bounded to 1 intransformed coordinates.

      rc=4.0/y
      delyw=rc*delxw
      m=1+int((1.0/delyw))
      rl=0.0
      write(55,3)m,n
 3    format(I4,3x,I4)

c**********************************************************************

      dxtherm=0.005
      open(unit =60, file='profile',status ='old',access='sequential')
      read(60,6)pro_t1, pro_t2, pro_t3, pro_t4, pro_t5
 6    format(5(f5.2, /))
      pro_t1=pro_t1+273.0
      pro_t2=pro_t2+273.0
      pro_t3=pro_t3+273.0
      pro_t4=pro_t4+273.0
      pro_t5=pro_t5+273.0
```

```
      nini= int(0.005/delxe)+1
      yini= 1.0- (1.0/(1.0+rc*0.005))
      mini=int(yini/delyw)+1

      do 5 i=1,nini
            te(i,1,2)=0.0
            te(i,2,1)=0.0
            te(i,2,2)=0.0
            xini=(float(i-1)*delxe)
            t_eini=pro_t4+ xini*(pro_t3-pro_t4)/0.005
            te(i,1,1)= t_eini

 5    continue

      do 7 i= 1,nini
            j=nini-1+i
            te(j,1,2)=0.0
            te(j,2,1)=0.0
            te(j,2,2)=0.0
            xini=(float(i-1)*delxe)
            t_eini=pro_t3+ xini*(pro_t2-pro_t3)/0.005
            te(j,1,1)= t_eini

 7    continue

      do 8 i=1,nini
            j= 2*nini-2+i
            te(j,1,2)=0.0
            te(j,2,1)=0.0
            te(j,2,2)=0.0
            xini=(float(i-1)*delxe)
            t_eini=pro_t2+ xini*(pro_t1-pro_t2)/0.005
            te(j,1,1)= t_eini

 8    continue

      do 9 i= 1, mini
            tw(i,1,2)=0.0
            tw(i,2,1)=0.0
            tw(i,2,2)=0.0
            xwini=(float(i-1)*delxw)
            t_wini=pro_t4-xwini*(pro_t4-pro_t5)/0.005
            tw(i,1,1)=t_wini

 9    continue

c***  Initialize the temperatures

      do 15 i=mini+1,m
            tw(i,1,2)=0.0
            tw(i,2,1)=0.0
            tw(i,2,2)=0.0
            tw(i,1,1)=tin
 15   continue

c** Surface temperature is set equalt to the temperature of the
```

```
c   n th node in the emulsion region.

      tes=te(n,1,1)
      rl=0.0
      j=0


c*** Calculations for part I

      a=0
      cte1=1.0
      cte2=0.0
      ctw1=2.0
      ctw2=1.0

c** The loop is repeated till the temperature of the grid point
c   second from the surface reaches emulsion braking temperature.

      do while (te(n-1,1,1).lt.teb)

c** j is the number of TIME stpes from the start of the model.

            j=j+1
            resid=1.0
            ictr=0

            do 20 i=1,n

                  te(i,1,2)=te(i,1,1)
 20         continue

            do 25 i=1,m

                  tw(i,1,2)=tw(i,1,1)
 25         continue

c** calculated residual is compared with the permissible error.

            do while (resid.gt.err)

                  resid=10.0
                  sum=0.0
                  sum1=0.0
                  ictr=ictr+1
                  tm1=te(n,1,1)

c** Since we would alrady have the previous pseudotime temp for
c    the n-1 node we use that to quicken the convergence.

                  tm2=te((n-1),1,2)
                  tm3=te(n,1,2)
                  tm4=te(n,2,2)

c** Part 1 surface node subroutine is called to calculate surface
c   temperature.
                  call p1surf(tm1,tm2,tm3,tm4)
```

```
c*** Surface temperature value returned by the subroutine is assigned
c    to the surface node.

                  te(n,2,2)=tm4

c** The temperatures at the interior nodes are calculated using a
c   subroutine general. To specify that the region is emulsion region
c   the cte1, cte2 values are passed. Entire array of te and the no of
c   grid points is also passed. The subroutine updates the te array.

                  call general(te,n,cte1,cte2,a)

                  tm5=te(2,2,2)
                  tm6=te(1,1,1)
                  tm7=tw(2,1,2)
                  tm8=te(1,1,2)
                  tm9=te(1,2,2)

c** Subroutine for emulsion-water interface is called to calculate the
c   emulsion water interface temperature.

                  call ewintfc(tm5,tm6,tm7,tm8,tm9)

c** tm9 is the emulsion-water interface temperature. Its value is
c   assigned to the respective grid pts in water and emulsion zones.

                  te(1,2,2)=tm9
                  tw(1,2,2)=tm9

c** Subroutine genral is called to calculate temperaures inside the
c   water body. To specify that the region is water, ctw1 and ctw2
c   values are passed to the subroutine. The subroutine updates the
c   water temperature array tw.

                  call general(tw,m,ctw1,ctw2,a)

c** The last node in the water region is assigned the temperature
c   equal to the initial temperature.

                  tw(m,2,2)=tin

c** The temperatures calculated are the (new tau, new t) temperatures
c   If these are close to the (old tau, new t) temperatures, then we
c   march in real time or else we march further in pseudotime. This
c   decided by calculating the residuals next.
c   'sum' is the difference between (new tau, new t) and
c   (old tau, new t) temperatures at all points, squared and summed,
c   divided by total no of points and then taken square root.
c   'sum1' is the difference between (new tau, new t) and
c   (old tau, old t) temperatures at all points, squared and summed,
c   divided by total no of points and then taken square root.
c  residual is calculated as difference in temp 'sum' normalized by the
c   'sum1' divided by deltau.

                  do 30 i=1,n
                        sum=sum+((te(i,2,2)-te(i,1,2))**2)
```

```
                        sum1=sum1+((te(i,2,2)-te(i,1,1))**2)
 30                continue

                   do 35 i=1,m
                        sum=sum+((tw(i,2,2)-tw(i,1,2))**2)
                        sum1=sum1+((tw(i,2,2)-tw(i,1,1))**2)
 35                continue

                   pts=dfloat(m+n)
                   sum=sum/pts
                   sum1=sum1/pts
                   sum=dsqrt(sum)
                   sum1=dsqrt(sum1)
                   resid=sum/sum1

                   do 40 i=1,n
                        te(i,1,2)=te(i,2,2)
 40                continue

                   do 45 i=1,m
                        tw(i,1,2)=tw(i,2,2)
 45                continue

                   end do

c As the condition of residual is met, the (new tau, new t) temp is
c assigned to the (old tau, old t) as we march in real time.

              do 50 i=1,n
                   te(i,1,1)=te(i,2,2)
                   te(i,1,2)=0.0
                   te(i,2,1)=0.0
                   te(i,2,2)=0.0
 50           continue

              do 60 i=1,m
                   tw(i,1,1)=tw(i,2,2)
                   tw(i,1,2)=0.0
                   tw(i,2,1)=0.0
                   tw(i,2,2)=0.0
 60           continue

              tes=te(n,1,1)
              time=delt*j
              itime=int(time)

              if(time-itime.lt.delt)then
                   write(59,*)'time=',time,'sur temp=',tes

              else

              endif


c ictr is the iteration counter that keeps track of the no of
c iterations needed to converge in pseudotime.
```

```
            xitercheck=time/50
            itercheck=int(xintercheck)
            check=xitercheck-itercheck

      end do

            write(59,*)'time=',time,'sur temp=',tes

c*** Write out the temperature and the distance from surface to tempout
c    file and the temperatures to the efrpt2 and wfrpt2 files.

      do 122 i=n,1,-1
            xe=h-(float(i-1)*delxe)
            write(57,21)xe,te(i,1,1)
            write(56,4)te(i,1,1)
 122  continue

 21   format(f6.4,3x,f12.7)
 4    format(f12.7)

      do 123 i=1,m
            xw=0.5+float(i-1)*delyw
            write(57,21)xw,tw(i,1,1)
            write(54,4)tw(i,1,1)
 123        continue

      stop
      end

c**********************************************************************
c** SUBROUTINE FOR PART I SURFACE NODE
      subroutine p1surf(tso,t1o,tso2,tsn)
c**********************************************************************
      implicit double precision(a-h,o-z)

c**********************************************************************
      common/list1/ho,epso,cono,difo,rhoo,cpo,qlo,qcom,co,tov,beta
      common/list2/conw,difw,rhow,hfgw,cpw,qmacks
      common/list3/y,delt,delxe,delxw,tin,h,c1,teb,err,deltau,q,gamma
      common/list4/epse,he
      common/list5/cone,dife,rhoe,qle
      common/list6/stboltz,delyw,rc,rl
c**********************************************************************
      fact=1.0/((gamma/deltau)+(1.0/delt))
      temp2=stboltz*epse*(((tso*tso)*(tso*tso))-((tin*tin)*(tin*tin)))
      temp1=t1o-tso-(delxe/cone)*(he*(tso-tin)-q+temp2)
      tsn=((gamma/deltau)*tso2+tso/delt
     $       +2*dife*temp1/(delxe*delxe))*fact

      return
      end
```

```
c*********************************************************************
c*** SUBROUTINE FOR EMULSION-WATER INTERFACE
      subroutine ewintfc(te2,tino,tw2,tino2,tinn)
c*********************************************************************
      implicit double precision(a-h,o-z)

c*********************************************************************
      common/list1/ho,epso,cono,difo,rhoo,cpo,qlo,qcom,co,tov,beta
      common/list2/conw,difw,rhow,hfgw,cpw,qmacks
      common/list3/y,delt,delxe,delxw,tin,h,c1,teb,err,deltau,q,gamma
      common/list4/epse,he
      common/list5/cone,dife,rhoe,qle
      common/list6/stboltz,delyw,rc,rl
c*********************************************************************
      tempp=2.0*difw*rc*rc/(delyw*delyw)
      tempq=cone*difw*rc*(2.0+4.0*delyw)/(conw*delyw)
      tempr=gamma/tempq+gamma*delxe/(2.0*dife)
      temps=1.0/tempq+delxe/(2.0*dife)
      fact=1.0/((tempr/deltau)+(temps/delt))
      temp1=(tempr/deltau)*tino2
      temp2=tempp*tw2/(tempq)
      temp3=((temps/delt)-(tempp/tempq)
     $            -(1.0/delxe))*tino
      temp4=te2/delxe
      tinn=(temp1+temp2+temp3+temp4)*fact
      return
      end


c*********************************************************************
c**** SUBROUTINE FOR GENERAL DIFFERENTIAL EQUATION
      subroutine general(t,n,ct1,ct2,a)
c*********************************************************************
      implicit double precision(a-h,o-z)
      parameter (imax=3000)
      dimension t(imax,2,2)
c*********************************************************************
      common/list1/ho,epso,cono,difo,rhoo,cpo,qlo,qcom,co,tov,beta
      common/list2/conw,difw,rhow,hfgw,cpw,qmacks
      common/list3/y,delt,delxe,delxw,tin,h,c1,teb,err,deltau,q,gamma
      common/list4/epse,he
      common/list5/cone,dife,rhoe,qle
      common/list6/stboltz,delyw,rc,rl
c*********************************************************************

      fact=1.0/((gamma/deltau)+(1.0/delt))
      if(ct1.eq.1.0)then
            if (a.eq.0.0)then
                  dx=delxe
                  d=h
                  alpha=dife
            else
                  dx=delxo
                  d=rl
                  alpha=difo
            endif
```

```
          do 10 i=n-1,2,-1
            x=d-((i-1)*dx)
            fx=a*co*q*beta*dexp(-beta*(rl-x))/(rhoo*cpo)
            to1=t(i,1,1)
            to2=t(i,1,2)
            top=t(i+1,2,2)
            tom=t(i-1,1,2)
            tn=((gamma/deltau)*to2+to1/
     $               delt+alpha*(top+tom-2.0*to1)
     $                /(dx*dx)+fx)*fact
            t(i,2,2)=tn
10        continue

       else
            dx=delyw
            alpha=difw

          do 20 i=2,(n-1)
            yw=(i-1)*dx
            ct1=(rc**2)*(1.0-yw)**4
            ct2=4.0*alpha*(rc*rc)*((1.0-yw)*(1.0-yw)*(1.0-yw))
            to1=t(i,1,1)
            to2=t(i,1,2)
            top=t(i+1,1,2)
            tom=t(i-1,2,2)
            tn=((gamma/deltau)*to2+to1/
     $               delt+ct1*alpha*(top+tom-2.0*to1)
     $               /(dx*dx)-ct2*(to1-tom)/dx)*fact
            t(i,2,2)=tn
20        continue

       endif

       return
       end
```

Program for Intermediate Regime

```
c**********************************************************************
c
c           PROGRAM FOR PART II
c
c**********************************************************************
      implicit double precision(a-h,o-z)
      parameter (imax = 3000)
c**********************************************************************
c     ho - convective heat rtansfer coefficient for oil/air
c     he - convective heat rtansfer coefficient for emulsion/air
c     hfgw - enthalpy of evaporation of water
c     epse - emissivity of emulsion
c     espo - emissivity of oil
c     cone - conductivity of emulsion
c     cono - conductivity of oil
c     conw - conductivity of water
c     dife - diffusivity of emulsion
c     difo - diffusivity of oil
c     difw - diffusivity of water
c     stboltz - Stefan - Boltzmann Constant
c     rhoe - emulsion density
c     rhoo - oil density
c     rhow - water density
c     cpo - specific heat of oil
c     co - fraction of incident heat flux not absorbed at the surface
c     teb - emulsion breaking temperature
c     tov - oil vaporization temperature
c     beta - inverse absorption depth
c     qle - latent heat of emulsion breaking
c     qlo - latent heat of oil vaporization
c     qcom - energy released by oil combustion
c     rl - thickness of oil layer
c     y - region of interest in water
c     delt - time step
c     delxe - grid spacing in emulsion zone
c     delxw - grid spacing in water region
c     tin - ambient/initial temperature
c     h -  emulsion thickness
c     c1 -inverse oil content of emulsion, by mass

c**********************************************************************
c Declaring Common variables for the main program as well as the
c subroutines

      common/list1/ho,epso,cono,difo,rhoo,cpo,qlo,qcom,co,tov,beta
      common/list2/conw,difw,rhow,hfgw,cpw,qmacks
      common/list3/y,delt,delxe,delxw,tin,h,c1,teb,err,deltau,q,gamma
        common/list4/epse,he,delxo
      common/list5/cone,dife,rhoe,qle
      common/list6/stboltz,delyw,rc,rl

c**********************************************************************

      namelist/list1/ho,epso,cono,difo,rhoo,cpo,qlo,qcom,co,tov,beta
      namelist/list2/conw,difw,rhow,hfgw,cpw,qmacks
```

```
      namelist/list3/y,delt,delxe,delxw,tin,h,c1,teb,err,deltau,q,
     $                   gamma
      namelist/list4/epse,he

c**********************************************************************
c The temperature in emulsion, water and oil. First index is for space,
c second is for pseudotime tau such that 1 is for old tau and
c 2 is for new tau,and third for time t such that 1 is old time 2 is
c new time

      dimension te(imax,2,2), tw(imax,2,2),to(imax,2,2)

c**********************************************************************

c**** read the oil data
      open (unit =11, file='oil.in', status = 'old')
c**** read the variables in list 1 declared above from oil property
c     input file.
      read (11, list1)
c**** save oil data
      open (unit =12, file='oil.out', status = 'unknown')
      write(12, list1)
c**** read the water data
      open (unit =13, file='water.in', status = 'old')
c**** read the variables in list 2 declared above from water property
c     input file.
      read(13, list2)
c**** save water data
      open (unit =14, file='water.out', status = 'unknown')
      write(14, list2)
c**** read the input
      open (unit =15, file='data.in', status = 'old')
c**** read the variables in list 3 declared above from data file.
      read (15,list3)
c**** save the input
      open (unit =16, file='data.out', status = 'unknown')
      write (16,list3)
c**** read the emulsion input
      open (unit =18, file='imuls.in', status = 'old')
c**** read the variables in list 4 declared above from emulsion
property
c     input file.
      read (18,list4)
c**** save the emulsion input
      open (unit =19, file='imuls.out', status = 'unknown')
      write (19,list4)

c**********************************************************************
c wfrpt2--> file containing water temeprature profile input for
c           part 2 of the model
c mandn --> file containing no of nodes in water (m) and in emulsion
(n)
c efrpt2 --> file containing temperature profile in emulsion layer at
c            the end of part 1 for input to part2.
c tempout2 --> file containing a typical temp profile during part2.
c residual2 --> file containig residuals
c wfrpt3 --> file containing water temperature profile to be input for
```

```
c            part 3 model
c ofrpt3 --> file containing oil temperature profile to be input for
c            part 3 model
c efrpt3 --> file containing emulsion temperature profile to be input
c            for part 3 model

      open (unit =17, file='emuls.out', status = 'unknown')
      open (unit =50, file='mnandl', status = 'unknown')
      open (unit =51, file='ofrpt3', status = 'unknown')
      open (unit =52, file='efrpt3', status = 'unknown')
      open (unit =53, file='wfrpt3', status = 'unknown')
      open (unit =54, file='wfrpt2', status = 'old')
      open (unit =55, file='mandn', status = 'old')
      open (unit =56, file='efrpt2', status = 'old')
      open (unit =57, file='tempout2', status = 'unknown')
      open (unit =58, file='watin2', status = 'unknown')
      open (unit =59, file='residual2', status = 'unknown')

c*** Calculation of emulsion properties using weighted fractions
c    of oil and water in emulsion.

      rhoe=rhow+(rhoo-rhow)/c1
      cone=conw+(cono-conw)/c1
      cpe=cpw+(cpo-cpw)/c1
      dife=cone/(rhoe*cpe)

c**********************************************************************
      stboltz=5.67e-8
c**********************************************************************
*

c**** Write out the emulsion properties calculated above to a file.

      write (17,2)qle,rhoe,cone,dife,epse,he,cpe
 2    format('Qle=',e9.3,/,'Rhoe=',f9.3,/,'Cone=',e10.3,/,'Dife=',
     $           e10.3,/,'Epse=',f6.3,/,'He=',f6.3,/,'cpe=',f10.3,/)
 3    format(I4,3x,I4)
 4    format(f12.7)
 9    format(3(2x,I4))
 21   format(f6.4,3x,f12.7)

c*** n= no of grid points in emulsion region
c*** m=no grid points in transformed water region
c*** l=no of grid points in oil region

      read(55,3)m,n
      rc=4.0/y
      delyw=rc*delxw
      rl=0.0

c** Oil grid spacing is chosen so that one grid length of emulsion
c  volume contains oil equivalent to one grid length in oil.

      delxo=(rhoe*delxe)/(c1*rhoo)

c**********************************************************************
*
```

```
c Read the water and emulsion temperature profiles at the end of part 1

      do 5 i=1,m
      read(54,4)tw(i,1,1)
 5    continue

      do 7 i=n,1,-1
      read(56,4)te(i,1,1)
 7    continue

c***  Initialize the temperatures
      l=2

      do 8 i=1,l
            to(i,1,2)=to(i,1,1)
            to(i,2,1)=0.0
            to(i,2,2)=0.0
 8    continue

      do 10 i=1,n
            te(i,1,2)=te(i,1,1)
            te(i,2,1)=0.0
            te(i,2,2)=0.0
 10   continue

      do 15 i=1,m
            tw(i,1,2)=tw(i,1,1)
            tw(i,2,1)=0.0
            tw(i,2,2)=0.0
 15   continue

c** Surface temperature is initialized to the temperature of the
c   n th node in the emulsion region.

      tes=te(n,1,1)

c Initial oil layer thickness is set to zero.
      rl=delxo
      j=0

      do 17 i=2,1,-1
        to(i,1,1)=teb
 17   continue

c** Part I ends when temp of two top most nodes of the emulsion have
c   reached the emulsion breaking temperature. Thus one grid length of
c  of emulsion breaks. This will produce one grid length of oil. Hence
c  2 nodes are placed in the oil and two nodes are deleted from the
c  emulsion region.

      n=n-1

c*** Calculations for part II

      ano=0.0
      ao=1.0
      cte1=1.0
```

```
      cte2=0.0
      ctw1=2.0
      ctw2=1.0

c **buffh is the variable that stores the emulsion layer broken
c  that has not produced enough oil to occupy one grid length in
c  the oil region. This variable keeps on growing till the emulsion
c  layer broken is enough to produce an extra node in the oil region.

      buffh=0.0
      mflag=0
      buffw=0.0
      twb=373.0

c** The loop is repeated till the surface temperature of the oil
c  reaches the oil valoprization temperature.

      do while (tes.lt.tov)

            j=j+1
            resid=10.0
            ictr=0
            hn=0.0
            rln=0.0

            do 27 i=1,l
                 to(i,1,2)=to(i,1,1)
                 to(i,2,1)=0.0
                 to(i,2,2)=0.0
 27         continue

            do 20 i=1,n
                 te(i,2,1)=0.0
                 te(i,2,2)=0.0
                 te(i,1,2)=te(i,1,1)
 20         continue

            do 25 i=1,m
                 tw(i,2,1)=0.0
                 tw(i,2,2)=0.0
                 tw(i,1,2)=tw(i,1,1)
 25         continue

            do while (resid.gt.err)

                  resid=10.0
                  sum=0.0
                  sum1=0.0
                  ictr=ictr+1
                  tm1=to(l,1,1)
                  tm2=to((l-1),1,2)
                  tm3=to(l,1,2)
                  tm4=to(l,2,2)

c** Subroutine for oil boundary is called and the oil surface
c  temperature is calculated.
```

```
                  call p2surf(tm1,tm2,tm3,tm4)
                  to(l,2,2)=tm4

c** The temperature profile inside the oil layer is calculated.

                  call general(to,l,cte1,cte2,ao)

                  if(mflag.eq.0)then

                    tm5=to(2,2,2)
                    tm6=to(1,1,1)
                    tm7=te(n-1,1,2)
                    tm8=to(1,1,2)
                    tm9=to(1,2,2)

c** Call subroutine to calculate oil-emulsion interface temperature.

                    call oeintfc(tm5,tm6,tm7,tm8,tm9)
                    te(n,2,2)=tm9
                    to(1,2,2)=tm9

c** Temperature inside the emulsion layer is calculated.

                    call general(te,n,cte1,cte2,ano)
                    tm5=te(2,2,2)
                    tm6=te(1,1,1)
                    tm7=tw(2,1,2)
                    tm8=te(1,1,2)
                    tm9=te(1,2,2)

c** Call subroutine to calculate emulsion-water interface temperature.

                    call ewintfc(tm5,tm6,tm7,tm8,tm9)
                    te(1,2,2)=tm9
                    tw(1,2,2)=tm9

c** Calculate the temperature profile inside the water region.

                    call general(tw,m,ctw1,ctw2,ano)
                    tw(m,2,2)=tin

                  else

                    if(tw(1,2,2).lt.twb)then

                      tm5=to(2,2,2)
                      tm6=to(1,1,1)
                      tm7=tw(2,1,2)
                      tm8=to(1,1,2)
                      tm9=to(1,2,2)

c** Call subroutine to calculate oil-water interface temperature.

                      call owintfc(tm5,tm6,tm7,tm8,tm9)
                      te(1,2,2)=tm9
                      tw(1,2,2)=tm9
```

```
                  else

                    tw(1,2,2)=twb

                  endif

                endif


c** The temperatures calculated are the (new tau, new t) temperatures
c   If these are close to the (old tau, new t) temperatures, then we
c   march in real time or else we march further in pseudotime. This
c   decided by calculating the residuals next. Here along with the temp
c   gradients, the H gradients are also included in the calculation of
c  the residuals.
c   'sum' is the difference between (new tau, new t) and
c   (old tau, new t) temperatures at all points, squared and summed,
c   divided by total no of points and then taken square root.
c   'sum1' is the difference between (new tau, new t) and
c   (old tau, old t) temperatures at all points, squared and summed,
c   divided by total no of points and then taken square root.
c   residual is calculated as difference in temp 'sum' normalized by
c   'sum1'.

                do 537 i=1,l
                      sum=sum+((to(i,2,2)-to(i,1,2))**2)
                      sum1=sum1+((to(i,2,2)-to(i,1,1))**2)
 537            continue

                do 530 i=1,n
                      sum=sum+((te(i,2,2)-te(i,1,2))**2)
                      sum1=sum1+((te(i,2,2)-te(i,1,1))**2)
 530            continue

                do 535 i=1,m
                      sum=sum+((tw(i,2,2)-tw(i,1,2))**2)
                      sum1=sum1+((tw(i,2,2)-tw(i,1,1))**2)
 535            continue

                pts=dfloat(m+n)
                sum=sum/pts
                sum1=sum1/pts
                sum=dsqrt(sum)
                sum1=dsqrt(sum1)
                resid=(sum/sum1)

c** The (new tau, new t)temperature is assigned to (old tau, new t)

                do 547 i=1,l
                      to(i,1,2)=to(i,2,2)
 547            continue

                do 540 i=1,n
                      te(i,1,2)=te(i,2,2)
 540            continue
```

```
                  do 545 i=1,m
                        tw(i,1,2)=tw(i,2,2)
 545              continue

                  end do

c As the condition of residual is met, the (new tau, new t) temp is
c assigned to the (old tau, old t) as we march in real time.

            do 50 i=1,n
                  te(i,1,1)=te(i,2,2)
                  te(i,1,2)=0.0
                  te(i,2,1)=0.0
                  te(i,2,2)=0.0

 50         continue

            do 55 i=1,l
                  to(i,1,1)=to(i,2,2)
                  to(i,1,2)=0.0
                  to(i,2,1)=0.0
                  to(i,2,2)=0.0
 55         continue

            do 60 i=1,m
                  tw(i,1,1)=tw(i,2,2)
                  tw(i,1,2)=0.0
                  tw(i,2,1)=0.0
                  tw(i,2,2)=0.0
 60         continue

            if(tw(1,1,1).lt.twb)then
            iboilover=0
            else
            iboilover=1
            endif

            i=n-1
            ncount=0

            do while (te(i,1,1).ge.teb.and.i.gt.1)

            ncount=ncount+1

            i=i-1

            end do

            if(ncount.gt.0)then

                  n=n-ncount

                  xe=(ncount)*delxe
                  heat=(1-1/c1)*rhoe*xe*cpw*(teb-tw(1,1,1))
                  h=(n-1)*delxe
                  deltaTe=heat/(rhoe*h*cpe)
```

```
            do 63 i=1,n

                  te(i,1,1)=te(i,1,1)+deltaTe

 63         continue

c** ncount calculates the decrease in the no of nodes of emulsion as
c  some emulsion volume is broken into oil and water.

                  if(n.lt.2)then

                        mflag=1

                  else

                  endif

c** Since the oil grid spacing is so chosen that volume of one grid
c  length of oil is produced upon breaking of emulsion volume of
c  emulsion from one emulsion grid length, ndn no of nodes will be
c  added to the oil region.

                  l=l+ncount
                  rl=(l-1)*delxo
                  h=(n-1)*delxe

c** The oil layer produced is at teb temp. As this layer is added
c  at the bottom of the existing oil layer, the temperatures of the
c nodes in the oil region need to be reassigned.

                  do 65 i=l,ncount+1,-1
                        ncnt=i-ncount
                        to(i,1,1)=to(ncnt,1,1)
 65               continue

                  do 70 i=1,ncount
                         to(i,1,1)=to(i+1,1,1)
 70               continue

c                 te(n,1,1)=teb
c                 write(59,*)time

            else

            endif

            if (iboilover.eq.1)then
                  tm6=to(2,1,1)
                  tm7=tw(2,1,1)

                  call boilover(tm6,tm7,m,wnew)

                  wold=float(m-1)*delyw
                  buffw=buffw+wold-wnew

                  if(buffw.gt.delyw)then
```

```
                else
                endif

            else
            endif


        tes=to(l,1,1)
        time=delt*j

            itime=int(time)
            tdiff= time-itime
            if(tdiff.lt.delt)then

        write(58,*)'time=',time,'sur temp=',tes

c ictr is the iteration counter that keeps track of the no of
iterations
c needed to converge in pseudotime.

      else

      endif

      end do


c*** Write out temperature and the distance from surface to tempout2
c    file and the temperatures to the  ofrpt3, efrpt3 and wfrpt3 files.

  228 do 121 i=l,1,-1
            xo=rl-(float(i-1)*delxo)
            write(57,21)xo,to(i,1,1)
            write(51,4)to(i,1,1)
 121  continue

      do 122 i=n,1,-1
            xe=xo+h-(float(i-1)*delxe)
            write(57,21)xe,te(i,1,1)
            write(52,4)te(i,1,1)
 122  continue

      do 123 i=1,m
            xw=xe+float(i-1)*delyw
            write(57,21)xw,tw(i,1,1)
            write(53,4)tw(i,1,1)
 123        continue

      write(50,9)m,n,l
      stop
      end
```

```
c*********************************************************************
c** SUBROUTINE FOR PART II SURFACE NODE
      subroutine p2surf(tso,t1o,tso2,tsn)
c*********************************************************************
      implicit double precision(a-h,o-z)

c*********************************************************************
      common/list1/ho,epso,cono,difo,rhoo,cpo,qlo,qcom,co,tov,beta
      common/list2/conw,difw,rhow,hfgw,cpw,qmacks
      common/list3/y,delt,delxe,delxw,tin,h,c1,teb,err,deltau,q,gamma
      common/list4/epse,he,delxo
      common/list5/cone,dife,rhoe,qle
      common/list6/stboltz,delyw,rc,rl
c*********************************************************************

      fact=1.0/((gamma/deltau)+(1.0/delt))
      temp2=stboltz*epso*(((tso*tso)*(tso*tso))-((tin*tin)*(tin*tin)))
      temp1=t1o-tso-(delxo/cono)*(ho*(tso-tin)-(1.0-co)*q+temp2)

      tsn=((gamma/deltau)*tso2+tso/delt
     $       +2.0*difo*temp1/(delxo*delxo))*fact

      return
      end


c*********************************************************************
c*** SUBROUTINE FOR OIL-EMULSION INTERFACE
      subroutine oeintfc(te2,tino,tw2,tino2,tinn)
c*********************************************************************
      implicit double precision(a-h,o-z)

c*********************************************************************
      common/list1/ho,epso,cono,difo,rhoo,cpo,qlo,qcom,co,tov,beta
      common/list2/conw,difw,rhow,hfgw,cpw,qmacks
      common/list3/y,delt,delxe,delxw,tin,h,c1,teb,err,deltau,q,gamma
      common/list4/epse,he,delxo
      common/list5/cone,dife,rhoe,qle
      common/list6/stboltz,delyw,rc,rl
c*********************************************************************

      tempp=gamma*0.5*(delxe*rhoe*cpe+delxo*rhoo*cpo)
      tempq=0.5*(delxe*rhoe*cpe+delxo*rhoo*cpo)

      fact=1.0/((tempp/deltau)+(tempq/delt))

      temp1=(tempq/delt)*tino
      temp2=cone*tw2/delxe
      temp3=((tempp/deltau)-(cone/delxe)
     $            -(cono/delxo))*tino2
      temp4=cono*te2/delxo
      temp5=a*co*q*dexp(-beta*rl)

      tinn=(temp1+temp2+temp3+temp4-temp5)*fact

      return
      end
```

```
c*********************************************************************
c*** SUBROUTINE FOR EMULSION-WATER INTERFACE
      subroutine ewintfc(te2,tino,tw2,tino2,tinn)
c*********************************************************************
      implicit double precision(a-h,o-z)

c*********************************************************************
      common/list1/ho,epso,cono,difo,rhoo,cpo,qlo,qcom,co,tov,beta
      common/list2/conw,difw,rhow,hfgw,cpw,qmacks
      common/list3/y,delt,delxe,delxw,tin,h,c1,teb,err,deltau,q,gamma
      common/list4/epse,he,delxo
      common/list5/cone,dife,rhoe,qle
      common/list6/stboltz,delyw,rc,rl
c*********************************************************************

      tempp=2.0*difw*rc*rc/(delyw*delyw)
      tempq=cone*difw*rc*(2.0+4.0*delyw)/(conw*delyw)
      tempr=gamma/tempq+gamma*delxe/(2.0*dife)
      temps=1.0/tempq+delxe/(2.0*dife)

      fact=1.0/((tempr/deltau)+(temps/delt))

      temp1=(tempr/deltau)*tino2
      temp2=tempp*tw2/(tempq)
      temp3=((temps/delt)-(tempp/tempq)
     $            -(1.0/delxe))*tino
      temp4=te2/delxe

      tinn=(temp1+temp2+temp3+temp4)*fact

      return
      end



c*********************************************************************
c**** SUBROUTINE FOR GENERAL DIFFERENTIAL EQUATION
      subroutine general(t,n,ct1,ct2,a)
c*********************************************************************
      implicit double precision(a-h,o-z)
      parameter (imax=3000)
      dimension t(imax,2,2)
c*********************************************************************
      common/list1/ho,epso,cono,difo,rhoo,cpo,qlo,qcom,co,tov,beta
      common/list2/conw,difw,rhow,hfgw,cpw,qmacks
      common/list3/y,delt,delxe,delxw,tin,h,c1,teb,err,deltau,q,gamma
      common/list4/epse,he,delxo
      common/list5/cone,dife,rhoe,qle
      common/list6/stboltz,delyw,rc,rl
c*********************************************************************

      fact=1.0/((gamma/deltau)+(1.0/delt))
      if(ct1.eq.1.0)then
            if (a.eq.0.0)then
```

```
                dx=delxe
                d=h
                alpha=dife

          else

                dx=delxo
                d=rl
                alpha=difo

          endif

        do 10 i=n-1,2,-1

          x=((i-1)*dx)
          fx=a*co*q*beta*dexp(-beta*(rl-x))/(rhoo*cpo)
          to1=t(i,1,1)
          to2=t(i,1,2)
          top=t(i+1,2,2)
          tom=t(i-1,1,2)

          tn=((gamma/deltau)*to2+to1/
    $               delt+alpha*(top+tom-2.0*to1)
    $                /(dx*dx)+fx)*fact

          t(i,2,2)=tn

10      continue

     else

          dx=delyw
          alpha=difw

        do 20 i=2,(n-1)

          yw=(i-1)*dx
          ct1=(rc**2)*(1.0-yw)**4
          ct2=4.0*alpha*(rc*rc)*((1.0-yw)*(1.0-yw)*(1.0-yw))
          to1=t(i,1,1)
          to2=t(i,1,2)
          top=t(i+1,1,2)
          tom=t(i-1,2,2)

          tn=((gamma/deltau)*to2+to1/
    $               delt+ct1*alpha*(top+tom-2.0*to1)
    $               /(dx*dx)-ct2*(to1-tom)/dx)*fact

          t(i,2,2)=tn

20      continue

     endif

     return
     end
```

```
c*********************************************************************
c*** SUBROUTINE FOR OIL-WATER INTERFACE (NO BOILOVER)
      subroutine owintfc(to2,tino,tw2,tino2,tinn)

c*** This does account for the indepth radiation absorption
c*********************************************************************
      implicit double precision(a-h,o-z)

c*********************************************************************
      common/list1/ho,epso,cono,difo,rhoo,cpo,qlo,qcom,co,tov,beta
      common/list2/conw,difw,rhow,hfgw,cpw,qmacks
      common/list3/y,delt,delxe,delxw,tin,h,c1,teb,err,deltau,q,gamma
      common/list4/epse,he,delxo
      common/list5/cone,dife,rhoe,qle
      common/list6/stboltz,delyw,rc,rl
c*********************************************************************

      tempp=2.0*difw*rc*rc/(delyw*delyw)
      tempq=cono*difw*rc*(2.0+4.0*delyw)/(conw*delyw)
      tempr=gamma/tempq+gamma*delxo/(2.0*difo)
      temps=1.0/tempq+delxo/(2.0*difo)
      tempt=((2.0*difw*rc*rc/delyw + 4.0*difw*rc*rc*rc)*co*q*dexp
     $  (-beta*rl))/(conw*rc)

      fact=1.0/((tempr/deltau)+(temps/delt))

      temp1=(tempr/deltau)*tino2
      temp2=tempp*tw2/(tempq)
      temp3=((temps/delt)-(tempp/tempq)
     $            -(1.0/delxo))*tino
      temp4=to2/delxo
      temp5=tempt/tempq

      tinn=(temp1+temp2+temp3+temp4+temp5)*fact

      return
      end


c*********************************************************************
c*** SUBROUTINE FOR OIL-WATER INTERFACE AT BOILOVER
      subroutine boilover(tm10,tm11,mold,wnew)
c*********************************************************************
      implicit double precision(a-h,o-z)

c*********************************************************************
      common/list1/ho,epso,cono,difo,rhoo,cpo,qlo,qcom,co,tov,beta
      common/list2/conw,difw,rhow,hfgw,cpw,qmacks
      common/list3/y,delt,delxe,delxw,tin,h,c1,teb,err,deltau,q,gamma
      common/list4/epse,he,delxo
      common/list5/cone,dife,rhoe,qle
      common/list6/stboltz,delyw,rc,rl
c*********************************************************************

      temp1=delt/(rhow*hfgw)
      temp2=cono*(tm10-twb)/delxo+conw*(twb-tm11)/delxw+co*q*
```

```
     $            dexp(-beta*rl)
      wold=float((mold-1)*delyw)
      wnew=wold-temp1*temp2

      return
      end
```

Program for Final Regime

```
c*********************************************************************
c
c           PROGRAM FOR PART III
c
c*********************************************************************
      implicit double precision(a-h,o-z)
      parameter (imax = 3000)
c*********************************************************************

c     ho - convective heat rtansfer coefficient for oil/air
c     he - convective heat rtansfer coefficient for emulsion/air
c     hfgw - enthalpy of evaporation of water
c     epse - emissivity of emulsion
c     espo - emissivity of oil
c     cone - conductivity of emulsion
c     cono - conductivity of oil
c     conw - conductivity of water
c     dife - diffusivity of emulsion
c     difo - diffusivity of oil
c     difw - diffusivity of water
c     stboltz - Stefan - Boltzmann Constant
c     rhoe - emulsion density
c     rhoo - oil density
c     rhow - water density
c     cpo - specific heat of oil
c     co - fraction of incident heat flux not absorbed at the surface
c     teb - emulsion breaking temperature
c     tov - oil vaporization temperature
c     beta - inverse absorption depth
c     qle - latent heat of emulsion breaking
c     qlo - latent heat of oil vaporization
c     qcom - energy released by oil combustion
c     rl - thickness of oil layer
c     y - region of interest in water
c     delt - time step
c     delxe - grid spacing in emulsion zone
c     delxw - grid spacing in water region
c     tin - ambient/initial temperature
c     h -  emulsion thickness
c     c1 -inverse oil content of emulsion, by mass

c*********************************************************************
c Declaring Common variables for the main program as well as the
c subroutines

      common/list1/ho,epso,cono,difo,rhoo,cpo,qlo,qcom,co,tov,beta
```

```
      common/list2/conw,difw,rhow,hfgw,cpw,qmacks
      common/list3/y,delt,delxe,delxw,tin,h,c1,teb,err,deltau,q,gamma
        common/list4/epse,he,delxo
      common/list5/cone,dife,rhoe,qle
      common/list6/stboltz,delyw,rc,rl


c*********************************************************************

      namelist/list1/ho,epso,cono,difo,rhoo,cpo,qlo,qcom,co,tov,beta
      namelist/list2/conw,difw,rhow,hfgw,cpw,qmacks
      namelist/list3/y,delt,delxe,delxw,tin,h,c1,teb,err,deltau,q,
     $                   gamma
      namelist/list4/epse,he

c*********************************************************************
c The temperature in emulsion, water and oil. First index is for space,
c second is for pseudotime tau such that 1 is for old tau and
c 2 is for new tau,and third for time t such that 1 is old time 2 is
c new time

      dimension te(imax,2,2), tw(imax,2,2),to(imax,2,2)

c*********************************************************************

c**** read the oil data
      open (unit =11, file='oil.in', status = 'old')
      read (11, list1)
c**** save oil data
      open (unit =12, file='oil.out', status = 'unknown')
c**** read the variables in list 1 declared above from oil property
c     input file.
      write(12, list1)
c**** read the water data
      open (unit =13, file='water.in', status = 'old')
c**** read the variables in list 2 declared above from water property
c     input file.
      read(13, list2)
c**** save water data
      open (unit =14, file='water.out', status = 'unknown')
      write(14, list2)
c**** read the input
      open (unit =15, file='data.in', status = 'old')
c**** read the variables in list 3 declared above from data file.
      read (15,list3)
c**** save the input
      open (unit =16, file='data.out', status = 'unknown')
      write (16,list3)
c**** read the emulsion input
      open (unit =18, file='imuls.in', status = 'old')
c**** read variables in list 4 declared above from emulsion property
c     input file.
      read (18,list4)
c**** save the emulsion input
      open (unit =19, file='imuls.out', status = 'unknown')
      write (19,list4)
```

```
c*********************************************************************
c wfrpt3--> file containing water temeprature profile at end of part 2
c            as input for part 3 of the model
c mnandnl --> file containing no of nodes in water (m), in emulsion (n)
c           and oil (l)
c efrpt3 --> file containing temperature profile in emulsion layer at
c            the end of part 2 for input to part 3.
c tempout3 --> file containing a typical temp profile during part 3.
c residual3 --> file containig residuals
c wfrpt4 --> file containing water temperature profile at end of part 3
c ofrpt4 --> file containing oil temperature profile at end of part 3
c efrpt4 --> file containing emulsion temp profile at end of part 3
c dldt --> file containing burning rate versus time data.

      open (unit =17, file='emuls.out', status = 'unknown')
      open (unit =51, file='ofrpt4', status = 'unknown')
      open (unit =52, file='efrpt4', status = 'unknown')
      open (unit =53, file='wfrpt4', status = 'unknown')
      open (unit =54, file='wfrpt3', status = 'old')
      open (unit =55, file='mnandl', status = 'old')
      open (unit =56, file='efrpt3', status = 'old')
      open (unit =50, file='ofrpt3', status = 'old')
      open (unit =57, file='tempout3', status = 'unknown')
      open (unit =58, file='watin3', status = 'unknown')
      open (unit =59, file='residual3', status = 'unknown')
      open (unit =60, file='dldt', status = 'unknown')
      open (unit =61, file='heatflx', status = 'unknown')
      open (unit =62, file='mnl', status = 'unknown')

c*** Calculation of emulsion properties using weighted fractions
c    of oil and water in emulsion.

      qle=0.0*(1.0-(1/c1))*hfgw
      rhoe=rhow+(rhoo-rhow)/c1
      cone=conw+(cono-conw)/c1
      cpe=cpw+(cpo-cpw)/c1
      dife=cone/(rhoe*cpe)

c*********************************************************************
      stboltz=5.67e-8
c*********************************************************************

c**** Write out the emulsion properties calculated above to a file.
      write (17,2)qle,rhoe,cone,dife,epse,he,cpe
 2    format('Qle=',e9.3,/,'Rhoe=',f9.3,/,'Cone=',e10.3,/,'Dife=',
     $           e10.3,/,'Epse=',f6.3,/,'He=',f6.3,/,'cpe=',f10.3,/)
 3    format(I4,3x,I4)
 4    format(f12.7)
 9    format(3(2x,I4))
 21   format(f6.4,3x,f12.7)

c*** n= no of grid points in emulsion region
c*** m=no grid points in transformed water region
c*** l=no of grid points in oil region

      read(55,9)m,n,l
      rc=4.0/y
```

```
      delyw=rc*delxw

c** Oil grid spacing is chosen so that one grid length of emulsion
c  volume contains oil equivalent to one grid length in oil.

      delxo=(rhoe*delxe)/(c1*rhoo)
      rloil=h*delxo/delxe
      qign=q

c**********************************************************************

c Read water and emulsion temperature profiles at the end of part II

      do 5 i=1,m
      read(54,4)tw(i,1,1)
 5    continue

      do 7 i=n,1,-1
      read(56,4)te(i,1,1)
 7    continue

      do 13 i=l,1,-1
      read(50,4)to(i,1,1)
 13   continue

c***  Initialize the temperatures

      do 8 i=1,l
            to(i,1,2)=to(i,1,1)
            to(i,2,1)=0.0
            to(i,2,2)=0.0
 8    continue

      do 10 i=1,n
            te(i,1,2)=te(i,1,1)
            te(i,2,1)=0.0
            te(i,2,2)=0.0
 10   continue

      do 15 i=1,m
            tw(i,1,2)=tw(i,1,1)
            tw(i,2,1)=0.0
            tw(i,2,2)=0.0
 15   continue

c** Surface temperature is initialized to the temperature of the
c   l th node in the oil region.
      tes=to(l,1,1)
      j=0

c*** Calculations for part III

      ano=0.0
      ao=1.0
      cte1=1.0
      cte2=0.0
      ctw1=2.0
```

```
      ctw2=1.0
      buffh=0.0
      buffl=0.0
      nchk=0
      qmax=0.0
      qcomp=qmacks-q
      qmin=0.05*qmacks
      mflag=0
      nflag=0
      nnflag=0
      twb=373.0
      drldtmax=0.0
      drldt=1000.0
      icount=0
      iextenchk=0

c** icount counts no of time steps after emulsion has completely broken
c  down into oil and water. (if it happens, we take 500 time steps
c  before the program is terminated. Else the loop terminates as oil
c  is completely depleted.

      do while (iextenchk.lt.10.and.l.gt.1)

            j=j+1
            resid=10.0
            ictr=0
            hn=0.0
            rln=0.0
            dlp=0.0
            dld=0.0

c** Oil layer thickness (rl) and emulsion layer thickness (h) are
c  calculated.

            rl=float(l-1)*delxo
            h=float(n-1)*delxe

            do 27 i=1,l
                 to(i,1,2)=to(i,1,1)
                 to(i,2,1)=0.0
                 to(i,2,2)=0.0
 27         continue

            do 20 i=1,n
                 te(i,2,1)=0.0
                 te(i,2,2)=0.0
                 te(i,1,2)=te(i,1,1)
 20         continue

            do 25 i=1,m
                 tw(i,2,1)=0.0
                 tw(i,2,2)=0.0
                 tw(i,1,2)=tw(i,1,1)
 25         continue

c** lold is the no of grid pts in oil (old tau, old t)
```

```
            lold=l

            do while (resid.gt.err)

                  resid=10.0
                  sum=0.0
                  sum1=0.0
                  ictr=ictr+1

c** The oil surface temperature is held at the oil vaporization temp.

                  to(l,2,2)=tov

c** Temp profile inside the oil layer is calculated.

                  call general(to,l,cte1,cte2,ao)
                  to(l,2,2)=tov

c** If the emulsion layer exists.....

                if(mflag.eq.0)then

                    tm5=to(2,2,2)
                    tm6=to(1,1,1)
                    tm7=te(n-1,1,2)
                    tm8=to(1,1,2)
                    tm9=to(1,2,2)

c** Call subroutine to calculate oil-emulsion interface temperature.

                    call oeintfc(tm5,tm6,tm7,tm8,tm9)
                    te(n,2,2)=tm9
                    to(1,2,2)=tm9

c** Temperature profile inside the emulsion layer is calculated.

                  call general(te,n,cte1,cte2,ano)

                  tm1=te(2,2,2)
                  tm2=te(1,1,1)
                  tm3=tw(2,1,2)
                  tm4=te(1,1,2)
                  tm5=te(1,2,2)

c** Emulsion water interface consition is applied.

                  call ewintfc(tm1,tm2,tm3,tm4,tm5)

                  te(1,2,2)=tm5
                  tw(1,2,2)=tm5

c** Temperature profile inside the water layer is calculated.

                  call general(tw,m,ctw1,ctw2,ano)

                  tw(m,2,2)=tin
```

```
c** If the emulsion layer has depleted....

                else

                  if(tw(1,1,1).lt.twb)then

                        tm1=to(2,2,2)
                        tm2=to(1,1,1)
                        tm3=tw(2,1,2)
                        tm4=to(1,1,2)
                        tm5=to(1,2,2)

                        call owintfc(tm1,tm2,tm3,tm4,tm5)

                        to(1,2,2)=tm5
                        tw(1,2,2)=tm5

                  else

                  tw(1,2,2)=twb

                  endif

c** Temperature profile inside the water layer is calculated.

                        call general(tw,m,ctw1,ctw2,ano)

                        tw(m,2,2)=tin

c** Oil-water interface is at the emulsion breaking temperature.

               endif

c** Residual calculation: Same as that for part I and II

                  do 537 i=1,l

                        sum=sum+((to(i,2,2)-to(i,1,2))**2)
                        sum1=sum1+((to(i,2,2)-to(i,1,1))**2)

 537              continue

                  do 530 i=1,n

                        sum=sum+((te(i,2,2)-te(i,1,2))**2)
                        sum1=sum1+((te(i,2,2)-te(i,1,1))**2)

 530              continue

                  do 535 i=1,m

                        sum=sum+((tw(i,2,2)-tw(i,1,2))**2)
                        sum1=sum1+((tw(i,2,2)-tw(i,1,1))**2)

 535              continue
```

```
                  pts=dfloat(m+n)
                  sum=sum/pts
                  sum1=sum1/pts
                  sum=dsqrt(sum)
                  sum1=dsqrt(sum1)
                  resid=(sum/sum1)

                  do 547 i=1,l
                        to(i,1,2)=to(i,2,2)
 547              continue

                  do 540 i=1,n
                        te(i,1,2)=te(i,2,2)
 540              continue

                  do 545 i=1,m
                        tw(i,1,2)=tw(i,2,2)
 545              continue

c** The loop of tau ends if the residual goes below acceptable
threshold
                  end do

c** the (new tau, new t) temperatures are assigned to the
c   (old tau, old t) temperatures upon convergence in tau.

            do 50 i=1,n
                  te(i,1,1)=te(i,2,2)
                  te(i,1,2)=0.0
                  te(i,2,1)=0.0
                  te(i,2,2)=0.0
 50         continue

            do 55 i=1,l
                  to(i,1,1)=to(i,2,2)
                  to(i,1,2)=0.0
                  to(i,2,1)=0.0
 55         continue

            do 60 i=1,m
                  tw(i,1,1)=tw(i,2,2)
                  tw(i,1,2)=0.0
                  tw(i,2,1)=0.0
                  tw(i,2,2)=0.0
 60         continue

            i=n-1
            ncount=0

            do while (te(i,1,1).ge.teb.and.i.gt.1)

            ncount=ncount+1

            i=i-1

            end do
```

```
            if(ncount.gt.0)then

                  n=n-ncount
                  xe=(ncount)*delxe
                  heat=(1-1/c1)*rhoe*xe*cpw*(teb-tw(1,1,1))
                  h=(n-1)*delxe
                  deltaTe=heat/(rhoe*h*cpe)

            do 63 i=1,n

                  te(i,1,1)=te(i,1,1)+deltaTe

 63         continue

c** ncount calculates the decrease in the no of nodes of emulsion as
c  some emulsion volume is broken into oil and water.
c** Since the oil grid spacing is so chosen that volume of one grid
c  length of oil is produced upon breaking of emulsion volume of
c  emulsion from one emulsion grid length, ndn no of nodes will be
c  added to the oil region.

                        l=l+ncount
                        rl=(l-1)*delxo
                        h=(n-1)*delxe

c** The oil layer produced is at teb temp. As this layer is added
c  at the bottom of the existing oil layer, the temperatures of the
c nodes in the oil region need to be reassigned.

                    do 65 i=l,ncount+1,-1
                        ncnt=i-ncount
                        to(i,1,1)=to(ncnt,1,1)
 65                 continue

                    do 70 i=1,ncount
                         to(i,1,1)=to(i+1,1,1)
 70                 continue

            else

            endif

                  if(n.gt.2)then

                  else

                        mflag=1

                        if(tw(1,1,1).ge.twb)then

                              tm6=to(2,1,1)
                              tm7=tw(2,1,1)

                              call boilover(tm6,tm7,dwdt)

                              if (nnflag.eq.0)then
```

```
                        write(58,*)time,'Boil:dwdt=',dwdt
                              nnflag = 1
                              else
                              endif
                              buffw=buffw+dwdt
                              ndm=int(buffw/delyw)
                              if(ndm.gt.0)then
                                m=m-ndm
                                buffw=buffw-float(ndm*delyw)
                                do 67 i=1,n
                                  tw(i,1,1)=tw(i+ndm,1,1)
 67                               continue
                              else
                              endif
                        else
                        endif
                  endif
              if(mflag.eq.1.and.nflag.eq.0)then
              write(58,*)time,'Emulsion depleted',tw(1,1,1)
              nflag=1
              else
              endif
          tm8=to(l-1,1,1)
c*** Oil surface auxiliary condition is used to calculate oil
c  evaporation rate dld. Must be negative.
          call oilsurf(tm8,dld)
          if(dld.gt.0.0)then
              dld=0.0
          else
          endif
```

```
      qcomb=-0.02*rhoo*qcom*dld

      drldt=-(dld)

      if(n.gt.2)then

      else

      icount=icount+1

      endif

c*********************************************************************
c this is a new part of the code to handle the heat flux calculation.

      if(qcomb.gt.0)then
            if(qcomb.lt.qcomp.and.qmax.lt.qmacks)then
                  q=qign-0.02*rhoo*qcom*dld
                  qmax=q

            else

                  q=qmacks
                  qmax=q

            endif

      else

            q=qmax

      endif


c*********************************************************************

        rln=rl+delt*(dld)

        drl=buffl+rl-rln

        dl=drl/delxo
        ldl=abs(int(dl))
        buffl=drl

            if (ldl.gt.0)then

                  l=l-ldl
                  if(l.lt.1)then

                        l=1

                  else

                  endif

                  rl=(l-1)*delxo
```

```
                to(l,1,1)=tov
                buffl=buffl-(ldl*delxo)

            else

            endif

          tes=to(l,1,1)
          time=delt*j

          itime=int(time)
          test_diff=time-itime

          if(test_diff.lt.delt)then

              write(61,*)time, q
              write(60,*)time,drldt

              if(drldt.lt.1e-9)then
              iextenchk=iextenchk+1

              else

              iextenchk=0

              endif

          else
          endif

          if(n.eq.2.and.nchk.eq.0)then
          t3=time
          nchk=1
          else
          endif

          if (time.eq.300.0)then

 228 do 121 i=l,1,-1
              xo=rl-(float(i-1)*delxo)
              write(57,21)xo,to(i,1,1)
              write(51,21)xo,to(i,1,1)
121   continue

      do 122 i=n,1,-1
              xe=xo+h-(float(i-1)*delxe)
              write(57,21)xe,te(i,1,1)
              write(52,21)xe,te(i,1,1)
122   continue

      do 123 i=1,m
              xw=xe+float(i-1)*delyw
              write(57,21)xw,tw(i,1,1)
              write(53,21)xw,tw(i,1,1)
123   continue

      else
```

```
      endif

      end do

      rl=rl+buffl

      eff=(rloil-rl)/rloil

        write(59,*)'T3=',t3, 'Time =',time, 'Iextenchk=', iextenchk
      write(59,99)eff,rloil,rl,l,m,n
  99  format(     1x, 'Efficiency=', f6.4,2x,'Initial
Oil=',f8.6,2x,'Final
     &   Oil= ',f8.6,/,' Oil Nodes left= ',I3,' Water Nodes= ',I3,
     & ' Emulsion Nodes= ',I3)


      stop
      end



c*********************************************************************
c*** SUBROUTINE FOR OIL-EMULSION INTERFACE
      subroutine oeintfc(te2,tino,tw2,tino2,tinn)
c*********************************************************************
      implicit double precision(a-h,o-z)

c*********************************************************************
      common/list1/ho,epso,cono,difo,rhoo,cpo,qlo,qcom,co,tov,beta
      common/list2/conw,difw,rhow,hfgw,cpw,qmacks
      common/list3/y,delt,delxe,delxw,tin,h,c1,teb,err,deltau,q,gamma
      common/list4/epse,he,delxo
      common/list5/cone,dife,rhoe,qle
      common/list6/stboltz,delyw,rc,rl
c*********************************************************************

      tempp=gamma*0.5*(delxe*rhoe*cpe+delxo*rhoo*cpo)
      tempq=0.5*(delxe*rhoe*cpe+delxo*rhoo*cpo)

      fact=1.0/((tempp/deltau)+(tempq/delt))

      temp1=(tempq/delt)*tino
      temp2=cone*tw2/delxe
      temp3=((tempp/deltau)-(cone/delxe)
     $            -(cono/delxo))*tino2
      temp4=cono*te2/delxo
      temp5=a*co*q*dexp(-beta*rl)

      tinn=(temp1+temp2+temp3+temp4-temp5)*fact

      return
      end
```

```
c**********************************************************************
c** SUBROUTINE FOR PART III SURFACE NODE
      subroutine oilsurf(tso,dld)
c**********************************************************************
      implicit double precision(a-h,o-z)

c**********************************************************************
      common/list1/ho,epso,cono,difo,rhoo,cpo,qlo,qcom,co,tov,beta
      common/list2/conw,difw,rhow,hfgw,cpw,qmacks
      common/list3/y,delt,delxe,delxw,tin,h,c1,teb,err,deltau,q,gamma
      common/list4/epse,he,delxo
      common/list5/cone,dife,rhoe,qle
      common/list6/stboltz,delyw,rc,rl
c**********************************************************************

      fact=1.0/(rhoo*qlo)
      temp2=stboltz*epso*(((tov*tov)*(tov*tov))-((tin*tin)*(tin*tin)))
      temp1=cono*(tov-tso)/delxo-(ho*(tso-tin)+(1.0-co)*q-temp2)

      dld=temp1*fact


      return
      end


c**********************************************************************
c*** SUBROUTINE FOR EMULSION-WATER INTERFACE
      subroutine ewintfc(te2,tino,tw2,tino2,tinn)
c**********************************************************************
      implicit double precision(a-h,o-z)

c**********************************************************************
      common/list1/ho,epso,cono,difo,rhoo,cpo,qlo,qcom,co,tov,beta
      common/list2/conw,difw,rhow,hfgw,cpw,qmacks
      common/list3/y,delt,delxe,delxw,tin,h,c1,teb,err,deltau,q,gamma
      common/list4/epse,he,delxo
      common/list5/cone,dife,rhoe,qle
      common/list6/stboltz,delyw,rc,rl
c**********************************************************************

      tempp=2.0*difw*rc*rc/(delyw*delyw)
      tempq=cone*difw*rc*(2.0+4.0*delyw)/(conw*delyw)
      tempr=gamma/tempq+gamma*delxe/(2.0*dife)
      temps=1.0/tempq+delxe/(2.0*dife)

      fact=1.0/((tempr/deltau)+(temps/delt))

      temp1=(tempr/deltau)*tino2
      temp2=tempp*tw2/(tempq)
      temp3=((temps/delt)-(tempp/tempq)
     $            -(1.0/delxe))*tino
      temp4=te2/delxe

      tinn=(temp1+temp2+temp3+temp4)*fact

      return
```

```
      end

c**********************************************************************
c**** SUBROUTINE FOR GENERAL DIFFERENTIAL EQUATION
      subroutine general(t,n,ct1,ct2,a)
c**********************************************************************
      implicit double precision(a-h,o-z)
      parameter (imax=3000)
      dimension t(imax,2,2)
c**********************************************************************
      common/list1/ho,epso,cono,difo,rhoo,cpo,qlo,qcom,co,tov,beta
      common/list2/conw,difw,rhow,hfgw,cpw,qmacks
      common/list3/y,delt,delxe,delxw,tin,h,c1,teb,err,deltau,q,gamma
      common/list4/epse,he,delxo
      common/list5/cone,dife,rhoe,qle
      common/list6/stboltz,delyw,rc,rl
c**********************************************************************

      fact=1.0/((gamma/deltau)+(1.0/delt))
      ct2=0.0

      if(ct1.eq.1.0)then

            if (a.eq.0.0)then

                  dx=delxe
                  d=h
                  alpha=dife

            else

                  dx=delxo
                  d=rl
                  alpha=difo

            endif

          do 10 i=n-1,2,-1

            x=((i-1)*dx)
            fx=a*co*q*beta*dexp(-beta*(rl-x))/(rhoo*cpo)
            to1=t(i,1,1)
            to2=t(i,1,2)
            top=t(i+1,2,2)
            tom=t(i-1,1,2)

            tn=((gamma/deltau)*to2+to1/
     $               delt+alpha*(top+tom-2.0*to1)
     $                /(dx*dx)+fx)*fact


            t(i,2,2)=tn

 10       continue

      else
```

```
            dx=delyw
            alpha=difw

          do 20 i=2,(n-1)

            yw=(i-1)*dx
            ct1=(rc**2)*(1.0-yw)**4
            ct2=4.0*alpha*(rc*rc)*((1.0-yw)*(1.0-yw)*(1.0-yw))
            to1=t(i,1,1)
            to2=t(i,1,2)
            top=t(i+1,1,2)
            tom=t(i-1,2,2)

            tn=((gamma/deltau)*to2+to1/
     $              delt+ct1*alpha*(top+tom-2.0*to1)
     $              /(dx*dx)-ct2*(to1-tom)/dx)*fact

            t(i,2,2)=tn

 20       continue

       endif

       return
       end



c**********************************************************************
c*** SUBROUTINE FOR OIL-WATER INTERFACE (NO BOILOVER)
       subroutine owintfc(to2,tino,tw2,tino2,tinn)

c*** This does account for the indepth radiation absorption
c**********************************************************************
       implicit double precision(a-h,o-z)

c**********************************************************************
       common/list1/ho,epso,cono,difo,rhoo,cpo,qlo,qcom,co,tov,beta
       common/list2/conw,difw,rhow,hfgw,cpw,qmacks
       common/list3/y,delt,delxe,delxw,tin,h,c1,teb,err,deltau,q,gamma
       common/list4/epse,he,delxo
       common/list5/cone,dife,rhoe,qle
       common/list6/stboltz,delyw,rc,rl
c**********************************************************************

       tempp=2.0*difw*rc*rc/(delyw*delyw)
       tempq=cono*difw*rc*(2.0+4.0*delyw)/(conw*delyw)
       tempr=gamma/tempq+gamma*delxo/(2.0*difo)
       temps=1.0/tempq+delxo/(2.0*difo)
       tempt=((2.0*difw*rc*rc/delyw + 4.0*difw*rc*rc*rc)*co*q*dexp
      $  (-beta*rl))/(conw*rc)

       fact=1.0/((tempr/deltau)+(temps/delt))

       temp1=(tempr/deltau)*tino2
       temp2=tempp*tw2/(tempq)
       temp3=((temps/delt)-(tempp/tempq)
```

```
     $            -(1.0/delxo))*tino
      temp4=to2/delxo
      temp5=tempt/tempq

      tinn=(temp1+temp2+temp3+temp4+temp5)*fact

      return
      end

c**********************************************************************
c*** SUBROUTINE FOR OIL-WATER INTERFACE AT BOILOVER
      subroutine boilover(tm10,tm11,dwdt)
c**********************************************************************
      implicit double precision(a-h,o-z)

c**********************************************************************
      common/list1/ho,epso,cono,difo,rhoo,cpo,qlo,qcom,co,tov,beta
      common/list2/conw,difw,rhow,hfgw,cpw,qmacks
      common/list3/y,delt,delxe,delxw,tin,h,c1,teb,err,deltau,q,gamma
      common/list4/epse,he,delxo
      common/list5/cone,dife,rhoe,qle
      common/list6/stboltz,delyw,rc,rl
c**********************************************************************

      temp1=1.0/(rhow*hfgw)
      temp2=cono*(tm10-twb)/delxo+conw*rc*(twb-tm11)/delyw
     $            +co*q*dexp(-beta*rl)
      dwdt=-temp1*temp2

      return
      end
```

VITA

Ajey Yeshwant Walavalkar was born in Ratnagiri, India on January 7th, 1973. He completed his high-school education in the town of Pune in western India. He received Bachelor of Engineering degree in Mechanical Engineering in 1994 from University of Pune, India. Ajey began graduate study in August 1995 at The Pennsylvania State University, University Park, USA. He has focused on experimental and numerical heat transfer for emulsion pool fires. He married Leena Kolhatkar in August 1998. After graduation, Ajey plans to work for Carrier Corporation in Syracuse, New York.